UNIVERSIDADE DA BEIRA INTERIOR
Engenharia

Guidance of Interceptor Missiles Based on Robust Control

(versão final após defesa)

António Rui Moreira Tinoco da Costa

Dissertação para obtenção do Grau de Mestre em
Engenharia Aeronáutica
(Ciclo de Estudo Integrado)

Orientador: Prof. Doutor Kouamana Bousson

Covilhã, dezembro de 2018

“It has become appallingly obvious that our technology has exceeded our humanity.” –Albert Einstein, 1909

Acknowledgements

First and foremost, I would like to express my deepest gratitude to my family, most especially to my parents for all the support given and because without them, this dissertation would not be possible to accomplish.
Secondly, I would like to give special thanks to my supervisor Professor Kouamana Bousson, for all the support, patience and trust laid on my work.
I also have to give special thanks to my laboratory colleague Adriano Brum, for all the support given on the Python code.
Lastly, to all my friends that directly and indirectly contributed to the accomplishment of this project work.

Abstract

Missiles development are constantly evolving. This is mainly due to the significantly increase in the performance of the missiles means of transportation (aircrafts, vessels, submarines, trucks and trains), allowing bigger and heavier armament, which results directly in much more precise control systems, with a capacity for different types of warheads, as well as an ability to store larger amounts of fuel.

Regarding the subject addressed in this thesis, it should be taking into consideration that a tactical missile has to be quite versatile, as it can either aim to shoot down an aircraft with high manoeuvrability or a cruise missile with a predefined trajectory, being thus necessary to withstand high speeds and g force.

A control system for a missile is responsible for its attitude, while missile guidance system is responsible for controlling its trajectories and, therefore, being able to detect that the missile is outside the interception trajectory, requiring an input signal to put it back on collision course.

The focus of this dissertation is on the control of the trajectories of a tactical missile, which has to be capable of performing the basic function of detecting the signals received by the command, which in its turn will be applied to the control system.

An H_∞/LTR controller and the Artstein method applied on a Robust LQR controller were applied to the missile, where it's concluded that the first one has a better performance for manoeuvrable or non-manoeuvrable targets. However, Robust LQR method reveals a strong potential when implemented to solve systems in which perturbations predominate, thus making the behaviour of both methods very similar.

Keywords

H_∞; H_∞/LTR; Robust LQR; Tactic Missile; Guidance; Artstein Method

Resumo

O desenvolvimento dos mísseis está em constante evolução. Tal se deve principalmente ao aumento significativo do desempenho dos meios de transporte destes (aeronaves, embarcações, submarinos, camiões e comboios), permitindo assim transportar armamento de maiores dimensões e peso, o qual resulta diretamente em sistemas de controlo muito mais precisos, com uma capacidade para diferentes tipos de ogivas e armazenamento de maiores quantidades de combustível.

Relativamente ao assunto abordado neste trabalho, é preciso ter em conta que um míssil tático tem de ser bastante versátil, pois tanto pode ter como alvo a abater uma aeronave com elevada manobrabilidade ou um míssil de cruzeiro com uma trajetória pré-definida, sendo assim necessário suportar elevadas velocidades e força g.

Um sistema de controlo para um míssil é responsável pela sua atitude, enquanto o sistema de orientação deste é responsável pelo controlo das suas trajetórias, tendo assim de ser capaz de detetar que o míssil se encontra fora da trajetória de interceção com o alvo, necessitando de receber uma entrada que o volte a colocar na rota de colisão. O foco desta dissertação é no controlo das trajetórias de um míssil tático, tendo este de ser capaz de cumprir a função básica de detetar os sinais recebidos pelo comando, os quais por sua vez serão aplicados ao sistema de controlo, o que se resume em alterações do rumo do míssil.

Foi aplicado um sistema de orientação H_∞/LTR, bem como o método de Artstein a um LQR Robusto, onde se conclui que o primeiro apresenta um melhor desempenho tanto para alvos sem manobrabilidade como com manobrabilidade. Porém, é necessário ter em conta que o método do LQR Robusto revela um forte potencial quando implementado para solucionar sistemas nos quais predominem perturbações, fazendo assim com que o comportamento dos dois métodos seja bastante semelhante.

Palavras-chave

H_∞; H_∞/LTR; LQR Robusto; Míssil Tático; Orientação; Método de Artstein

Content

Introduction

1.1. General Context 1
1.2. Missile Classification according to its mission 2
1.2.1. Basic Principles of Missile Guidance and Control Devices 4
1.3. Objective 15
1.4. Structure 15

Missile Guidance and Flight Dynamic

2.1. Traditional body coordinate frame, Missile Coordinate frame and Moment Reference Point Coordinate Frame 18
2.1.1. Static Coefficient Model 18
2.1.2. Aerodynamic Damping Model 19
2.1.3. Aerodynamic Forces and Moments 20
2.2. Velocity Equations (or Forces) and Manoeuvre Rates (or Moments) for short period .. 22
2.3. Pursuit Modelling associated to Guidance (Proportional Navigation) 25
2.3.1. Pure Proportional Navigation (PPN) 27
2.3.2. True Proportional Navigation (TPN) 27
2.3.3. Generalized True Proportional Navigation (GTPN) 28
2.3.4. Ideal Proportional Navigation (IPN) 28

Optimal Guidance of Air-to-Air Missiles and Surface-to-Air Missiles

3.1. Introduction to $H\infty$ and LQR methods 31
3.2. Target/Interceptor Kinematics Model 3D Approach 32
3.3. Classic Linear Quadratic Regulator (LQR) method 34
3.3.1. Artstein Method with application on LQR Robust 36
3.4. $H\infty$ Method 37
3.4.1. State-Space Solutions to Standard $H\infty$ 37
3.4.2. $H\infty$/LTR control for the mixed sensibility problem and through the exit 39
3.5. Case of Study Application 39

Simulation and Results

4.1. Implementation of the problem, using a non-manoeuvring target 43
4.1.1. Implementation of the first analysis (X1) 44
4.1.2. Implementation of the first analysis (X2) 50
4.2. Implementation of the problem, using a manoeuvring target 56
4.2.1. Implementation of the first evasive manoeuvre trajectory X3 57
4.2.2. Implementation of the first evasive manoeuvre trajectory X4 67

Contributions and Future works

5.1. Contributions 77
5.2. Future Works 78

Bibliography 79

Appendix A

A.1. Numerical Resolution of Ordinary Equations (Butcher Algorithm) 85

Appendix B 87

List of Figures

Chapter 1

1.1. Missile Guidance System in the form of a control loop [5] 1
1.2. Guidance Phases for a Ballistic Missile [9] 3
1.3. Guidance Phases for an AAM [9] 3
1.4. Guidance Phases for an SAM [10] 4
1.5. Flight path of zero-lift inertial system on ASM or AGM [12] 4
1.6 Typical Guided Missile [7] 5
1.7. Classification of Jet Powerplants [13] 5
1.8. External Control Devices on Missiles: A. Plan Forms of Airfoils; B. Movable parts of Fixed Airfoils [13] 6
1.9. Forces and Moments represented in missile body axis system [16] 8
1.10. Different types of missile classification [16] 9
1.11. Three Basic Types of Missile Seeker Systems [17] 10
1.12. A. Command Guidance; B. Beam-Rider Guidance [18] 11
1.13. Velocity Pursuit Kinematics [21] 12
1.14. Proportional Navigation [23] 13
1.15. N′ Effecting various missile flight [21] 14
1.16. Pursuit: pure pursuit/deviated pursuit/lead pursuit [24] 14

Chapter 2

2.1. Rotational dynamics of rigid body [16] 17
2.2. Static Coefficients applied on a missile [34] 18
2.3. Definition of the Euler Angles on a Missile [35] 22
2.4. Parallel-navigation trajectories for nonmaneuvering targets: a) Velocity collision triangle; b) trajectories triangle; c) relative trajectory [1] 26
2.5. Proportional Navigation guidance loop in terms of missile acceleration [1] 26
2.6. Proportional Navigation variants: a) Pure Proportional Navigation; b) True Proportional Navigation; c) Generalized True Proportional Navigation; d) Ideal Proportional Navigation [39] 28

Chapter 3

3.1. 3D Pursuit-Evasion Geometry [37] 33
3.2. The closed loop LQR system [46] 34
3.3. Block diagram of the feedback control system [43] 37

Chapter 4

4.1. Intersection of target and missile using Robust LQR control in three dimensions for X1 44
4.2. Missile and target accelerations until the intersection occurs using Robust LQR control for X1 45
4.3. Missile and target velocities until the intersection occurs using Robust LQR method for X1. 45
4.4. Intersection of target and missile using Hinfinit/LTR control in three dimensions for X1 46
4.5. Missile and target accelerations until the intersection occurs using Hinfinit/LTR method for X1 46
4.6. Missile and target velocities until the intersection occurs using Hinfinit/LTR method for X1 47
4.7. Intersection of target and missile using Hinfinit/LTR and Robust LQR methods in three dimensions for X1 47
4.8. Missile and target positions until the intersection occurs using Hinfinit/LTR and Robust LQR methods for X1 48
4.9. Missile accelerations until the intersection occurs using Hinfinit/LTR and Robust LQR methods for X1 48
4.10. Missile velocities until the intersection occurs using Hinfinit/LTR and Robust LQR methods for X1 49
4.11. Intersection of target and missile using Robust LQR control in three dimensions for X2 50
4.12. Missile and target acceleration until the intersection occurs using Robust LQR method for X2 51
4.13. Missile and target velocities until the intersection occurs using Robust LQR method for X2 51
4.14. Intersection of target and missile using Hinfinit/LTR control in three dimensions for X2 52
4.15. Missile and target acceleration until the intersection occurs using Hinfinit/LTR method for X2 52
4.16. Missile and target velocity until the intersection occurs using Hinfinit/LTR method for X2 53
4.17. Intersection of target and missile using Hinfinit/LTR and Robust LQR control in three dimensions for X2 53
4.18. Missile position until the intersection occurs using Hinfinit/LTR and Robust LQR methods for X2 54

4.19. Missile acceleration until the intersection occurs using Hinfinit/LTR and Robust LQR methods for X2 54
4.20. Missile velocity until the intersection occurs using Hinfinit/LTR and Robust LQR methods for X2 55
4.21. Intersection of target and missile using Robust LQR control in three dimensions for X3.1..... 57
4.22. Target and missile course using Robust LQR control in two dimensions for X3.1..... 58
4.23. Missile and target acceleration until the intersection occurs using Robust LQR method for X3.1 58
4.24. Missile and target velocity until the intersection occurs using Robust LQR method for X3.1..... 59
4.25. Intersection of target and missile using Hinfinit/LTR control in three dimensions for X3.1..... 59
4.26. Target and missile course using Hinfinit/LTR control in two dimensions for X3.1 ... 60
4.27. Missile and target acceleration until the intersection occurs using Hinfinit/LTR method for X3.1 60
4.28. Missile and target velocity until the intersection occurs using Hinfinit/LTR method for X3.1..... 61
4.29. Intersection of target and missile using Robust LQR control in three dimensions for X3.2..... 62
4.30. Target and missile course using LQR Robust control in two dimensions for X3.2..... 63
4.31. Missile and target acceleration until the intersection occurs using Robust LQR method for X3.2 63
4.32. Missile and target velocity until the intersection occurs using Robust LQR method for X3.2..... 64
4.33. Intersection of target and missile using Hinfinit/LTR control in three dimensions for X3.2..... 64
4.34. Target and missile course using Hinfinit/LTR control in two dimensions for X3.2 ... 65
4.35. Missile and target acceleration until the intersection occurs using Hinfinit/LTR method for X3.2 65
4.36. Missile and target velocity until the intersection occurs using Hinfinit/LTR method for X3.2..... 66
4.37. Intersection of target and missile using Robust LQR control in three dimensions for X4.1..... 67
4.38. Target and missile course using LQR Robust control in two dimensions for X4.1..... 68
4.39. Missile and target acceleration until the intersection occurs using Robust LQR method for X4.1 68
4.40. Missile and target velocity until the intersection occurs using Robust LQR method for X4.1..... 69

4.41. Intersection of target and missile using Hinfinit/LTR control in three dimensions for X4.1 69
4.42. Target and missile course using Hinfinit/LTR control in two dimensions for X4.1 ... 70
4.43. Missile and target acceleration until the intersection occurs using Hinfinit/LTR method for X4.1 70
4.44. Missile and target velocity until the intersection occurs using Hinfinit/LTR method for X4.1 71
4.45. Intersection of target and missile using Robust LQR control in three dimensions for X4.2 72
4.46. Target and missile course using Robust LQR control in two dimensions for X4.2..... 73
4.47. Missile and target acceleration until the intersection occurs using Robust LQR method for X4.2 73
4.48. Missile and target velocity until the intersection occurs using Robust LQR method for X4.2 74
4.49. Intersection of target and missile using Hinfinit/LTR control in three dimensions for X4.2 74
4.50. Target and missile course using Hinfinit/LTR control in two dimensions for X4.2 ... 75
4.51. Missile and target acceleration until the intersection occurs using Hinfinit/LTR method70 for X4.2..... 75
4.52. Missile and target velocity until the intersection occurs using Hinfinit/LTR method for X4.2 76

List of Acronyms

LOS	Line-of-Sight
CLOS	Command to Line-of-Sight
FOV	Field of View
AAM	Air-to-Air Missile
AIM	Air-Intercept Missile
SAM	Surface-to-Air Missile
ASM	Air-to-Surface Missile
AGM	Air-to-Ground Missile
SSM	Surface-to-Surface Missile
GGM	Ground-to-Ground Missile
EOB	End of Boost
PIP	Predicted intercept point
TERCOM	Terrain contour matching
GPS	Global Positioning System
IR	Infrared Radiation
RH	Radar Homing
RF	Radio/radar Frequency
TV	Television Waves
PN	Proportional Navigation
PPN	Pure Proportional Navigation
TPN	True Proportional Navigation
GTPN	Generalized True Proportional Navigation
IPN	Ideal Proportional Navigation
UV	Ultraviolet
MMW	Millimetre Wave
LASER	Light Amplification by Stimulated Emission of Radiation
LADAR	Laser Detection and Ranging
LATAX	Missile lateral acceleration
LQR	Linear Quadratic Regulator
LQG	Linear Quadratic Gaussian
LTI	Linear Time-Invariant

LFT	Linear Fractional Transformation
LTR	Loop Transfer Recovery
SISO	Single Input and Single Output
MIMO	Multiple Input and Multiple Output
MRP	Moment Reference Point for Missile Aerodynamics on the missile centreline
MACH	Number indicating the ratio of the speed of an object to the speed of sound in the medium through which the object is moving
DOF	Degrees of Freedom
2D	Two Dimensions
3D	Three Dimensions
CG	Centre of Gravity
REF	Reference

Nomenclature

Symbols	Description
$A(t)$	State Matrix
A_Z	Translational acceleration normal to the missile longitudinal axis
$B(t)$	Control Matrix
C	Missile Lead angle
$C(t)$	Output Matrix
C_A	Axial Force Coefficient
C_l	Rolling Moment Coefficient
C_m	Pitching Moment coefficient
C_N	Normal Force Coefficient
C_S	Side Force
C_{T_M}	Thrust Coefficient
C_Y	Side Force Coefficient
C_{yaw}	Yawing Moment Coefficient
D	Drag
D_{ref}	Missile Aerodynamic reference length
$\bar{d}_{cm}$	Position of the mass centre from the ogive
$\bar{d}_{mrc}$	Position of the moments reference centre from a fixed point
$F_Z(\alpha, \delta)$	Forces applied to the missile
F^B	Force resulting from the rocket Propulsion
g	Gravitational Acceleration
$G(s)$	Process Plant
H	Hamiltonian Matrix
HE	Heading Error
I	Moment of Inertia
J	Performance Index
K	Controller
k	Time-varying feedback gain matrix
K_C	Feedback matrix
K_F	State observer matrix
m	Missile Mass
$M(\alpha, \delta)$	Moment applied to the missile airframe
N'	Navigation Constant
n_C	Missile lateral acceleration
n_M, a_M	Missile acceleration
n_T	Target acceleration

P	Riccati solution
p	Roll Rate
q	Pitch Rate
$\bar{Q}$	Missile Dynamic Pressure
$Q(t)$	Weighting Matrix for the state variables
r	Yaw Rate
R_{TM}	Length of LOS
$\dot{R}_{TM}$	Rate of change between Missile and Target
$R(t)$	Matrix
S_{ref}	Missile Aerodynamic reference area
t	Time
T	Transposed Matrix
T_M	Missile Thrust
T_{zw}	Matrix
u	Longitudinal Speed
$u(t)$	Plant Control input vector
v	Lateral Speed
V_C	Missile-Target Closing Velocity
V_M^B, V_M	Missile velocity
$\dot{V}_M^B$	Missile velocity rate
V_T	Target Velocity
$\dot{V}_T$	Target Velocity rate
V_R	Relative Speed
V_{sound}	Speed of sound
w	Vertical Speed
W	Rate of rotation of the LOS
x	Longitudinal Position
X	Matrix
$x(t)$	State Vector
y	Lateral Position
Y	Matrix
$y(t)$	Output Vector
z	Vertical Position
z_T	Small deviations of Target
z_M	Small deviations of Missile

Greek Alphabet

Symbols	Description
α	Angle of Attack
$\dot{\alpha}$	Angle of attack rate
α_{tot}	Total Angle of Attack, measured in the X-Z plane with the missile coordinate frame with the origin at the MRP
γ	Flight-Path Angle of the missile
$\dot{\gamma}$	Flight-Path angle rate
λ	LOS angle
$\dot{\lambda}$	LOS rate
ε	Flight-path angle of the target
$\dot{\varepsilon}$	Angular velocity of the target
θ	Pitch angle
ϕ , ϕ_A	Roll angle
Ψ, β	Yaw angle
δ	Control input
$\ddot{\theta}$	Angular acceleration
ω_M^B	Angular Velocity
γ	Norm bound
Γ	Angle between missile acceleration and the normal to range
$\dot{\beta}$	Yaw Rate
$\dot{\theta}$	Pitch Rate

In this dissertation, some symbols may refer to more than one variable. However, when necessary it will be referenced in the text.

Chapter 1

Introduction

1.1. General Context

In 1870, the first theory application of a guidance law was made, when Werner von Siemens submitted a proposal to the Prussian ministry of war for a project of guided torpedoes to destroy the enemy vessels and in 1916, it had become the first operational guided-weapon system in history. [1]

To understand the definition of a guided-weapon, first it's necessary to distinguish guidance from navigation. So, guidance is "the process for guiding the path of an object towards a given point, which in general may be moving", which means that the target moves in a way that is not quite predictable and there will be an evader and a pursuer. On the other hand, in navigation there will be one given point (the target) that is fixed, so the pursuer doesn't need to predict the trajectory to occur the intersection. [2]

Since the first operational guided-weapon (the guidance of the proposed torpedo would have been of LOS), this technology has evolved into an exponential way and today guidance is being treated in technological disciplines from the point of view of kinematics, dynamics and control, trying to predict zones of interception, launch envelopes, stability of guidance process, trajectories, accuracy effects, structural limits, costs, energy expenditure and many other topics. [3] [4]

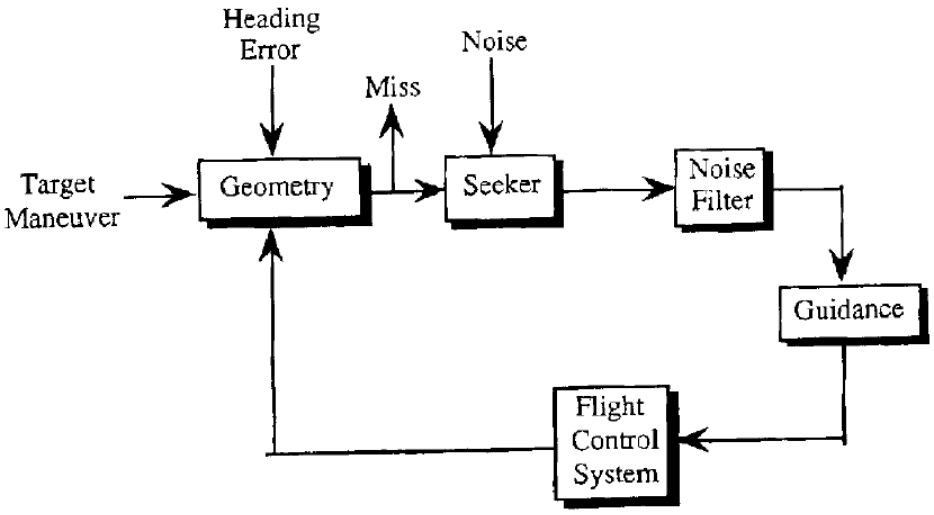

Figure 1.1. Missile Guidance System in the form of a control loop [5]

From figure 1.1 it's possible to see how control engineers in today's society implement a guidance system on a missile. Starting with the Geometry section, the missile acceleration is subtracted from target acceleration to obtain a relative acceleration. After that, two integrations will occur to provide the distance and the miss distance will be obtained through the relative separation between the missile and the target (in conventional missiles systems, it is used a warhead to destroy the target, because the missile designer can't eliminate the miss distance).
The missile seeker will attempt to track the target (with the use of a certain filter to smooth the noisy seeker signal) and then a guidance command is generated from the noise filter output. Finally, the flight control system must enable the missile to manoeuvre until the achieved acceleration matches the acceleration commands from the guidance law. [5]
To conclude, the motivation for the accomplishment of this dissertation is that a current fast progress of guided weaponry is being made, due to the advances of different areas of technology as inertial instrumentation (gyroscopes), electronics (microelectronics and radar), rocket engines and computer engineering.

1.2. Missile Classification according to its mission

A Guided missile is widely categorized according to its mission, which is generally stated in terms of its intended target and launching platform: Air-Air Missile (AAM) or Air-Intercept Missile (AIM), Surface-Air Missile (SAM), Air-Surface Missile (ASM) or Air-Ground Missile (AGM) and Surface-to-Surface Missile (SSM) or Ground-to-Ground Missile (GGM). [6] [7]
Starting with SSM, one of the most famous weaponry systems are the Ballistic Missiles, that follow a predefined trajectory that cannot be modified after all the fuel is expended. As shown in figure 1.2, a ballistic Missile typically experiences three different flight phases: boost, coast and re-entry. In the boost phase, the missile experiences a powered flight from launch to thrust cut-off; in the coast phase, the thruster is turned off and it flies freely without the influence of atmospheric drag because it's in a relatively high part of the atmosphere; in the re-entry phase, it reaches the lower part of the atmosphere and the atmospheric drag becomes considerable again and lasts until the impact on the ground occurs. [8]
SAM and AAM can also be classified into several "guidance phases", based on the guidance mode employed or on their specific mission. The AAM and the SAM have three different flight phases: programmed manoeuvre (for the AAM) or Boost Phase (for SAM), midcourse guidance and the terminal guidance, as shown in figures 1.3 and 1.4. The programmed manoeuvre is the first part of the trajectory, which is independent of the target information and is executed to ensure that the aircraft from where it is launched doesn't suffer any damage by the missile. After this phase is concluded, the midcourse guidance phase is initiated, placing the missile into the terminal acquisition range of the target with the missile seeker pointed to it and finally, the last phase (and the most important because it determines the success or failure of the mission)

is the terminal guidance, where the missile locks on the target and attempts to close the distance as quickly as possible, because all missiles have fuel and manoeuvre limitations. The success of the terminal guidance phase is directly related to the miss-distance that is the distance of closest approach of the missile to the target. [9] [10]

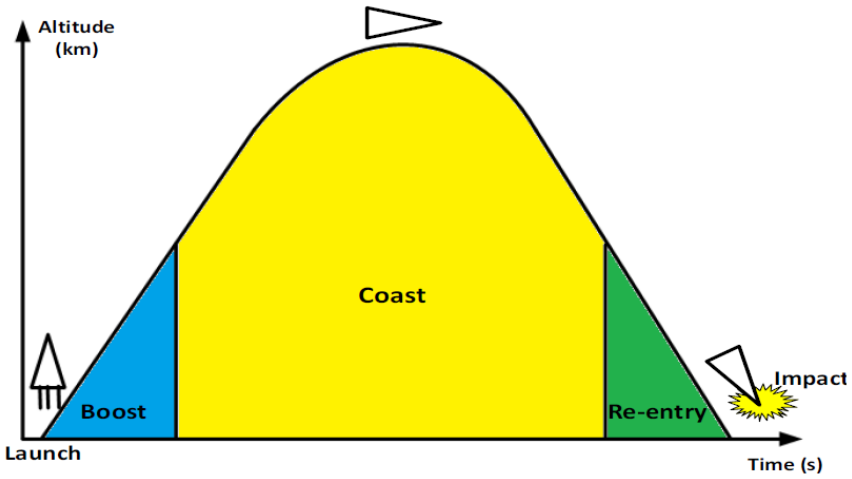

Figure 1.2. Guidance Phases for a Ballistic Missile (SSM or GGM) [8]

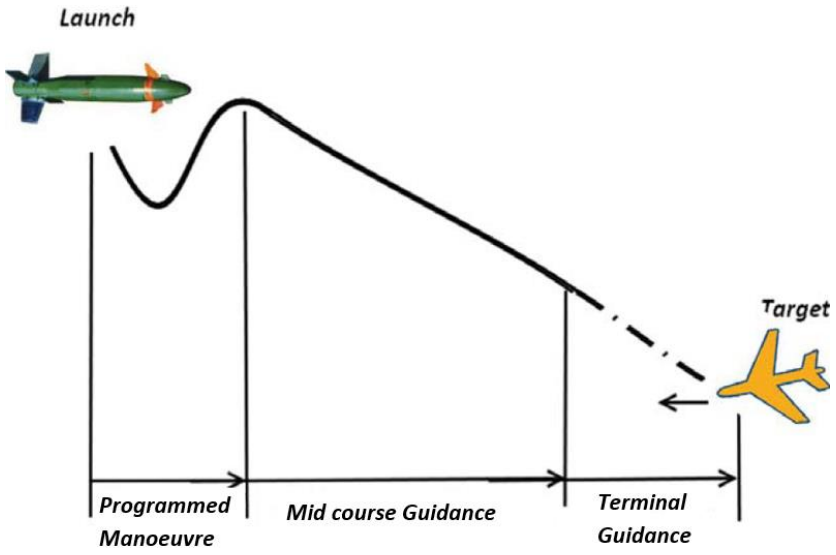

Figure 1.3. Guidance Phases for an AAM or AIM [9]

Missile trajectory for SAM is almost the same as in the AAM/AIM, except for the initial phase, which is called boost phase. As shown on figure 1.4, first the weapon control system decides if the target is reachable and if so, a launch solution is computed and the missile is initialized, launched and boosted to the intended flight speed. Inertial guidance is typically employed and the missile is boosted to flight speed and roughly establishes a flight path to intercept the target. [10] [11]

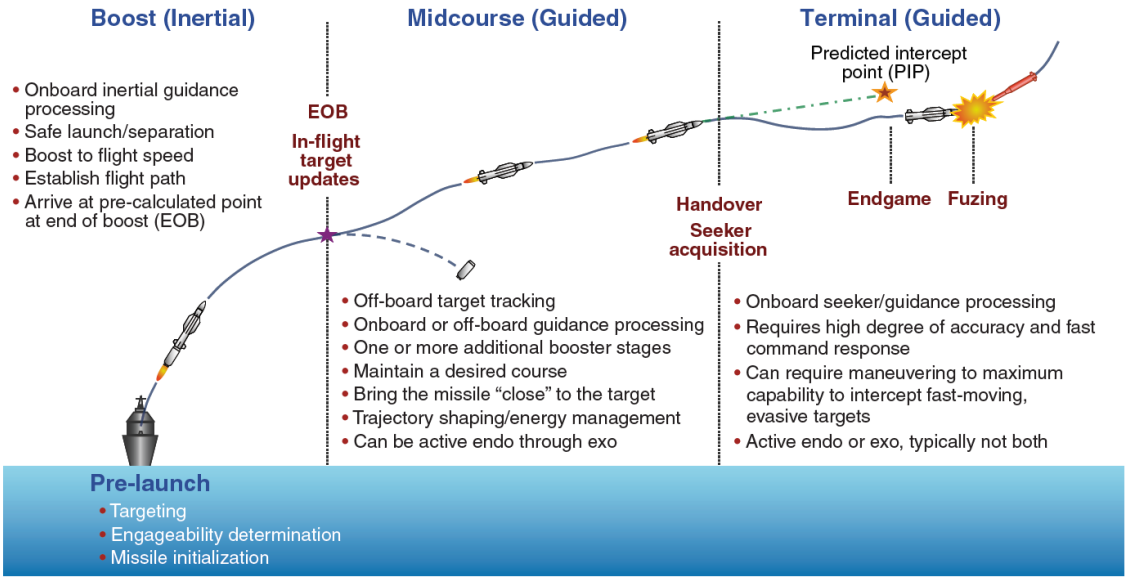

Figure 1.4. Guidance Phases for an SAM [10]

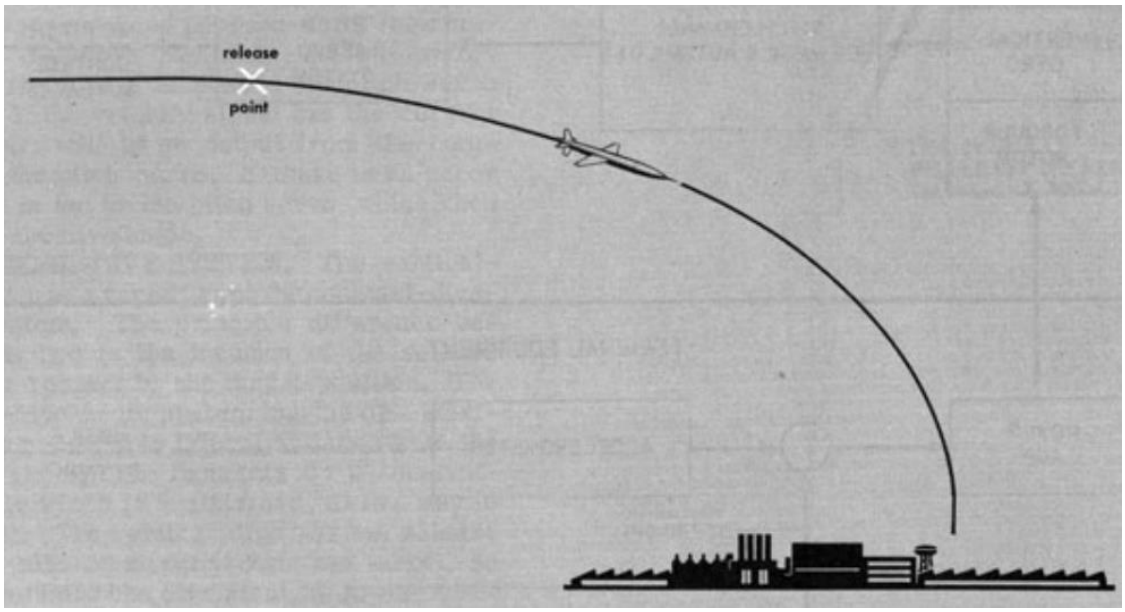

Figure 1.5. Flight path of zero-lift inertial system on ASM or AGM [12]

ASM or AGM will not be discussed in this dissertation, being the only focus the AAM and the SAM. However, in figure 1.5, an example is presented.

1.2.1. Basic Principles of Missile Guidance and Control Devices

All missiles have subsystems commonly associated that differ according to their mission. Depending on the design, some of the functions of these subsystems may be assisted or even replaced by equipment located in the launching platform (for example an airplane or a submarine). [7] [11]

Next, the subsystems shown in figure 1.6 will be discussed in the following sub chapters.

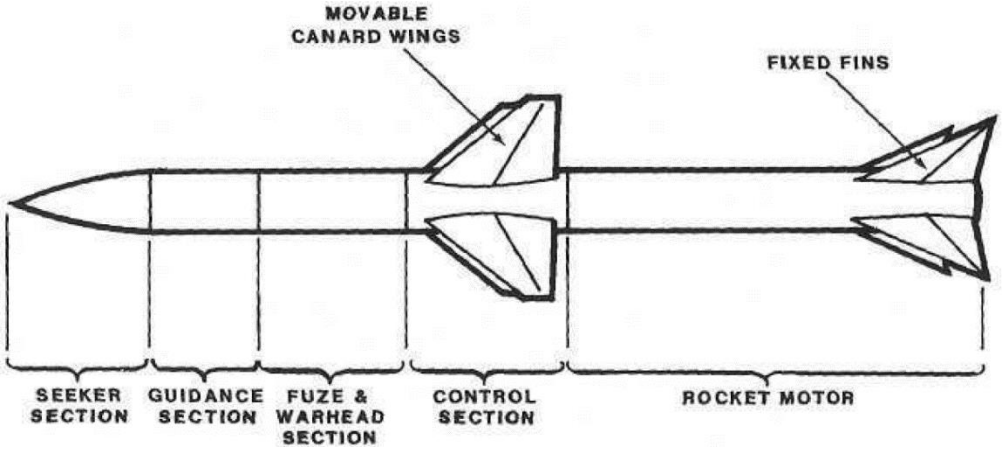

Figure 1.6.Typical Guided Missile [7]

1.2.1.1. Missile Propulsion

Normally, missile targets have high speeds, so missiles need to be rocket or jet powered (although the propulsion system of the missile may be of any type suitable for airborne vehicles).

As range requirements for the missile increase, so does the complexity of the motor design. For shorter-range missiles, solid-fuel rockets are usually preferred since this type of engine usually has very high thrust-to-weight, is simpler and rarely require throttling generating great acceleration and very high speeds during short duration. For medium-range missiles, solid-fuel rockets are also preferred but with two levels of thrust: an initial high-thrust booster and a longer-lasting, low-thrust sustainer. [7] [11]

For even greater ranges, liquid-fuel designs become more competitive in thrust-to-weight while also providing convenient thrust control. Despite this, ramjet propulsion is usually preferred over liquid-fuel for endo-atmospheric missiles.

Particularly with SAMs, a solid rocket booster will be provided to assist the missile in initial acceleration to efficient ramjet operating speed. [13] [16]

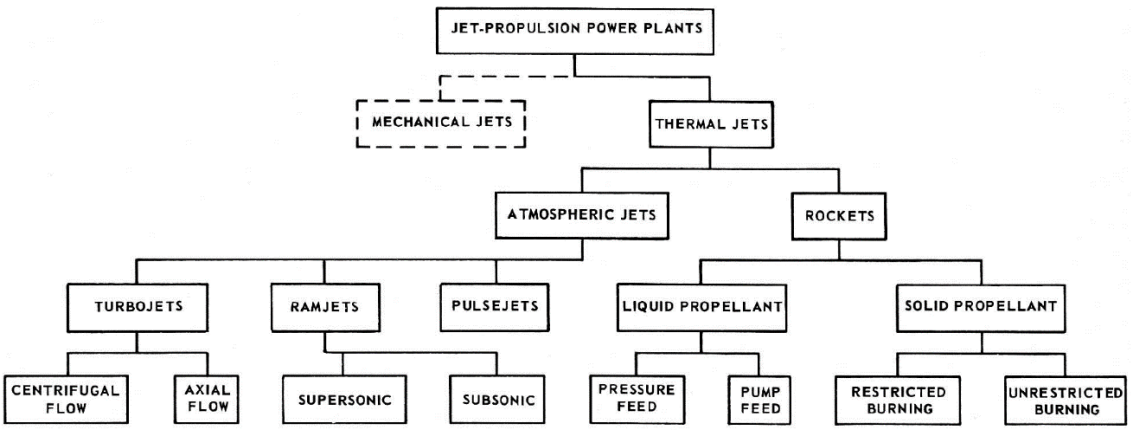

Figure 1.7. Classification of Jet Power plants [13]

1.2.1.2. Missile Control Devices

Missile control systems are responsible for the attitude during flight. The primary requirement is to detect when it's necessary to apply a control over the missile and for that, it needs to determinate the specific controls to manoeuvre and in what way. [7] [11]
So, the subsystems must comply with three basic functions: maintain the stability of the missile in pitch, roll and yaw; receive system command signals of the guidance system and convert those (by using suitable servomechanisms) in mechanical movements of the control surfaces, which will translate into missile direction changes; turn the missile towards the target soon after the launch. [14]
Missiles are often controlled aerodynamically, like conventional aircrafts, but they may also use thrust-vector control or an arrangement of fixed control jets as shown in figure 1.8. However, those are restricted to a limiting structural load factor and therefore, aerodynamically controlled missiles generally have their best turn performance at their highest speeds, being also able to provide control during the gliding (or unpowered) portion of missile flight. Nevertheless, this type of missile control is subject to the lift limitations of airfoils and the result of induced drag. [15] [16]

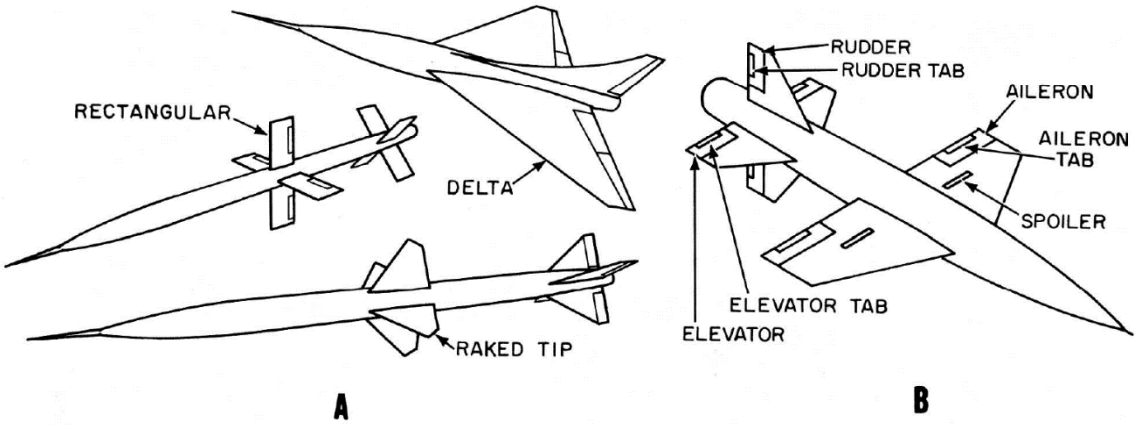

Figure 1.8. External Control Devices on Missiles: A. Plan Forms of Airfoils; B. Movable parts of Fixed Airfoils [13]

Thrust-vector control is a control system provided by altering the direction of the exhaust gases to change the thrust line that may be accomplished by rotating the nozzles (to do that, it needs deflector vanes in the exhaust or other means capable of making the missile to rotate on its CG in a severe sideslip). This method is highly unstable and requires a sophisticated and fast autopilot but enables great manoeuvrability. Besides, the missile needs to have the motor burning, making impossible to be controlled during a gliding flight segment. Therefore, Thrust-vector control is limited to applications on short-range weapons but it is quite useful for very high-altitude missiles since, unlike aerodynamic controls, doesn't dependent on the atmosphere. [14]

Another method of thrust-vector control is the use of fixed control jets arranged around the missile to make him rotate around its own CG. In this case, the thrust line is changed by rotating the entire missile rather than just the nozzles or exhaust gases. One advantage of this method is that may be lighter comparatively to a straight Thrust-vector control system since no large actuators are required. However, some manoeuvrability may be lost once greater control power is usually available from the main engine. [7] [11]

Almost any controller requires actuators of some sort for movement control surfaces, nozzles, valves, etc. The way the design and power source of these actuators are chosen also alters the performance of missile's manoeuvrability. Power sources can be pneumatic, electric or hydraulic or the combination of these. Hydraulic actuators usually provide the fastest reaction time to these three methods and they are capable of producing great control forces efficiently. Within hydraulic actuators, they can be "open" or "closed". In an open system, the used hydraulic fluid is vented overboard and in a closed system, the used fluid returns to the reservoir for reuse. Electric actuators are normally faster than pneumatic ones. Since all guided missiles already have electrical systems, this kind of power source may simplify the missile by eliminating additional systems. However, it's a very expensive source and tends to be heavy when great amounts of control power are required. [14]

Pneumatic actuators can be provided by bottles of compressed gas or by a gas generator. It's a system with a simple implementation and lightweight but they have a limited endurance and are slow in reacting, especially when heavy control loads are involved. [15]

1.2.1.3. Missile Fuzes and Warheads

The purpose of a missile fuse system is to cause the detonation of the warhead when the maximum target damage is achieved. However, it must ensure the safety of the firing platform and personnel and for that reason, the fuse only becomes armed to allow the detonation of the warhead when it senses that the firing platform is out of reach. Because of the wide range of interception conditions possible in engagements with targets, fuse design is one of the weakest link in missile defences.

Fuses can be classified as contact, time delay, command and proximity. Contact fuses are activated when the missile hits the target. They aren't very effective because normally the missile only approaches the target without hitting it.

Time-delay fuses are not usually used by missiles because of its lack of accuracy. However, in large-calibre anti-aircraft artillery they are very effective because they are pre-set before launch to explode at a given time that is calculated to place the projectile in close-range with the target.

Command Fuzes are activated by radio command from the guidance platform and requires relatively large warheads to improve the success of the mission significantly. Proximity fuses against manoeuvring targets are the most effective. They can be passive, semi-active and active. Passive fuses are activated by noise, heat, radio emissions, etc. that comes from the

target; Semi-Active fuses are generally used on an interacting Doppler frequency or high target LOS rates; Active fuses send out a signal and activate when he missile receives a reflection from the target (for example radio-proximity or LASER fuses).

Relatively to missile warheads, their lethality depends largely on the amount of explosive material and the number and size of the fragments. Warheads need to be designed for a specific target and must complement the missile guidance and fuse design.

The warheads used in AAMs are typically blast-fragmentation, incendiary or explosive pellets and expanding-rod types. Blast-fragmentation warheads combine the effects of high-velocity fragments and the explosive shock wave to cause damage. With the decreased air density at high altitude, the damage given to targets from the blast effect is not usually great unless the target take a direct hit, being penetrated.

Pellet warheads are similar to Blast-fragmentation, but with the exception of the fragments being actually small bomblets that burn or explode when contact or penetration occurs on the target. As in the previous case, the induced damage in high altitudes from blast effects is not very effective because of the decreasing air density, unless the missile actually penetrates and explode inside the target. It's necessary to note that fragments tend to spread out from the explosion, losing killing power as miss distance increases. Explosive or incendiary pellets minimize this effect since a single hit can do more damage.

The expanding-rod warhead is more likely to cut through control cables, hydraulic and fuel lines and structural members than individual fragments. However, these rods often separate early in the explosion, leaving large gaps in the warhead coverage. [7] [16]

1.2.1.4. Missile Guidance Systems

Missile-target dynamics are highly nonlinear. This is due to the fact that the equations of motion are best described in an inertial coordinated system and the aerodynamic moments and forces are represented in the missile and target body axis system, as shown in figure 1.9.

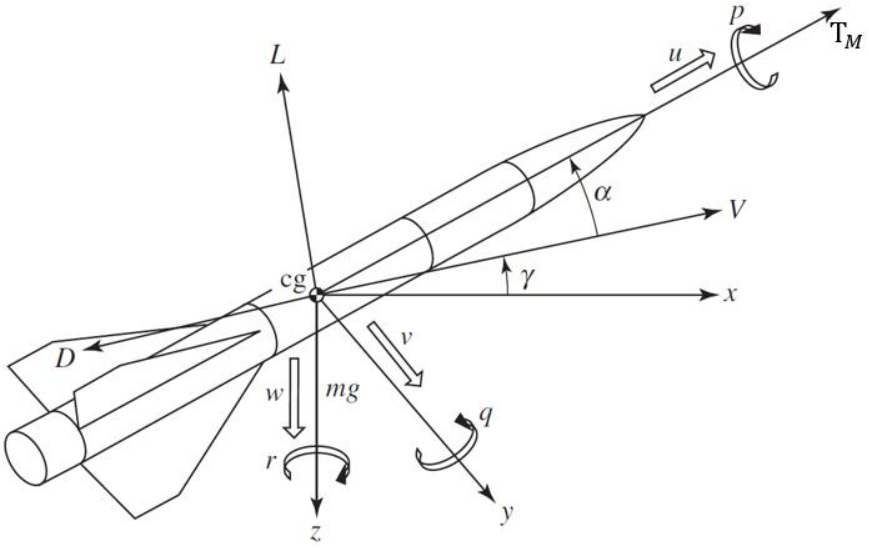

Figure 1.9. Forces and Moments represented in missile body axis system [16]

Four basic guidance concepts will be discussed: homing guidance system, which guides the interceptor to the target using a target seeker and an on-board computer (it can be passive, semi-active and active); command guidance, which relies on missile guidance commands calculated at the ground launching site and transmitted to the missile; inertial guidance, used mostly in ballistic missiles; position-fixing guidance, having as examples the TERCOM and GPS. One should also take into account that IR and RH devices are also employed in guidance systems for many AIMs. [14] [15] [16]

Various flight paths or trajectories may be deployed for fixed targets but for moving targets special requirements must be made. In figure 1.10, it is possible to observe some of the various missile types by their guidance methods that can be found nowadays. Despite all these methods, this dissertation will only approach the most fundamental ones and also most commonly used.

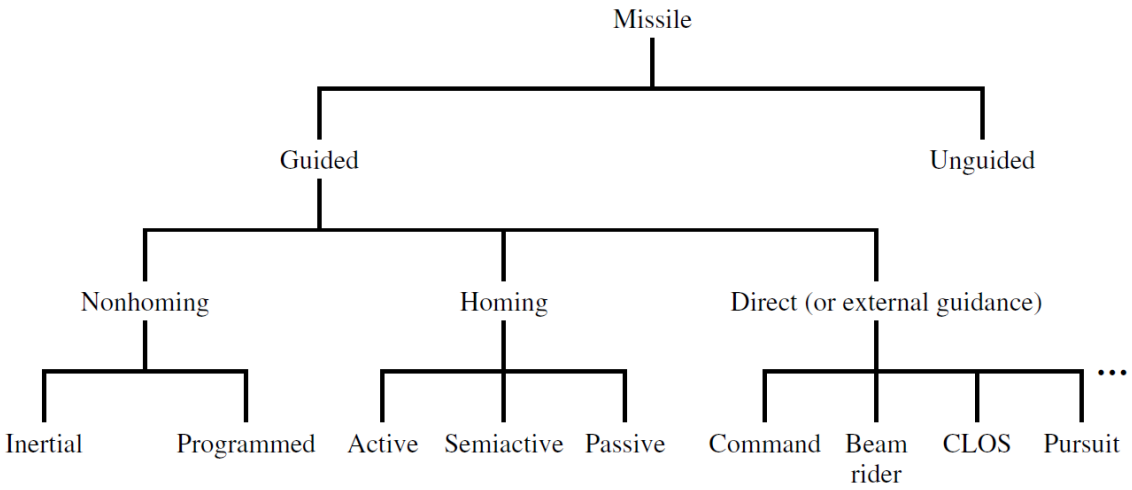

Figure 1.10. Different type of missile classification [16]

Homing Guidance

Homing guidance describes a process that can determine the position or position parameters of the target with respect to the pursuer, formulating its own commands to guide itself to the target. In other words, homing guidance is a specialized form of guidance, consisting in selecting, identifying and following a target through some distinguishing characteristic of it (for example heat, sound or reflection of radar waves), providing interception accuracy that is unsurpassed by any other form of missile guidance. This method can be used during the terminal phase of the missile or during the entire flight in some cases (particularly for short-range missiles) and it may be classified as active, semi active or passive, as shown in figure 1.11.

Passive homing systems (passive seekers) are design to detect the target by means of natural emanations or radiation such as heat, light and sound waves, which means that they don't illuminate the threat but, on the contrary, receive energy that emanates from the target. Passive seekers measure the angular direction of the target relative to the missile, but they can't provide closing velocity (range-rate) or range-to-target information, which can be a very

big disadvantage for some guidance techniques that require target range and/or range-rate information in addition to azimuth and elevation angles. The advantage is that because they don't emit energy, passive seekers make impossible for the target to determine whether it is being tracked. The typical seekers of passive homing system are IR, TV, UV, MMW and sound.

A semi active homing system illuminate (or designate) the target by directing a beam of light, LASER, IR or RF energy at it. The illuminating beam is transmitted from the launch platform or from another location and, therefore, the illuminating source is largely responsible for target selection. One of the biggest advantages of this type of guidance is that significantly increased power can be brought to bear on the target without adding weight or size to the missile. [9] [16]

In an active homing system, the target is illuminated and tracked by equipment on board the missile itself. Depending on modality and implementation, it can provide missile-target range and range rate in addition to the angular direction of the target. In other words, the missile carries the source of radiation on board in addition to the radiation sensor, having the advantage of launch-and-leave or fire-and-forget (allows the crew just to fire the missile without any further operations). However, power and weight considerations usually restrict active homing to be used only during the terminal phase of guidance, after some other form of guidance bringing the missile to within a short distance to the threat. [10] [18]

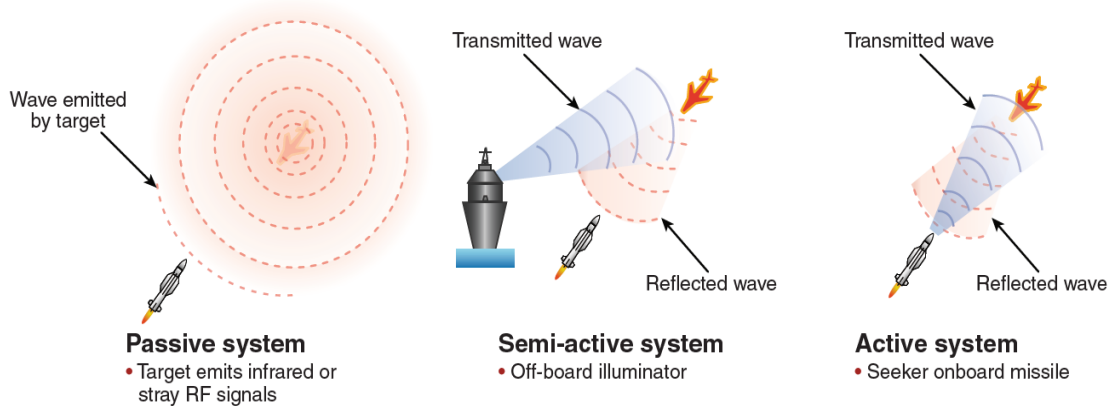

Figure 1.11. Three Basic Types of Missile Seeker Systems [10]

Command Guidance

Missiles where guidance instructions or commands come from external sources, are designated as Command guided missiles. A tracking system that is separated from the missile is used to track both the missile and the target, not being required a missile seeker.

The tracking system may consist in two different tracking units (one for the missile and one for the target) or it may consist in only one tracking unit that tracks both vehicles, which can be achieved using a radar, LASER, optical or IR systems. Target and missile ranges, elevations and bearings are analysed by a computer that uses the position and position rating and determines the flight path that the interceptor should take to a collision with the target occurs. In other

words, a computer at the launch platform determines if the interceptor is on the correct trajectory and if it's not, steering commands are generated by the computer on the platform and transmitted to the missile's own computer, where the computed flight path will be compared with the predicted flight path, and from this point on determining the correct signals required to move the missile control surfaces to change the path.

In command guidance, the launch point commands the missile all the way to the target, being most effective when applied on short-range missile systems because of the relatively large tracking errors that occur at long range. This method has associated disadvantages: as the external energy source must illuminate the target with a high data rate to make guidance effective, it will alert the target of the illuminating radar's presence and operation, causing evasive actions. [10] [17]

This tracking system is outlined in figure 1.12 A. and the Beam rider that is approached on the following sub chapter is outlined in figure 1.12 B.

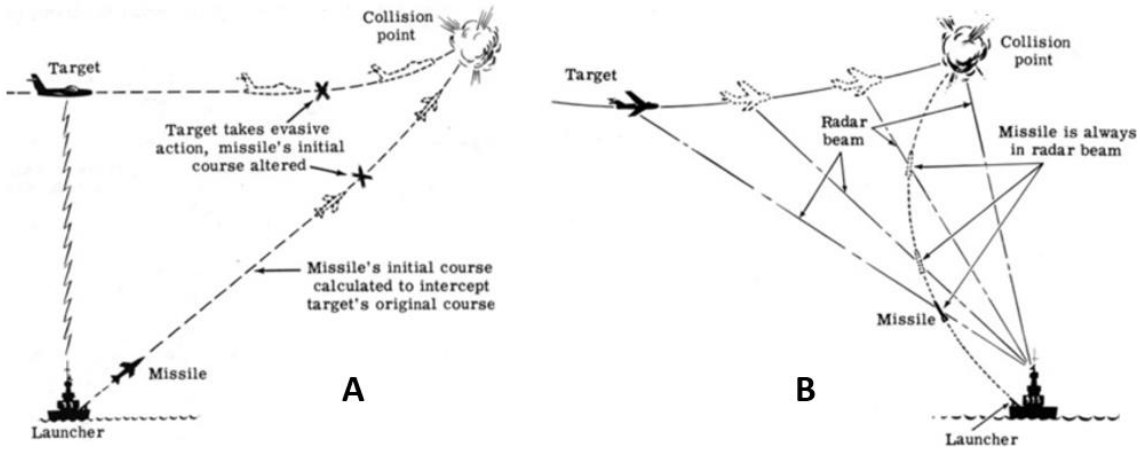

Figure 1.12. A. Command Guidance; B. Beam-Rider Guidance [17]

Beam Rider

In this type of guidance, the target is tracked by means of an electromagnetic beam, which may be transmitted by a ground radar or a LASER tracking system (for example a LADAR).

In order to follow the beam, the missile needs to have a rearward-facing antenna as on-board equipment that, through the modulation of the properties of the beam, computes steering signals that are a function of missile's position with respect to the centre of the target-tracking beam and sent to the control surfaces. [1] [10]

These correction signals keep the missile as nearly as possible in the centre of the target-tracking beam and for this reason, the interceptor is said to ride the beam. As long as the launch point continues to track the target, and the missile continues to ride the radar beam, the missile will intercept the target, having the advantage of allowing the launch of a large number of missiles into the same control or target-tracking beam. However, the tracking beam needs to be reasonably narrow to ensure a successful interception, decreasing the chance of

the missile to lose the track of the target (especially if the target is able to take evasive manoeuvres), restricting the use of this method to short-range missiles. [17] [18] [19]

Velocity Pursuit

Velocity pursuit guidance is based on the conceptual idea that a missile is always headed for the target current position. Provided that the missile's velocity is always greater than the target's, this strategy will result in an intercept. This method is usually implemented in LASER guided projectiles, where a simple seeker is set up on a vane (allowing to automatically align with the missile's velocity vector relatively to the wind), it's possible to obtain the required information for velocity pursuit. [19]

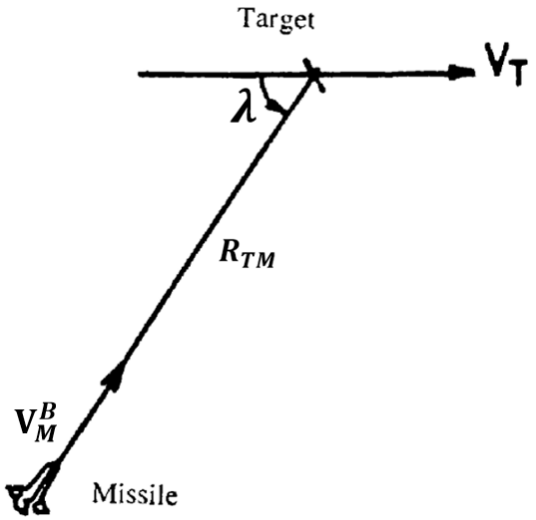

Figure 1.13. Velocity Pursuit Kinematics [20]

Using a target fixed polar coordinated system, as shown in figure 1.13, it's possible to write the equation that describes the distance between the missile and the target:

$$R_{TM} = R_{TM_0} * \frac{(1 + cos\,\lambda_0)^{\frac{V_M^B}{V_T}}}{(sin\,\lambda_0)^{\frac{V_M^B}{V_T}}} * \frac{(sin\,\lambda_0)^{\frac{V_M^B}{V_T}-1}}{(1 + cos\,\lambda_0)^{\frac{V_M^B}{V_T}}} \quad (1.1)$$

where the interception occurs at either $\lambda = 0$ or $\lambda = \pi$, that is, tail-chase or head-on, respectively. However, the only feasible case is the tail-chase interception because head-on has been proven instable.

It's also necessary to take into consideration that velocity pursuit guidance law results in a high demanded lateral acceleration (infinite at the final phase of the interception in some cases), causing the missile to miss the target. Besides that, this method is also sensible to target

velocity and disturbances like the wind, making the velocity pursuit not suitable for meter precision. [9] [20].

Proportional Navigation

Proportional Navigation (also known as Collision Homing) consists in the fact that the missile keeps a constant bearing to the target at all time, resulting in an eventual impact.
From figure 1.14, a typical two-dimensional missile-target engagement geometry for this law is presented: [5] [9]

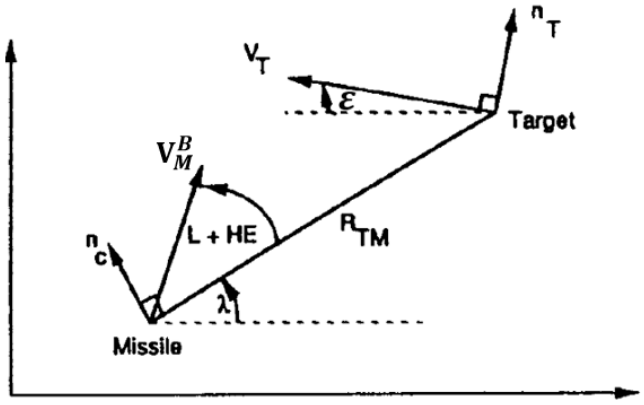

Figure 1.14. Proportional Navigation [22]

The missile measures the rotation of the LOS and turns at a rate proportional to it, being this law expressed as:

$$n_C = N' * V_C * \dot{\lambda} \quad (1.2)$$

where N′ is the constant of proportionality between the turn rate and LOS rate (the missile trajectory is heavily influenced by its navigation constant), and it should be between 3 and 4 to ensure good dynamic performance (a value of N′ greater than 2 is required for the missile to intercept manoeuvring targets). [16] [20]
This formulation requires an estimate or a measurement of the closing velocity (V_C), where if the missile uses active radar homing, a measurement of the closing velocity can be obtained using Doppler technology or in other cases, it can estimate the closing velocity from the geometry of the engagement and the altitude of the target. [21] [22]

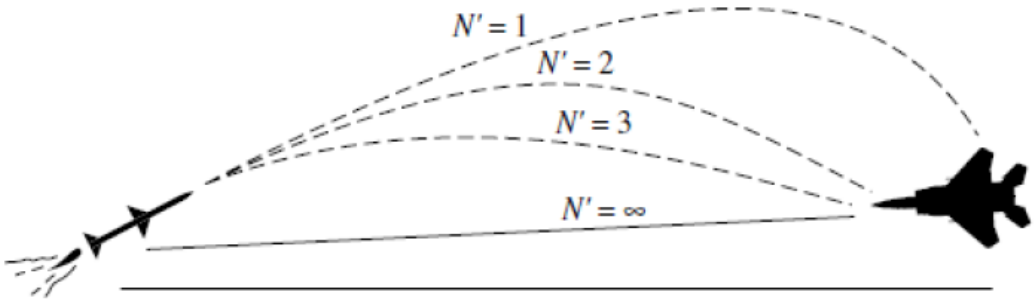

Figure 1.15. N′ Effecting various missile flight [20]

This sub-chapter regarding Proportional Navigation will be further analysed in chapter 2.

Pure Pursuit, Deviated Pursuit and Lead Pursuit

In the pure pursuit trajectory, the interceptor flies directly towards the target at all times, making the missile to constantly turning during the engagement (the heading of the missile is constantly maintained along the LOS between the missile and the target).

As a Homing Guidance law, the pursuit is considered impractical against moving targets, because during the pursuit course, the missile usually ends up in a tail-chase situation, making the manoeuvres required of the missile increasingly hard during the critical stage of the flight. Besides that, missile's speed must be considerably greater than the target, and at the end of the flight, the missile must overtake the target because the sharpest curvature of the missile flight occurs during this stage.

If the target tries to evade, the last-minute angular acceleration requirements of the persecutor could exceed the aerodynamic capability, causing a large miss distance. Also, because the motor thrust only lasts for a short period of the flight, in the last stage of flight it starts to slow down, making this guidance law only favourable to intercept slow-moving aircrafts (for example bombers), or head on towards an incoming aircraft.

Deviated pursuit is very similar to pure pursuit, except that the missile heading leads the LOS by a fixed angle (note that when the fixed lead angle is zero, deviated pursuit becomes pure pursuit). This method is not applicable in any missile but random errors and unwanted bias line often result in a deviated pursuit course. Lead Pursuit course is flown by an interceptor directing its velocity vector at an angle from the target so that projectiles launched from any point of the course will impact on the target. [16] [23]

Figure 1.16 shows the three different methods previously explained:

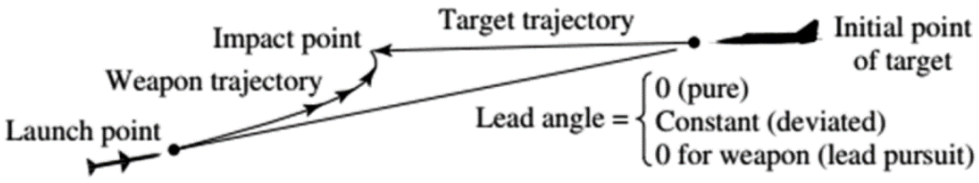

Figure 1.16. Pursuit: pure pursuit/deviated pursuit/lead pursuit [23]

1.3. Objective

All guidance laws are subjects to errors associated with the law itself, and for this reason, it's impossible to have a 100% flawless law. For example, in the case of the velocity pursuit, as previously mentioned, it results in high demand of lateral acceleration, in most cases infinite at the final phase of the interception, being also very sensitive to target velocity or even the wind, resulting in a finite miss distance. Another example is the proportional navigation, where most of the time the constant of proportionality N' is not a constant, because of the manoeuvrability of the target, which causes errors in the guidance law.

Besides those, one of the most used guidance law, the LQR method is also subject to errors (uncertainties), that can't be predicted and will cause instability to the controller.

Taking into account all the motivating factors previously discussed, the research carried out in this dissertation has as main objective the implementation of a H_∞/LTR controller in a SAM and AAM. For the approval of this method, the performance trajectories shall be compared to a Robust LQR controller using the Artstein Method.

1.4. Structure

In order to ensure a good understanding of this dissertation, it's divided into several chapters.

Chapter 1 approaches the introduction of the issue in question, where it begins with the arguments that constitute the motivation, as well as the bibliographic review in which an approach to the control and guidance of missiles is made. The dissertation objectives are also presented in this chapter.

Chapter 2 describes the modulation of pursuit, where missile dynamics and kinematics equations are presented, as well as a deeper approach to the Proportional Navigation Method.

Chapter 3 refers to the optimal guidance of the two study cases in this dissertation, which are the SAM and AAM. Besides that, it also contains the principles of the H_∞ Control Problem and Linear Quadratic Regulator (LQR), as well as the Artstein Method.

Chapter 4 refers to the simulation and results of the missile intersection for two different analysis. The first one, being referred in sub-chapter 4.1, corresponds to a non-manoeuvring target, where the missile is launched from two different locations, to prove that the program works for different data, as well as to show that H_∞/LTR controller is more efficient than the Robust LQR. On sub-chapter 4.2, the same target is applied but with evasive manoeuvres. Two different evasive routes after missile detection are analysed, being those generated randomly by the program, being the detection time also subjected to analysis.

Chapter 5 contains the conclusion of the results obtained on chapter 4, as well as future works to complement this dissertation.

Finally, the appendix A contains the Butcher Method, required in the simulation and appendix B contains the Article submitted to the International Review of Aerospace Engineering (IREASE).

Chapter 2

Missile Guidance and Flight Dynamics

In this chapter, only the missile in a three-dimensional-plane will be discussed, because from this, it's possible to deduce the respective equations of the pitch plane (two-dimensional plane). Note that missile equations of motion are written in the body-axes coordinate frame, the vehicle aerodynamics are nonlinear, a spherical Earth rotating at a constant angular velocity is assumed, the winds are defined with respect to the Earth and the gradients of the low-frequency winds are small enough to be neglected. [16]

To understand the concept of Modulation of Pursuit, figure 2.1 shows a rotational dynamics of a rigid body, where three different methods are integrated into computational sequence:

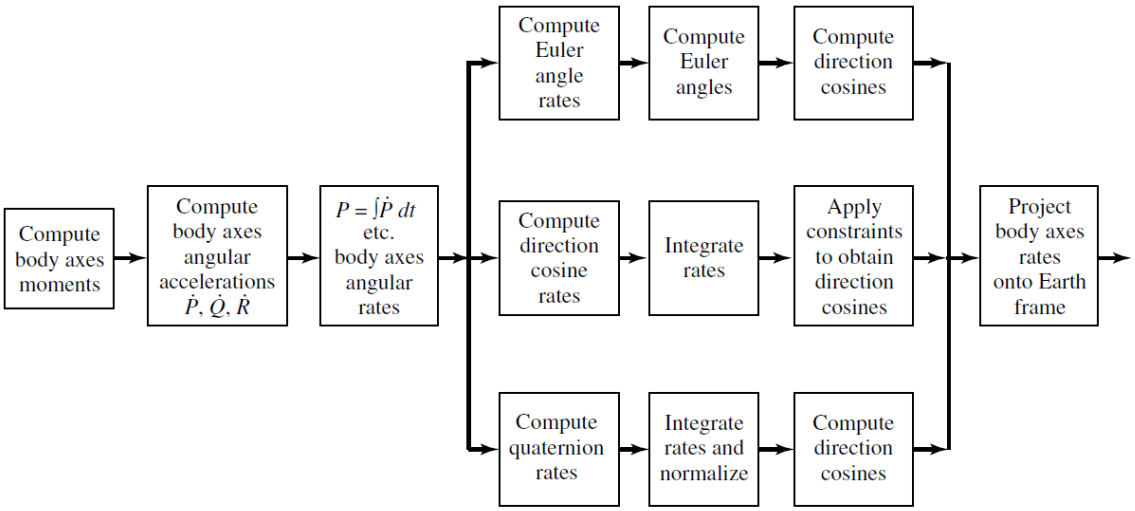

Figure 2.1. Rotational dynamics of rigid body [16]

Six simultaneous nonlinear equations of motion, with six variables (*u*, *v*, *w*, p, q and r) completely describe the behaviour of a rigid body (in this case a missile). These equations can be solved with a digital computer using numerical integration techniques, where an analytical solution of sufficient accuracy may be obtained by linearizing these equations (note that these equations are also called as Euler's equations).

2.1. Traditional body coordinate frame, Missile Coordinate frame and Moment Reference Point Coordinate Frame

2.1.1. Static Coefficient Model

In this sub-chapter, it will be discussed the flight equations (forces, moments, lateral acceleration, among others), as well as the modulation of the guidance problem. Therefore, figure 2.2 shows the static coefficients applied to a missile coordinate frame with origin at the moment reference point for missile aerodynamics on the missile centreline (MRP), being the X-axis forward along the missile centreline, and the X-Z plane oriented to contain the wind-relative velocity vector and also the static coefficients applied on the MRP coordinate frame (body-fixed), with origin at the MRP and with all the axes parallel to those of the traditional body coordinate frame (body-fixed), with origin at the missile CG. That is, X-axis forward, Y-axis starboard and Z-axis completing the right-handed system.

Note that green coordinates stands for the missile frame (represented by an "m") and red coordinates stands for the MRP frame (represented by a "p").Also, the equations shown below represented with a "b" are relative to the traditional body coordinate frame with origin at the missile centre-of-mass (this last case isn't represented in figure 2.1). [37]

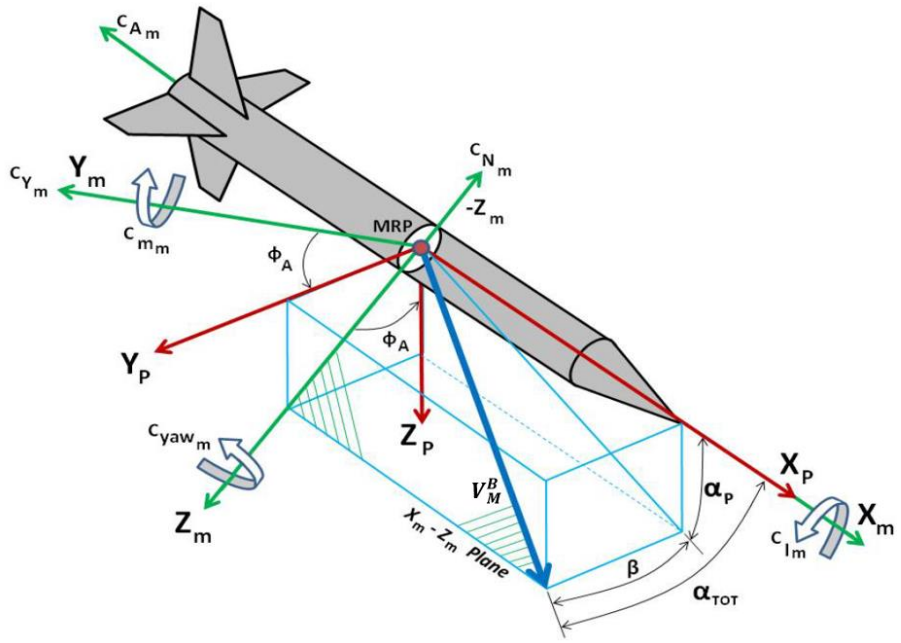

Figure 2.2. Static coefficients applied on a missile [37]

As it can be seen from the above figure, V_M^B has been translated from the missile centre-of-mass to the MRP and Y_m is pointed in the direction of V_M^B x $\hat{\imath}$ ($\hat{\imath}$ is a unit vector along the X_m), what means that V_M^B remains in the plane $X_m - Z_m$ regardless of the roll position of the missile. Beside those, α_{tot} is also measured in the plane $X_m - Z_m$ and has a range of 0^o to $+180^o$,

C_{Am} and C_{Nm} are positive in a direction opposite to that of the X-axis and Z-axis, respectively, C_{lm}, C_{mm} and C_{yawm} are positive by the right-hand rule, C_{Am} , C_{Nm} and C_{mm} are the longitudinal coefficients (also called the pitch plane coefficients), C_{Ym} , C_{lm} and C_{yawm} are the lateral-directional coefficients and can be set as zero in the missile coordinate frame with origin in the MRP for a missile that is axisymmetric about the centreline (because that the plane $X_m - Z_m$ is a plane of symmetry containing the V_M^B vector). Note that static coefficients for a missile are, in general, a function of α_{tot}, ϕ_A (as a range of -180^o to $+180^o$) and Mach number (note that for a missile axisymmetric about it centreline, the static coefficients in missile frame are only a function of α_{tot} and Mach number, because aerodynamic properties don't change with ϕ_A). The equations which represent each of the variables discussed previously are: [37]

$$\alpha_{tot} = arccos(\frac{u}{V_M^B}) \qquad (2.1)$$

$$\phi_A = arctg(\frac{v}{w}) \qquad (2.2)$$

$$MACH = \frac{V_M^B}{V_{sound}} \qquad (2.3)$$

From the above equations, u, v and w are components of V_M^B in the traditional body coordinate frame with origin at the missile centre-of-mass, translated to the MRP. It is imperative to understand that there are singularities in the equation (2.2) at $\alpha_{tot} = 0^o$ and $\alpha_{tot} = 180^o$, and these must be handled by specifying a value of ϕ_A(for example zero). [37]

2.1.2. Aerodynamic Damping Model

Missile aerodynamics damping model is based on traditional damping derivatives that are dimensionless and are used to calculate aerodynamic moments caused by angular rates of the missile, and they should be developed at the missile centre-of-mass rather than at the MRP. The damping derivatives should also be developed in a coordinate frame parallel to the missile frame, to properly separate the missile frame pitch and yaw damping effects. These derivatives correspond to C_{lpm}, $C_{mqm}$and C_{yawrm} for roll, pitch and yaw, respectively and they are all positive in the missile frame by the right-hand rule, being represented as: [37]

$$C_{lpm} = \frac{\partial C_{lm}}{\partial(\frac{p_m D_{ref}}{2V_M^B})} \qquad (2.4\ a)$$

$$C_{mqm} = \frac{\partial C_{mm}}{\partial(\frac{q_m D_{ref}}{2V_M^B})} \quad (2.4\text{ b})$$

$$C_{yawrm} = \frac{\partial C_{yawm}}{\partial(\frac{r_m D_{ref}}{2V_M^B})} \quad (2.4\text{ c})$$

These damping derivatives use missile frame angular rates (p_m, q_m and r_m) that are obtained by transforming the body rates from the traditional body coordinate frame with origin at the missile centre-of-mass to the missile coordinate frame with origin at the MRP by a negative rotation about the centreline ($-\phi_A$). At $\alpha_{tot} = 0^o$ and $\alpha_{tot} = 180^o$, the pitch damping derivative for the missile is assumed to be equal to the yaw damping derivative (the missile shape approximates to a vehicle that is axisymmetric about the longitudinal axis) and the yaw damping derivative at $\alpha_{tot} = 90^o$ is assumed to be much less than the corresponding pitch damping derivative (there is a difference between the orientation of the pitch and yaw axes regarding V_M^B).

If aerodynamic uncertainties are to be modelled in a simulation, in equations (2.4 a), (2.4 b) and (2.4 c) the dispersions should be applied, converting those in dimensionless damping moment coefficients, by assuming a linear relationship between coefficients and regular rates. Therefore, the following equations are obtained: [37]

$$C_{lmd} = \frac{p_m D_{ref}}{2V_M^B} C_{lpm} \quad (2.5\text{ a})$$

$$C_{mmd} = \frac{q_m D_{ref}}{2V_M^B} C_{mqm} \quad (2.5\text{ b})$$

$$C_{yawmd} = \frac{r_m D_{ref}}{2V_M^B} C_{yawrm} \quad (2.5\text{ c})$$

and they can be interpreted as the changes in the rolling, pitching and yawing moment coefficients caused by damping.

2.1.3. Aerodynamic Forces and Moments

For the missile coordinate frame with origin at the MRP, the vector equations for the aerodynamics forces and moments are, respectively:

$$\overrightarrow{F_m} = \begin{pmatrix} F_{Xm} \\ F_{Ym} \\ F_{Zm} \end{pmatrix} = \bar{Q}\, S_{ref} \begin{pmatrix} -C_{Am} \\ C_{Ym} \\ -C_{Nm} \end{pmatrix} \quad (2.6)$$

$$\overrightarrow{M_m} = \begin{pmatrix} M_{Xm} \\ M_{Ym} \\ M_{Zm} \end{pmatrix} = \bar{Q}\, S_{ref} D_{ref} \begin{pmatrix} C_{lm} + C_{lmd} \\ C_{mm} + C_{mmd} \\ C_{yawm} + C_{yawmd} \end{pmatrix} \quad (2.7)$$

Note that equations (2.6) and (2.7) must be transformed from the missile coordinate frame with origin at the MRP to the MRP coordinate frame with origin at the MRP by rotating about the centreline through ϕ_A, obtaining the following equations:

$$\overrightarrow{F_p} = \begin{pmatrix} F_{Xp} \\ F_{Yp} \\ F_{Zp} \end{pmatrix} = \begin{pmatrix} 1 & 0 & 0 \\ 0 & \cos(\phi_A) & \sin(\phi_A) \\ 0 & -\sin(\phi_A) & \cos(\phi_A) \end{pmatrix} \begin{pmatrix} F_{Xm} \\ F_{Ym} \\ F_{Zm} \end{pmatrix} \quad (2.8)$$

$$\overrightarrow{M_p} = \begin{pmatrix} M_{Xp} \\ M_{Yp} \\ M_{Zp} \end{pmatrix} = \begin{pmatrix} 1 & 0 & 0 \\ 0 & \cos(\phi_A) & \sin(\phi_A) \\ 0 & -\sin(\phi_A) & \cos(\phi_A) \end{pmatrix} \begin{pmatrix} M_{Xm} \\ M_{Ym} \\ M_{Zm} \end{pmatrix} \quad (2.9)$$

Finally, the aerodynamic forces and moments for the traditional body coordinate frame with origin at the missile centre-of-mass will be:

$$\overrightarrow{F_b} = \begin{pmatrix} F_{Xb} \\ F_{Yb} \\ F_{Zb} \end{pmatrix} = \begin{pmatrix} F_{Xp} \\ F_{Yp} \\ F_{Zp} \end{pmatrix} \quad (2.10)$$

$$\overrightarrow{M_b} = \begin{pmatrix} M_{Xb} \\ M_{Yb} \\ M_{Zb} \end{pmatrix} = \begin{pmatrix} M_{Xp} \\ M_{Yp} \\ M_{Zp} \end{pmatrix} + \begin{pmatrix} MRP_{Xb} \\ MRP_{Yb} \\ MRP_{Zb} \end{pmatrix} \times \begin{pmatrix} F_{Xp} \\ F_{Yp} \\ F_{Zp} \end{pmatrix} \quad (2.11)$$

Carrying the cross product in equation (2.11), $\overrightarrow{M_b}$ can be written as:

$$M_{Xb} = M_{Xp} + MRP_{Yb}F_{Zp} - MRP_{Zb}F_{Yp} \quad (2.12\ a)$$

$$M_{Yb} = M_{Yp} + MRP_{Zb}F_{Xp} - MRP_{Xb}F_{Zp} \quad (2.12\ b)$$

$$M_{Zb} = M_{Zp} + MRP_{Xb}F_{Yp} - MRP_{Yb}F_{Xp} \quad (2.12\ c)$$

2.2. Velocity Equations (or Forces) and Manoeuvre Rates (or Moments) for short period

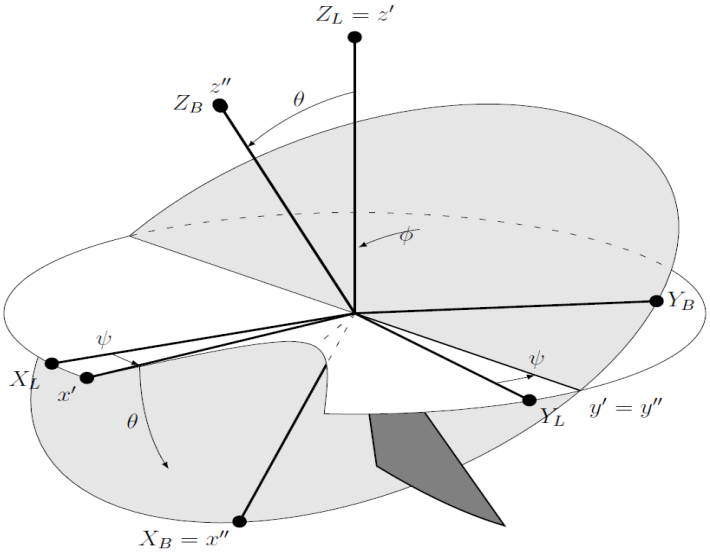

Figure 2.3 Definition of the Euler Angles on a Missile [38]

To fully understand the dynamics and kinematics present in a missile, first it's necessary to comprehend the Euler angles and the quaternions. Both will be explained with basis in figure 2.3, which represents the definition of the Euler angles for missiles.

Starting by defining the missile velocity (as explained in sub-chapter 2.1.1) and the angular velocity, respectively:

$$V_M^B = [u \quad v \quad w]^T \qquad (2.13\ a)$$

$$\omega_M^B = [p \quad q \quad r]^T \qquad (2.13\ b)$$

Euler angles define the axes transformation matrix $MX_BY_BZ_B$ of the inertial reference $MX_LY_LZ_L$, and they can written as:

$$S_{BL} = \begin{bmatrix} cos(\theta)\,cos(\psi) & cos(\theta)\,sin(\psi) & -sin(\theta) \\ sin(\phi)\,sin(\theta)\,cos(\psi) - cos(\phi)\,sin(\psi) & sin(\phi)\,sin(\theta)\,sin(\psi) + cos(\phi)\,cos(\psi) & sin(\phi)\,cos(\theta) \\ cos(\phi)\,sin(\theta)\,cos(\psi) + sin(\phi)\,sin(\psi) & cos(\phi)\,sin(\theta)\,sin(\psi) - sin(\phi)\,cos(\psi) & cos(\phi)\,cos(\theta) \end{bmatrix} \qquad (2.14)$$

However, when the value of θ is too big, it's preferable to use the quaternions approximation for missiles, and the equation is given by:

$$S_{BL} = \begin{bmatrix} q_0^2 + q_1^2 - q_2^2 - q_3^2 & 2(q_1q_2 + q_0q_3) & 2(q_1q_3 - q_0q_2) \\ 2(q_1q_2 - q_0q_3) & q_0^2 - q_1^2 + q_2^2 - q_3^2 & 2(q_2q_3 - q_0q_1) \\ 2(q_1q_3 + q_0q_2) & 2(q_2q_3 + q_0q_1) & q_0^2 - q_1^2 - q_2^2 + q_3^2 \end{bmatrix} \qquad (2.15)$$

Therefore, it's possible to relate the Euler angles with quaternions, using the equations (2.14) and (2.15), obtaining:

$$tan(\psi) = \frac{2(q_1 q_2 + q_0 q_3)}{(q_0^2 + q_1^2 - q_2^2 - q_3^2)} \qquad (2.16\ a)$$

$$tan(\phi) = \frac{2(q_2 q_3 + q_0 q_1)}{(q_0^2 - q_1^2 - q_2^2 + q_3^2)} \qquad (2.16\ b)$$

$$sin(\theta) = -2(q_1 q_3 - q_0 q_2) \qquad (2.16\ c)$$

Now, note that the rotation kinematics equation is obtained through the derivative of the quaternions in time, as shown on the following equation:

$$\begin{bmatrix} \dot{q_0} \\ \dot{q}_1 \\ \dot{q}_2 \\ \dot{q}_3 \end{bmatrix} = \frac{1}{2} \begin{bmatrix} 0 & -p & -q & -r \\ p & 0 & r & -q \\ q & -r & 0 & p \\ r & q & -p & 0 \end{bmatrix} \begin{bmatrix} q_0 \\ q_1 \\ q_2 \\ q_3 \end{bmatrix} \qquad (2.17)$$

The dynamic translation equation (with flat earth approach) is defined using the Newton's law:

$$m \frac{\partial V_M^B}{\partial t} + m \cdot \Omega_M^B V_M^B = F^B + m S_{BL} \cdot g^L \qquad (2.18)$$

where m is the missile mass and Ω_M^B is the symmetrical oblique tensioner of ω_M^B, being its equation given by:

$$\Omega_M^B = \begin{bmatrix} 0 & -r & q \\ r & 0 & -p \\ -q & p & 0 \end{bmatrix} \qquad (2.19)$$

Aerodynamic forces applied on the missile are represented as:

$$\begin{bmatrix} F_A \\ F_S \\ F_N \end{bmatrix} = \bar{Q} S_{ref} D_{ref} \begin{bmatrix} C_A \\ C_S \\ C_N \end{bmatrix} \qquad (2.20)$$

Note that the only moments being applied on the missile are the aerodynamics moments, (without considering the damping moments caused by the missile jet), and they may be written as:

$$M^B = \begin{bmatrix} L_{cm} \\ M_{cm} \\ N_{cm} \end{bmatrix} = \bar{Q} S_{ref} D_{ref} \begin{bmatrix} C_l \\ C_m + \bar{s}(t) \cdot C_N \\ C_n - \bar{s}(t) \cdot C_S \end{bmatrix} \qquad (2.21)$$

with $\bar{s}(t) = \bar{d}_{cm}(t) - \bar{d}_{mrc}$. When $\bar{s}(t) \neq 0$, there is coupling between the aerodynamic forces and moments. During the final stage of a missile, autopilot is responsible to control the missile acceleration and therefore, in the development of the autopilot, normally the system engineers only consider the dynamic of short period with a constant missile velocity.

To obtaining the translation equation, note that missile velocity V_M^B can be written as [38]:

$$V_M^B = \sqrt{u^2 + v^2 + w^2} \quad (2.22)$$

and the angle of attack and yaw angle are, respectively:

$$\alpha = arctg\left(\frac{w}{u}\right) \quad (2.23\text{ a})$$

$$\beta = arcsin\left(\frac{v}{V_M^B}\right) \quad (2.23\text{ b})$$

Therefore, from equations (2.22), (2.23 a) and (2.23 b), u, v and w become, respectively:

$$u = V_M^B \cos(\alpha)\cos(\beta) \quad (2.24\text{ a})$$

$$v = V_M^B \sin(\beta) \quad (2.24\text{ b})$$

$$w = V_M^B \sin(\alpha)\cos(\beta) \quad (2.24\text{ c})$$

and from the above equations (2.24 a), (2.24 b) and (2.24 c), the velocity equations are obtained:

$$\dot{u} = \dot{V}_M^B \cos(\alpha)\cos(\beta) - V_M^B \dot{\alpha}\sin(\alpha)\cos(\beta) - V_M^B \dot{\beta}\cos(\alpha)\sin(\beta) \quad (2.25\text{ a})$$

$$\dot{v} = \dot{V}_M^B \sin(\beta) + V_M^B \dot{\beta}\cos(\beta) \quad (2.25\text{ b})$$

$$\dot{w} = \dot{V}_M^B \sin(\alpha)\cos(\beta) + V_M^B \dot{\alpha}\cos(\alpha)\cos(\beta) - V_M^B \dot{\beta}\sin(\alpha)\sin(\beta) \quad (2.25\text{ c})$$

Now, if the Coriolis forces, due to the gas jet, are neglected and if the gravitational terms are despised, the angle of attack rate and yaw angle rate can also be obtained: [38]

$$\dot{\alpha} = \frac{\bar{Q}S_{ref}}{mV_M^B}\left(\frac{\sin(\alpha)}{cos(\beta)}C_A - \frac{\cos(\alpha)}{cos(\beta)}C_N\right) + q - pcos(\alpha)\tan(\beta) - \frac{\sin(\alpha)}{\cos(\beta)}\frac{\bar{Q}S_{ref}C_T}{mV_M^B} \quad (2.26)$$

$$\dot{\beta} = \frac{\bar{Q}S_{ref}}{mV_M^B}(\cos(\alpha)\sin(\beta)\,C_A - \cos(\beta)\,C_S + \sin(\alpha)\sin(\beta)C_N) + psin(\alpha) - rcos(\alpha) - \cos(\alpha)\sin(\beta)\frac{\bar{Q}S_{ref}C_T}{mV_M^B} \quad (2.27)$$

Finally, it's possible to obtain the equations:

$$\dot{p} = \frac{\bar{Q}S_{ref}d}{I_x^b}C_l \quad (2.28\text{ a})$$

$$\dot{q} = \frac{I_y^b - I_x^b}{I_y^b}pr + \frac{\bar{Q}S_{ref}d}{I_y^b}(C_m + \bar{s}\cdot C_N) \quad (2.28\text{ b})$$

$$\dot{r} = \frac{I_x^b - I_y^b}{I_y^b}pq + \frac{\bar{Q}S_{ref}d}{I_y^b}(C_n - \bar{s}\cdot C_S) \quad (2.28\text{ c})$$

2.3. Pursuit Modelling associated to Guidance (Proportional Navigation)

In the sub-chapter Missile Guidance Systems, a small introduction was made to the Proportional Navigation method. However, PN is, by far, the most important of the classical guidance laws and for that reason, it requires a deeper approach. A brief description of the several variants of the PN will also be made.

To fully understand the PN, first an approach to the parallel navigation is required, since the proportional navigation is a guidance law that implements it.

According to the Parallel Navigation, the direction of the LOS between the missile and the target is kept constant relative to inertial space, that is, the LOS is kept parallel to the initial LOS. For a 3D approach, this method can be stated as:

$$W = 0 \quad (2.29)$$

or:

$$\dot{\lambda} = 0 \quad (2.30)$$

where W is the rate of rotation of the LOS and λ is the angle that the LOS forms with the reference line on the said plane. For non-manoeuvring targets, parallel navigation can be defined as: [1] [5]

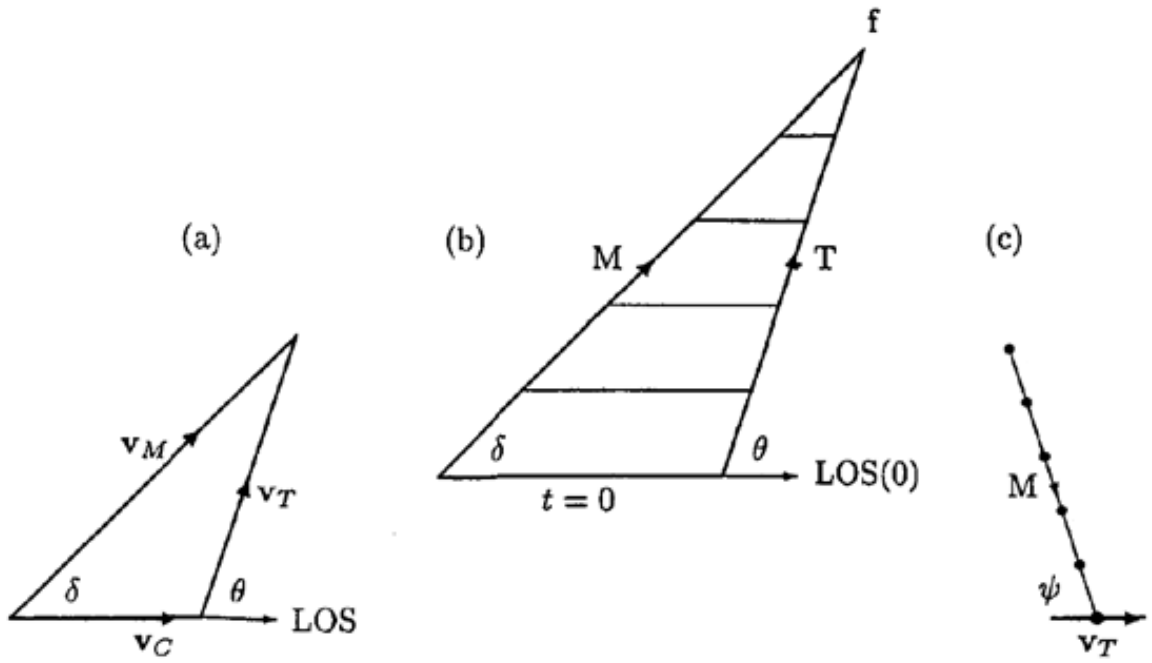

Figure 2.4. Parallel-navigation trajectories for nonmaneuvering targets: a) Velocity collision triangle; b) trajectories triangle; c) relative trajectory [1]

Note that if T (Target) has manoeuvrability, the approach of M (Missile) will no longer be a constant bearing line.

Now, going back to the PN method, since this implements parallel navigation, it will make W in the general case or $\dot{\lambda}$ in the planar case tend to zero, has shown in equations (2.29) and (2.30) and it can be represented by the following guidance loop schematic: [1] [5]

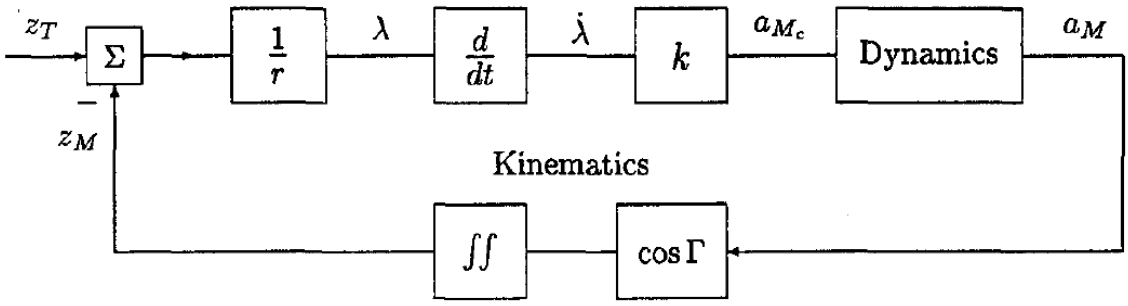

Figure 2.5. Proportional Navigation guidance loop in terms of missile acceleration [1]

where the guidance law for a 3D engagement can be given as:

$$\dot{a}_M = N * \mathrm{W} \qquad (2.31)$$

Over the years, PN has spawned an enormous variety of guidance laws that have attempted to improve the performance of the basic PN law, being called PN-variants. The structures of these

variants will be examined in the following sub-chapters, where figure 2.6 will portray the combination of those.

2.3.1. Pure Proportional Navigation (PPN)

According to the PPN law, missile lateral acceleration is given by:

$$a_M = N * \mathrm{W} * V_M \quad (2.32)$$

and is applied perpendicular to the velocity vector of the missile. If the missile's angle-of-attack is neglected, then LATAX is also in the natural direction of the lift force, which is generated by the missile's airframe and lifting surfaces whenever a manoeuvre is made (lift force is responsible for the LATAX) as shown in figure 2.6 a). However, the angle-of-attack is never zero and for many high manoeuvrable missiles, the values are quite high. [9] [20]

2.3.2. True Proportional Navigation (TPN)

For TPN, the relevant speed is the closing velocity and not the missile velocity itself, because it's the closing velocity that ultimately drives the LOS separation to zero. Note that the LOS rate also needs to tend to zero. Therefore, this method consists in applying the missile lateral acceleration perpendicular to the LOS and to the closing velocity as shown in figure 2.6 b). Besides this, missile velocity is not directly available unless the missile carries an inertial navigation unit while target velocity is easily available from the Doppler data of the seeker. The main problem relative to the implementation of this variant is that LATAX direction isn't a natural direction of the lifting forces generated by missile's airframe (which is ultimately responsible for lateral acceleration). However, the use of thrusters gives an additional longitudinal acceleration or deceleration that combined with the aerodynamic forces, generates the LATAX desired direction.
Note that if the missile is for exo-atmospheric interceptions, it requires the use of thrusters to generate lateral acceleration, because aerodynamic forces are non-existent. So, the use of TPN for these cases isn't a problem because it only adds a very little extra effort to deflect the force with these thrusters in the required direction.
The main difference between TPN and PPN is that missile lateral acceleration is applied perpendicular to the LOS for the first case and for the second one, LATAX is applied perpendicular to the missile velocity. [9] [20]
Therefore, TPN law can be given as:

$$a_M = N' * \mathrm{W} * V_C \quad (2.33)$$

2.3.3. Generalized True Proportional Navigation (GTPN)

GTPN is based on the fact that in the TPN law there is a certain freedom of choosing the lateral acceleration direction. So, Generalized True Proportional Navigation consists in making that a part of the guidance law and defining the LATAX direction as being deviated by some angle from the normal to the LOS, as shown in figure 2.6 c). [9] [20]

2.3.4. Ideal Proportional Navigation (IPN)

In this Proportional Navigation variant, missile lateral acceleration is applied perpendicular to the relative velocity between the missile and the target, as shown in figure 2.6 d). The performance of IPN is much superior to the PPN and TPN. However, it has a very difficult implementation, being the least interesting method to be applied on a missile. [9] [20]

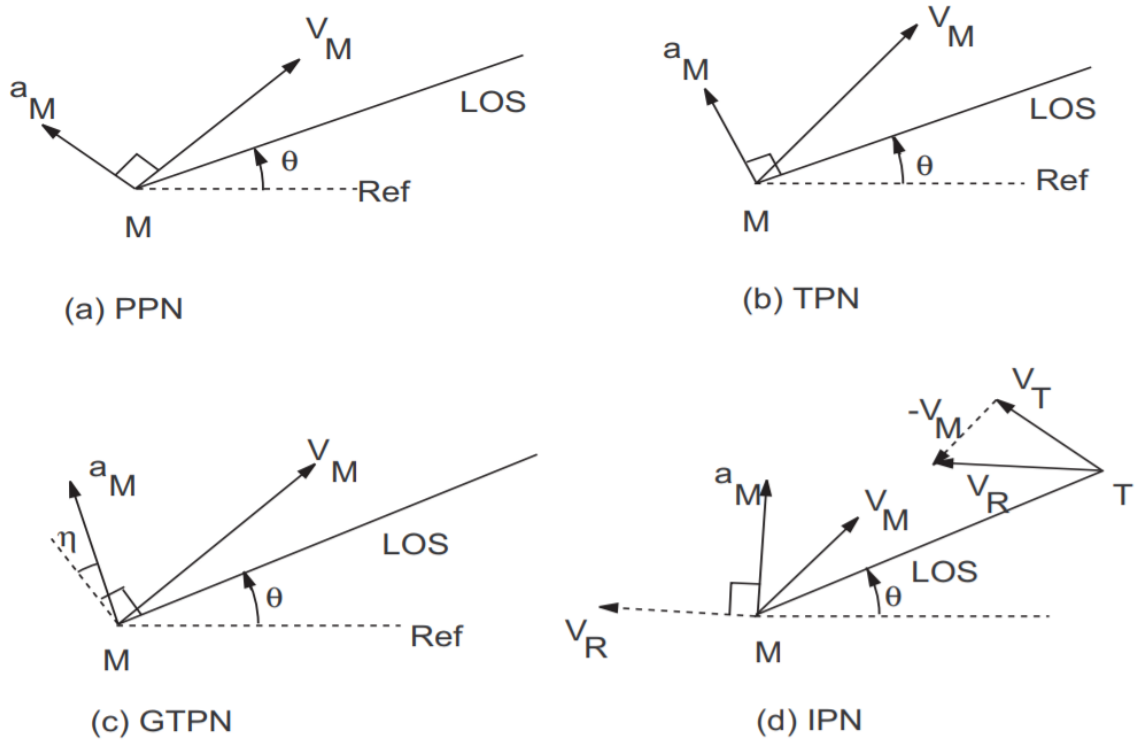

Figure 2.6. Proportional Navigation variants: a) Pure Proportional Navigation; b) True Proportional Navigation; c) Generalized True Proportional Navigation; d) Ideal Proportional Navigation [38]

A six degree of freedom simulation flight dynamics model is essential for the accurate prediction of short and long range trajectories of high and low spin-stabilized missiles. Therefore, a computational analysis must take into account the constant effects of the aerodynamic coefficients, as well as Mach number and variation of the angle of attack.

Moreover, the performance of low-cost guidance, navigation and control technologies (for example the measurement calibration or even the measurement time) must be compatible with the missile dynamic environment (high spin rate, short time of flight, among others) for a successful intersection occurs. [47] [48]

Chapter 3

Optimal Guidance of Air-to-Air Missiles and Surface-to-Air Missiles

3.1. Introduction to $\mathbf{H}_\infty$ and LQR methods

Although linear quadratic (H_2) optimal control was applied successfully during the 60's and the 70's (mainly to aerospace industry), it failed to explain address robustness.

The H_∞ control problem (and its connection to robustness) was introduced by George Zames in the late 70's, where he first presented the theory in the frequency domain and the computation of H_∞-optimal controllers were based on analytic function theory operator-theoretic methods. However, these methods were quite complicated and only gave a limited sight into the structure of the solutions.

The general state-space solution of the H_∞-optimal control problem was first given by Glover and Doyle and it revolutionized the practical numerical computation of the control, allowing to solve this method with approximately the same complexity as the standard linear quadratic control problem. Note that the Linear Quadratic Regulator (LQR) will be approached in sub-chapter 3.3 as a guidance problem.

The success of the optimal control method depends on the target/interceptor and missile acceleration requirements, which means that the optimal controller can be obtained from the corresponding Riccati differential equation. However, this approach only gives the optimal solution for non-manoeuvring targets. Moreover, a significant shortcoming of the optimal control approach is that all the states of the target/interceptor system are typically assumed to be precisely known. However, in all practical situations, only some states of the system are available for measurements and even those measurements are subject to noise and uncertainties (the precision missile guidance problem is an output feedback problem).

Another flaw of the optimal control theory is its lack of concern for the issue of robustness (especially in the design of feedback control systems). That is, the requirement that the control system will maintain an adequate level of performance in the face of significant Plant uncertainty (the Plant uncertainties may be due to variation on the Plant parameters and the effects on nonlinearities and unmodelled dynamics which have not been included in the Plant model). Indeed, the requirement for robustness is one of the main reasons for using feedback in control system design (note that robustness is extremely important in the precision missile guidance problem because of possible unknown target manoeuvres).

The use of H_∞ control methods has provided an important tool for the synthesis of robustly stable output feedback control systems and when this control theory is duly modified, it provides an effective framework for the precision missile guidance control, giving a much better performance than the LQR guidance law. [36] [39]

3.2. Target/Interceptor Kinematics Model 3D Approach

Most of the analytic studies in the past used a two-dimensional model for the kinematic studies of a missile. Whenever guidance and dynamics were considered, an oscillation of the optimal evasive manoeuvre became apparent, and for an optimal evasion approach, it was possible to guarantee a non-zero miss distance even from pursuers with unlimited manoeuvrability or from pursuers with optimal guidance strategies. However, the 2D approach is well known for its limitation to “head-on” or “tail-chase” engagements.

For a 3D linearized kinematic model, first it’s necessary to make the following assumptions: the pursuer and the evader are both considered as constant speed mass points; gravity can be neglected for both vehicles (note that the relative trajectory is not affected);Not only the missile but also the target both have perfect information on the relative state; the pursuer is a homing missile launched against an initial non-manoeuvring target in a collision course; the relative missile-target trajectory can be linearized around the initial line of sight; the pursuing missile has two identical and independent guidance channels to execute proportional navigation in two perpendicular directions in a plane normal to the LOS; the dynamics of each guidance channel is assumed to be of first order (note that is only to simplify the equations).

Based on the assumptions made, the control variable is the lateral acceleration vector of the evading target, where this acceleration is perpendicular to the velocity vector and its magnitude is bounded by the limit load factor and its direction is controlled by the missile roll-orientation. [40]

Therefore, the mathematical model of an unbounded missile manoeuvrability with an infinite missile roll-rate for a three-dimensional approach can be demonstrated as:

$$\dot{\vec{R}} = \vec{V}_T - \vec{V}_M \quad (3.1)$$

$$\vec{\Omega}_R = \frac{\vec{R}\mathrm{x}\dot{\vec{R}}}{\left|\vec{R}\right|^2} \quad [1] \quad (3.2)$$

[1] Vectorial Product or Cross Product for the equation (3.2): $\left|\vec{R}\mathrm{x}\dot{\vec{R}}\right| = \left|\vec{R}\right|\left|\dot{\vec{R}}\right|\sin\theta$, where θ is the angle between $\vec{R}$ and $\dot{\vec{R}}$ in the plane containing them [46]

where equation (3.1) represents the time derivative of the relative distance for a three-dimensional vector and the equation (3.2) represents the 3D vector of the angular velocity. Now, the acceleration command of the pursuing missile is given as:

$$(\dot{\vec{V}_M})_C = K_N \frac{(\vec{\Omega}_R \mathrm{x} \vec{R})}{|\vec{R}|} \quad (3.3)$$

and the actual acceleration is determined by:

$$\tau \ddot{\vec{V}_M} + \dot{\vec{V}_M} = (\dot{\vec{V}_M})_C \quad (3.4)$$

The acceleration of the constant speed evader is normal to its vector velocity, and it can be written as:

$$\dot{\vec{V}_T} = (\vec{\Omega}_T \mathrm{x} \vec{V}_T) \quad (3.5)$$

The final time of the pursuit is given by:

$$tf = \frac{|\vec{R_0}|}{V_R} \quad (3.6)$$

Therefore, the equation (3.3) can be reformulated as:

$$(\dot{\vec{V}_M})_C = \frac{N'}{(t_f - t)^2} \left[\vec{R}(t) + (t_f - t)\dot{\vec{R}}(t) \right] \quad (3.7)$$

The system of the differential equations (3.1), (3.4), (3.5) and the linearized feedback relation (3.7) determine the 9 components of the vectors $\vec{R}(t)$, $\vec{V}_T(t)$ and $\vec{V}_M$(t) if the initial conditions and the target angular velocity vector $\vec{\Omega}_T$(t) are given.

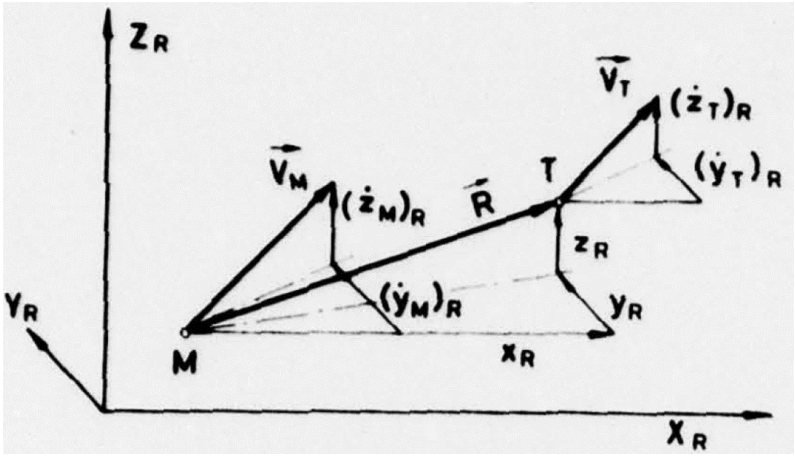

Figure 3.1. 3D Pursuit-Evasion Geometry [36]

From the above figure 3.1, a 3D evasion geometry during the persecution between the missile and the target is given.

3.3. Classic Linear Quadratic Regulator (LQR) method

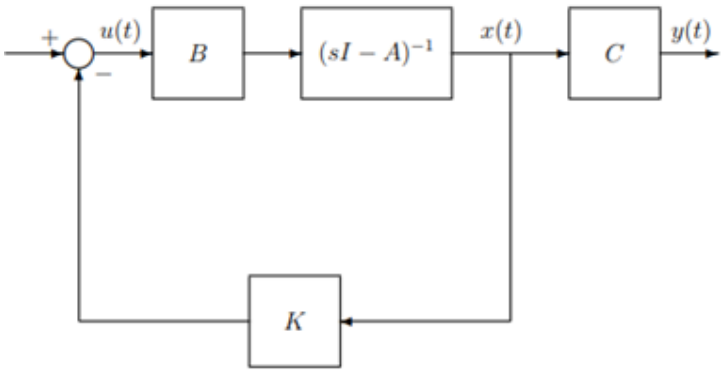

Figure 3.2. The closed loop LQR system [44]

Figure 3.2 represents the closed loop for the LQR system that will be approached in this sub-chapter, where the Plant P shown is given by:

$$P = C(sI - A)^{-1}B \quad (3.8)$$

Regulator design for a linear time-invariant state equation with the goal of minimizing a quadratic performance index naturally is referred to as a linear quadratic regulator problem.
Consider the continuous-time linear deterministic system that is characterized by the following equation that concerns the state equation and the second equation that concerns the output equation: [24] [25]

$$\begin{cases} \dot{x}(t) = A(t)x(t) + B(t)u(t) + uncertainties \\ y(t) = C(t)x(t) + others\_uncertainties \end{cases} \quad (3.9)$$

where x(t) is an n-dimensional state vector, u(t) is the r-dimensional plant control input vector (0<m≤r≤n) and y(t) is an m-dimensional output vector (m≤n). Regarding the matrices, A(t), B(t) and C(t) are nxn, nxr and mxn, respectively, where A(t) is the state matrix, B(t) is the control matrix (or entrance matrix) and C(t) is the output matrix.
Regarding the performance index (it may also be designated as cost function or objective function) to be minimized, it can be represented by the equation: [26] [27]

$$J(x, t0, tf, u(.)) = \frac{1}{2}\int_{t0}^{\infty} [x^T(t)Qx(t) + u^T(t)Ru(t)]dt \quad (3.10)$$

where the terminal time tf may be either fixed a priori or unspecified (tf>t0), the T denotes transposed matrix, Q(t) is a real symmetric nxn positive semi defined matrix, R(t) is a real symmetric rxr positive defined matrix and u(.) is a given element of Ω. [27] [28]
For the study of the LQR optimization, it is known that the Riccati equation is directly related to it. If the pair (A, B) is controllable (the solution is always greater than zero) and the pair (C, A) is observable, the use of the Riccati equation is valid and possible and its algebraic form is:

$$0 = PA + A^T P + Q - PBR^{-1}B^T P \quad (3.11)$$

Note that the pair (A, B) is given by "design" and can't be modified at this stage and the pair (Q, R) is the controller design parameter. Large Q penalizes transients of x and large R penalizes usage of control action u.
Therefore, the assigned weight of the matrices Q and R must be chosen very carefully. Two examples given for the implementation of the respective matrices are the Bryson Method and the Hamiltonian matrix. Regarding the first method, it suggests that each term of the diagonal matrices is the inverse square of the maximum value expected for the variable on the simulation time. These equations are:

$$Q = diag(Q_i) \Rightarrow Q_i = \frac{1}{x_{imax}^2} \quad (3.12\ a)$$

$$R = diag(R_i) \Rightarrow R_i = \frac{1}{u_{imax}^2} \quad (3.12\ b)$$

where x_{imax}^2 and u_{imax}^2 are the values indicating the extreme of the perturbations wanted for u_i or x_i for the closed loop during a manoeuvre. [30] [31]
Meanwhile, using the Hamiltonian matrix (H) to determine Q in its ideal form, the following matrix is given: [32]

$$H = \begin{bmatrix} A & -BR^{-1}B^T \\ -Q & -A^T \end{bmatrix} \quad (3.13)$$

After obtaining *P* through the Riccati equation, the parameterization of the control vector (u) as a linear function of the state vector (x) can be obtained:

$$u = -Kx \quad (3.14)$$

where K is the time-varying feedback gain matrix, being given as:

$$K = R^{-1}B^T P \quad (3.15)$$

Therefore, the control vector can be finally defined as:

$$u = -R^{-1}B^{T}Px \quad (3.16)$$

3.3.1. Artstein Method with application on LQR Robust

To be able to use a robust controller, first a system needs to meet a number of requirements, being those: The system must be able to resist to the disturbances while performing the function for the purpose it was created; the controller must accomplish the objective, even when subject to disturbances; the uncertainties given in equation (3.9) allows the state vector to be given as: [18] [33]

$$\dot{x} = \bar{A}x + \bar{B}u \quad (3.17)$$

Note that $\bar{A}$ and $\bar{B}$ have intercalated elements. Now, regarding the following equation (3.19), it must respect the following parameters:

$$\left\| \tilde{A} - A \right\| \leq \eta_1 \quad (3.18\ a)$$

$$\left\| \tilde{B} - B \right\| \leq \eta_2 \quad (3.18\ b)$$

Therefore, the controller is considered robust if it can return to its objective without having the accurate model of the system. When subject to disturbances, the state equation given in (3.9) becomes:

$$\dot{x} = (A + \Delta A)x + (B + \Delta \mathrm{B})u \quad (3.19)$$

Note that $\bar{A} = (A + \Delta A)$ and $\bar{B} = (B + \Delta \mathrm{B})$.

Since the objective of this dissertation is the implementation of a H_∞/LTR controller approached in the following sub-chapter) and the comparison with a Robust LQR, it's necessary to apply the Artstein method, to ensure that regardless of the input signal, the output signal will be controlled and stabilized as developed. [34] [35]

To conclude, the robust controller will adopt the following structure:

$$u = -R^{-1}B^{T}\left(P\left(x - x_{ref}(t)\right) + r\right) \quad (3.20)$$

where r and z are equal to, respectively:

$$r = -(A^{T} - PBR^{-1}B^{T})^{-1}Pz \quad (3.21)$$

$$z = -Ax_{ref}(t) \quad (3.22)$$

Note that the solution of matrix *(P)* for the Artstein method, is still obtained using the Riccati equation given by (3.11).

3.4. $\mathbf{H}_\infty$ Method

3.4.1. State-Space Solutions to Standard $\mathbf{H}_\infty$

To understand the H_∞-optimal control problem, consider a linear dynamic system with finite dimension and invariant on time, designated as a linear fractional transformation (LFT), which can be shown as a basic block diagram (control system diagram) as it follows: [41]

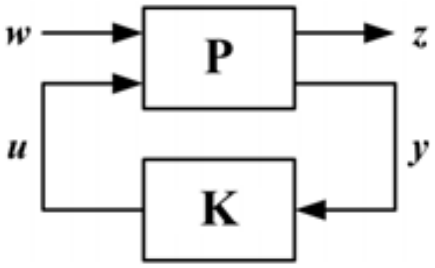

Figure 3.3. Block diagram of the feedback control system [41]

where P is the generalized plant and K is the controller, and both are finite-dimensional linear time-invariant (LTI) systems.

The generalized plant P (also called coefficient matrix for the LFT) contains what is usually called the plant in a control problem, plus all weighting functions, and it is expressed as:

$$P = \begin{cases} \dot{x} = Ax + Bu + Lw_x \\ z_x = Hx \\ z_u = \rho Iu \\ y = Cx + \mu Iw_y \end{cases} \quad (3.23)$$

The signal w (w_x and w_y) contains all external inputs (disturbance inputs), including Gaussian disturbances, sensor noises and commands; the output z (z_x and z_u) is an error signal (controlled output); y is the measured variables (measured output); and u is the control input. Note that the resulting closed-loop transfer function from w to z is denoted by T_{zw} and it's obtained from a fractional linear transformation. The matrices A, B and C form an embodiment in state variables of the usually called transfer matrix (or transfer function to the system SISO) of the process plant G(s), as demonstrated bellow: [40] [41]

$$G \coloneqq \begin{bmatrix} A & B \\ C & 0 \end{bmatrix} = C\Phi(s)B \quad (3.24)$$

where $\Phi(s)$ is represented as:

$$\Phi(s) = (sI - A)^{-1} \quad (3.25)$$

Therefore, if both pairs (A, B and A, L) are stable and both (A, C and A, H) are detectable, the plant P may be submitted to an optimization recurring to H_∞ and the problem will be based in finding a controller K, which with the information provided by y, generates a control signal u capable of commanding the generalized plant P and neutralizes the influence of w and z, using the minimization of the matrix T_{zw}.

The controller K admissible and represented in terms of state variable can be given as: [43] [44]

$$K \coloneqq \begin{bmatrix} A_\infty + BK_C + ZK_F & ZK_F \\ K_C & 0 \end{bmatrix} \quad (3.26)$$

Where A_∞ is represented as:

$$A_\infty = \mathrm{A} + \gamma^{-2}\mathrm{L}L^T\mathrm{X} \quad (3.27)$$

and Z as:

$$\mathrm{Z} = (\mathrm{I} - \gamma^{-2}\mathrm{YX})^{-1} \quad (3.28)$$

Finally, the solution for the generalized algebraic Riccati equation is given by the symmetric matrices X and Y:

$$A^TX + XA + \gamma^{-2}XLL^TX - \rho^{-2}XBB^TX + H^TH = 0 \quad (3.29\ \text{a})$$

$$K_C = \rho^{-2}B^TX \quad (3.29\ \text{b})$$

$$YA^T + AY + \gamma^{-2}YHH^T - \mu^{-2}YCC^T + L^TL = 0 \quad (3.29\ \text{c})$$

$$K_F = \mu^{-2}YC^T \quad (3.29\ \text{d})$$

Note that γ is the H_∞-norm bound and for the control K given in (3.26), the symmetric matrix of X and Y must be semi-definite positives and the spectral ray of the product XY must be lower than γ^{-2}. K_C is the feedback matrix and K_F is the state observer matrix.

However, this approach of the H_∞ control can lead to a poor performance in a closed-loop, because the controller is designed for the worst case scenario. [43] [44]

3.4.2. H_∞/LTR control for the mixed sensibility problem through the exit

To master the H_∞/LTR control, first it's necessary to understand the H_∞ method, represented in the sub-chapter 3.4.1, where the state-space solution for this problem is approached and a solution for the controller K is given by the equation (3.26). A set of the feedback matrix K_C (represented by equation 3.29 b) is projected to ensure that the transfer matrix with open mesh (G(s)K(s)) becomes the transfer matrix with objective mesh (C $\Phi(s)K_F$), which is reached using the state observer. This is the principle behind the LTR through the exit.

H_∞/LTR control through the exit can be divided in two steps. First, it's necessary to project one state observer matrix K_F (by choosing the L, μ and γ), to obtain the objective mesh and then design the feedback matrix K_C by reducing the value of ρ iteratively in order to approximate the open mesh to the objective mesh established in the beginning. If the value of ρ tends to zero, then the matrix X given by equation (3.29 a) will also tend to zero.

Note that if the pairs (A, B and A, L) are stabilized and the pair (A, C) is detectable, K_C will be chosen depending on the values obtained in equation (3.29 c). In the generalized plant P that is given by equation (3.23), if matrix H is equal to matrix C and ρ tends to zero, the controller K will tend to: [42]

$$\lim_{\rho \to 0^+} K(s) = [C\Phi(s)B]^{-1} C\Phi(s)K_F \quad (3.30)$$

and T_{zw} to:

$$\lim_{\rho \to 0^+} T(s) = C\Phi(s)K_F[I + C\Phi(s)K_F]^{-1} \quad (3.31)$$

3.5. Case of Study Application

For this case of study, the following terms must be taken into consideration: The matrixes A, B, L, H, C, ρI and μI were obtained based on experience; matrices Q and R were obtained recurring to Modified Bryson; state variables are referent to the position and velocity in 3D; the control variables refer to the acceleration in 3D; measured variables and the controlled output refer to the position in 3D; noise refers to the derivative of the position and velocity in 3D; trajectory for a non-manoeuvring and manoeuvring target was generated randomly using the Python program; LQR Robust controller was created using the Artstein method.

Chapter 4

Simulation and Results

This chapter will be addressed to the results of the missile interception simulation, where the sub-chapter 4.1 concerns the implementation of a pre-problem with a non-moving target and the sub-chapter 4.2 concerns for a target with manoeuvrability, being applied two different trajectories when the missile is detected, as well as two different detection time. All the graphics and matrices expose were generated with resource to the Butcher Algorithm (is presented in the Appendix A) and the Python program, where the colour green is referred to the target, the colour blue is referred to the missile using the H_∞/LTR method and the colour red is referred to the missile using the Robust LQR method.

Before analysing the different graphics of the position, velocity and acceleration, it's necessary to understand that the pursuer is a tactical missile with the ability for a 40 g force and a top speed of Mach 4. Also, the target was generated randomly by the program (as already referred), having this the ability for a 3 g force and a top speed of Mach 1.5. The main reason for such discrepancies between g force and Mach number of the missile and the target is mainly because the objective is to analyse the main differences of the two control methods in the shortest period of time.

Starting with H_∞/LTR method, the system that describes the missile movement is the system (3.23), where the state vector is represented by the position and velocity in 3D, the control vector is represented by the acceleration in 3D, the measured output and the controlled output are represented by the position in 3D and the disturbance input is represented by the position and velocity disturbances also in 3D. These vectors can be represented respectively as:

$$x = \begin{bmatrix} p_x & p_y & p_z & v_x & v_y & v_z \end{bmatrix}^T \quad (4.1\text{ a})$$

$$u = \begin{bmatrix} a_x & a_y & a_z \end{bmatrix}^T \quad (4.1\text{ b})$$

$$y = \begin{bmatrix} p_x & p_y & p_z \end{bmatrix}^T \quad (4.1\text{ c})$$

$$z = \begin{bmatrix} p_x & p_y & p_z \end{bmatrix}^T \quad (4.1\text{ d})$$

$$w = \begin{bmatrix} \dot{p}_x & \dot{p}_y & \dot{p}_z & \dot{v}_x & \dot{v}_y & \dot{v}_z \end{bmatrix}^T \quad (4.1\text{ e})$$

Besides these, the values for the generalized plant P represented by equation (3.23) that were used are:

$$\rho = 10^{-2} \quad \text{(4.2 a)}$$

$$\mu = 6 \quad \text{(4.2 b)}$$

Note that these values will be applied in the matrices (4.3 f) and (4.3 g).

For the Robust LQR controller maintain the accuracy of the data, the state vector, the control vector and the measured output are equal to those applied on the H_∞/LTR method. Therefore, they are represented by equations (4.1 a), (4.1 b) and (4.1 c), respectively.

Matrices A, B, L, H, C, ρI and μI of the Hinfinit/LTR system, were created based on the model in question resulting in, respectively:

$$A = \begin{bmatrix} 0 & 0 & 0 & 1 & 0 & 0 \\ 0 & 0 & 0 & 0 & 1 & 0 \\ 0 & 0 & 0 & 0 & 0 & 1 \\ 0 & 0 & 0 & 0 & 0 & 0 \\ 0 & 0 & 0 & 0 & 0 & 0 \\ 0 & 0 & 0 & 0 & 0 & 0 \end{bmatrix} \quad \text{(4.3 a)}$$

$$B = \begin{bmatrix} 0 & 0 & 0 \\ 0 & 0 & 0 \\ 0 & 0 & 0 \\ 1 & 0 & 0 \\ 0 & 1 & 0 \\ 0 & 0 & 1 \end{bmatrix} \quad \text{(4.3 b)}$$

$$L = \begin{bmatrix} 1 & 0 & 0 & 0 & 0 & 0 \\ 0 & 1 & 0 & 0 & 0 & 0 \\ 0 & 0 & 1 & 0 & 0 & 0 \\ 0 & 0 & 0 & 0 & 0 & 0 \\ 0 & 0 & 0 & 0 & 0 & 0 \\ 0 & 0 & 0 & 0 & 0 & 0 \end{bmatrix} \quad \text{(4.3 c)}$$

$$H = \begin{bmatrix} 1 & 0 & 0 & 0 & 0 & 0 \\ 0 & 1 & 0 & 0 & 0 & 0 \\ 0 & 0 & 1 & 0 & 0 & 0 \end{bmatrix} \quad \text{(4.3 d)}$$

$$C = \begin{bmatrix} 1 & 0 & 0 & 0 & 0 & 0 \\ 0 & 1 & 0 & 0 & 0 & 0 \\ 0 & 0 & 1 & 0 & 0 & 0 \end{bmatrix} \quad \text{(4.3 e)}$$

$$\rho I = \begin{bmatrix} \rho & 0 & 0 \\ 0 & \rho & 0 \\ 0 & 0 & \rho \end{bmatrix} \quad \text{(4.3 f)}$$

$$\mu I = \begin{bmatrix} \mu & 0 & 0 \\ 0 & \mu & 0 \\ 0 & 0 & \mu \end{bmatrix} \quad \text{(4.3 g)}$$

and for the Robust LQR method, matrices A and B are equal to those applied on the H_∞/LTR method. Therefore, they are represented by matrices (4.3 a) and (4.3 b), respectively.

4.1. Implementation of the problem, using a non-manoeuvring target

For the implementation of a non-manoeuvring target, Q and R were obtained recurring to modified Bryson, taking into consideration that the higher the values of the Q relative to the position, the more filtered the signal will be and for higher values of R, the lower the cost of the system will be. The matrices obtained were:

$$Q = \begin{bmatrix} 2000000 & 0 & 0 & 0 & 0 & 0 \\ 0 & 2000000 & 0 & 0 & 0 & 0 \\ 0 & 0 & 2000000 & 0 & 0 & 0 \\ 0 & 0 & 0 & 0 & 0 & 0 \\ 0 & 0 & 0 & 0 & 0 & 0 \\ 0 & 0 & 0 & 0 & 0 & 0 \end{bmatrix} \quad \text{(4.4 a)}$$

$$R = \begin{bmatrix} 0.001 & 0 & 0 \\ 0 & 0.001 & 0 \\ 0 & 0 & 0.001 \end{bmatrix} \quad \text{(4.4 b)}$$

Two different analysis were performed, by altering the state vector of the systems in question, being those, respectively: X1 = [0, 0, 0, 0, 0, 0] and X2 = [4500, 850, 250, 0, 0, 0]. For both simulations, the intersection occurred first for the Hinfinit/LTR controller, where for X1 it occurred at 6.21 seconds and for X2, it occurred at 5.45 seconds. Relatively to the Robust LQR, for X1, the intersection occurred at 7.07 seconds and for X2, it occurred at 6.37 seconds.
In the following sub-chapters 4.1.1 and 4.1.2, first an analysis of the Robust LQR method performance is made and then, the same analysis is made but for the H_∞/LTR method. In each one, the persecution between the missile and the target is presented in 3D, and the acceleration and speed of both are shown in 2D. Because the performance of both methods is very similar for the non-manoeuvring target generated by the program, a comparison between both is made regarding the acceleration and velocity in the end of each sub-chapter.

4.1.1. Implementation of the first analysis (X1)

4.1.1.1. Robust LQR Control

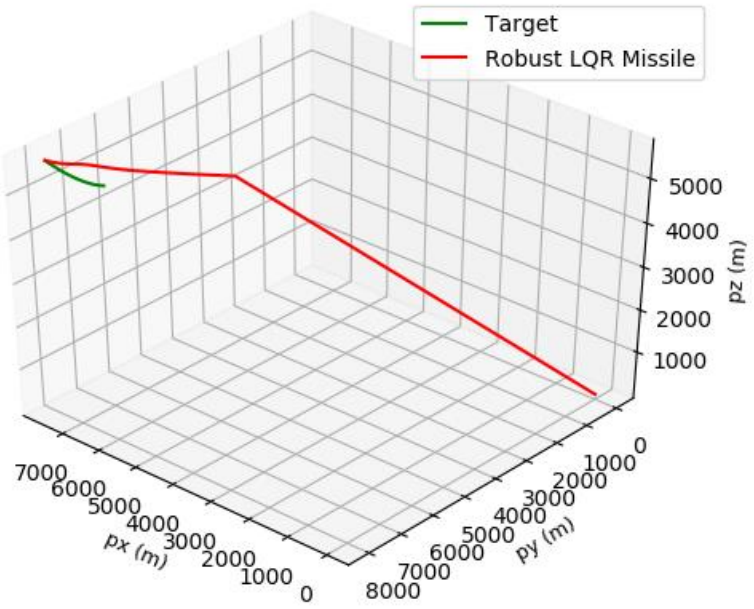

Figure 4.1. Intersection of target and missile using Robust LQR control in three dimensions for X1

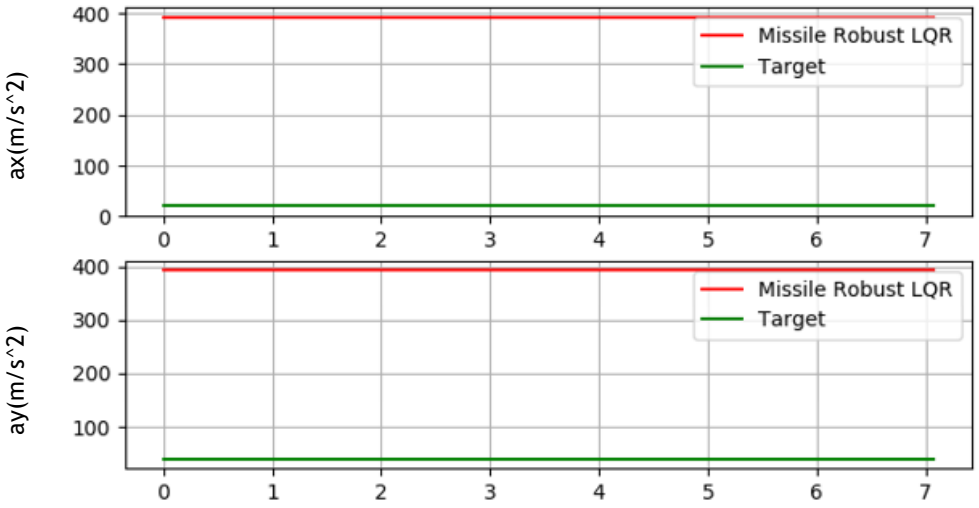

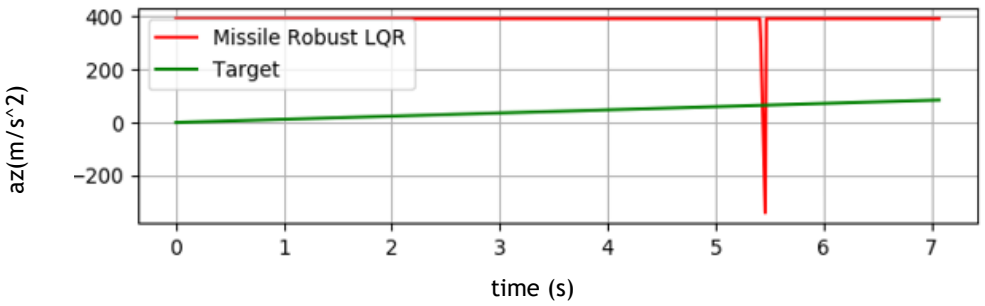

Figure 4.2. Missile and target accelerations until the intersection occurs using Robust LQR control for X1

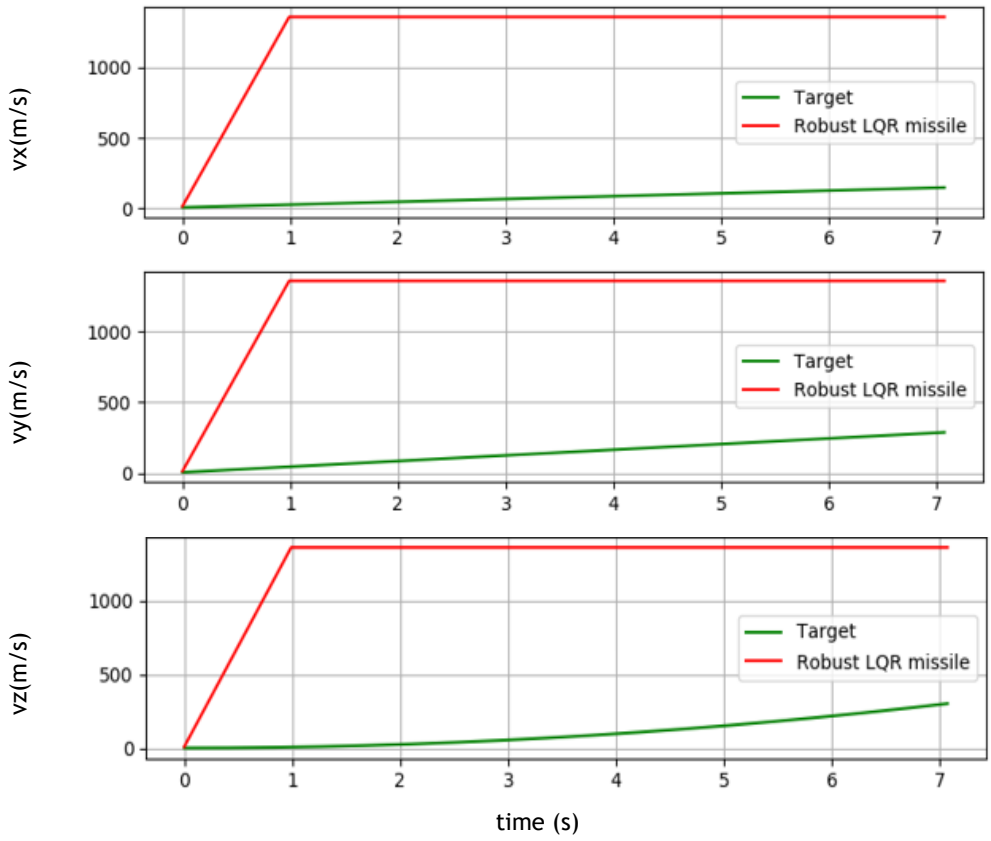

Figure 4.3. Missile and target velocities until the intersection occurs using Robust LQR method for X1

4.1.1.2. Hinfinit/LTR Control

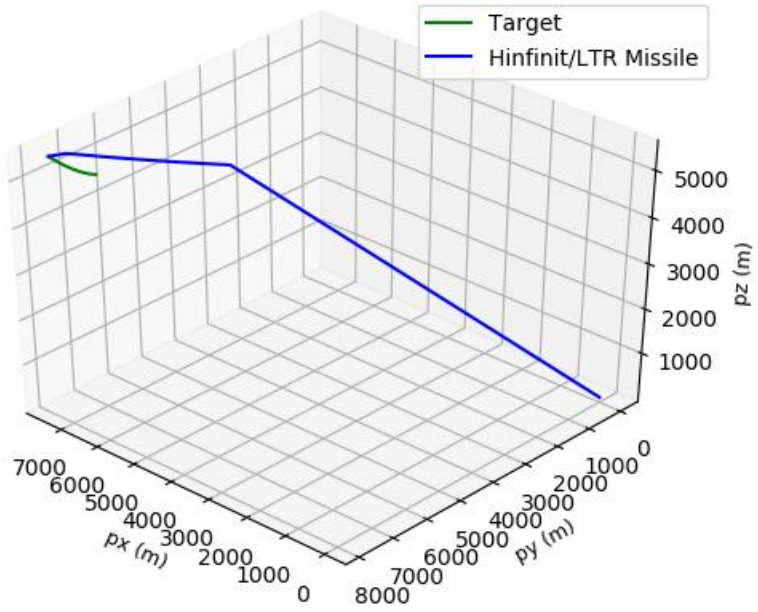

Figure 4.4. Intersection of target and missile using Hinfinit/LTR control in three dimensions for X1

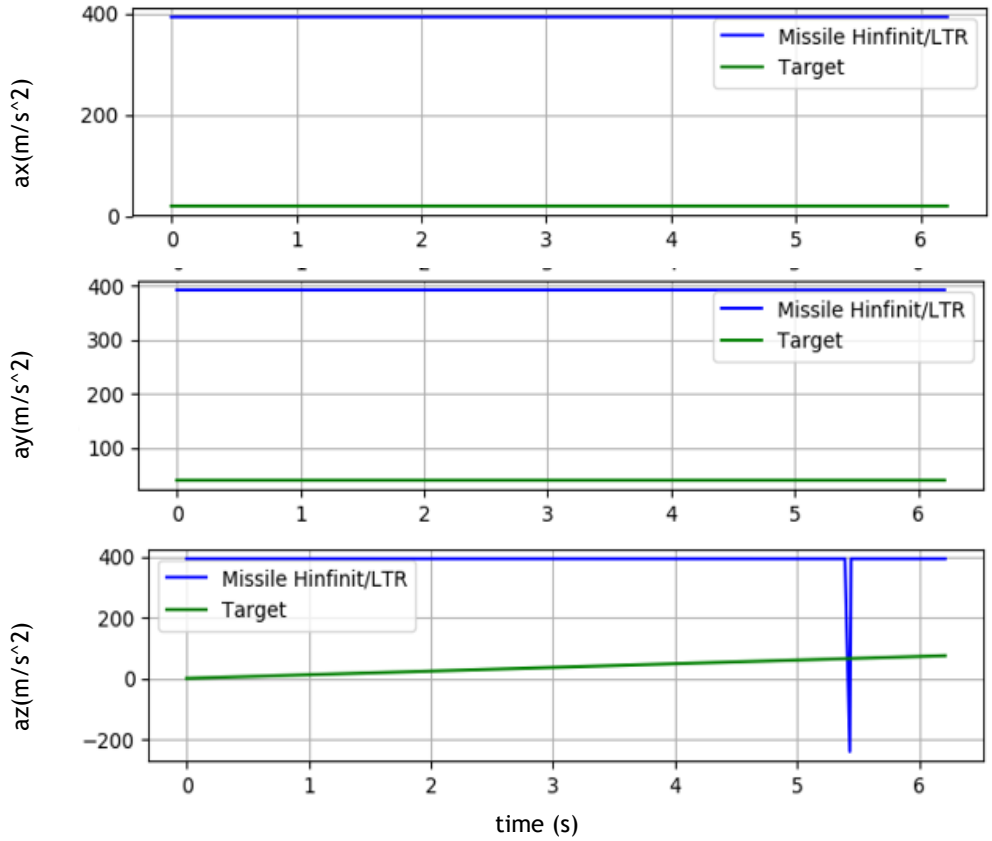

Figure 4.5. Missile and target accelerations until the intersection occurs using Hinfinit/LTR method for X1

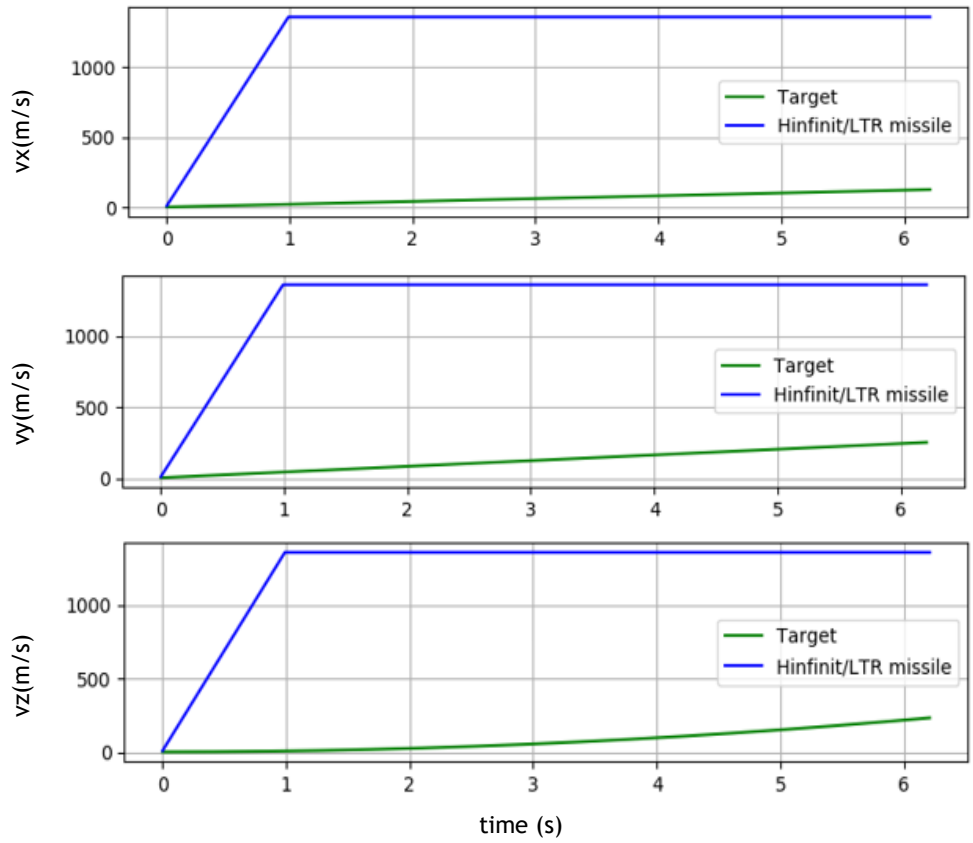

Figure 4.6. Missile and target velocities until the intersection occurs using Hinfinit/LTR method for X1

4.1.1.3. Comparison between the Robust LQR and Hinfinit/LTR methods

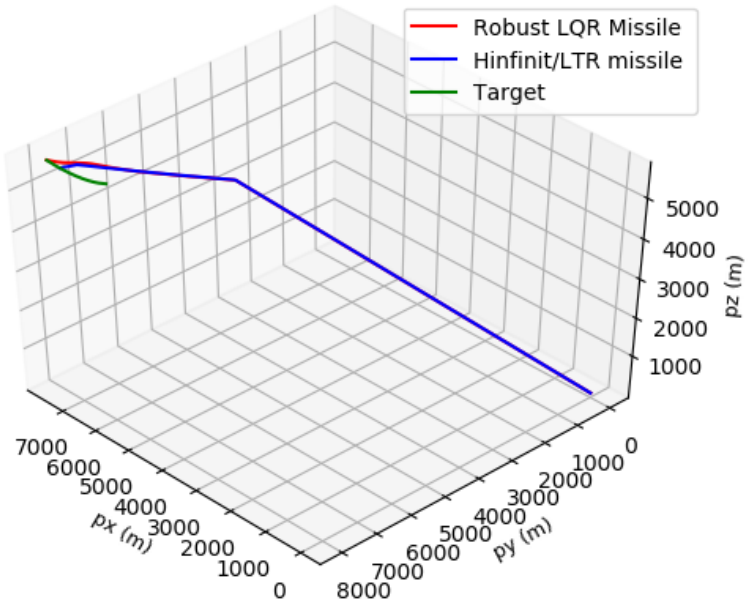

Figure 4.7. Intersection of target and missile using Hinfinit/LTR and Robust LQR methods in three dimensions for X1

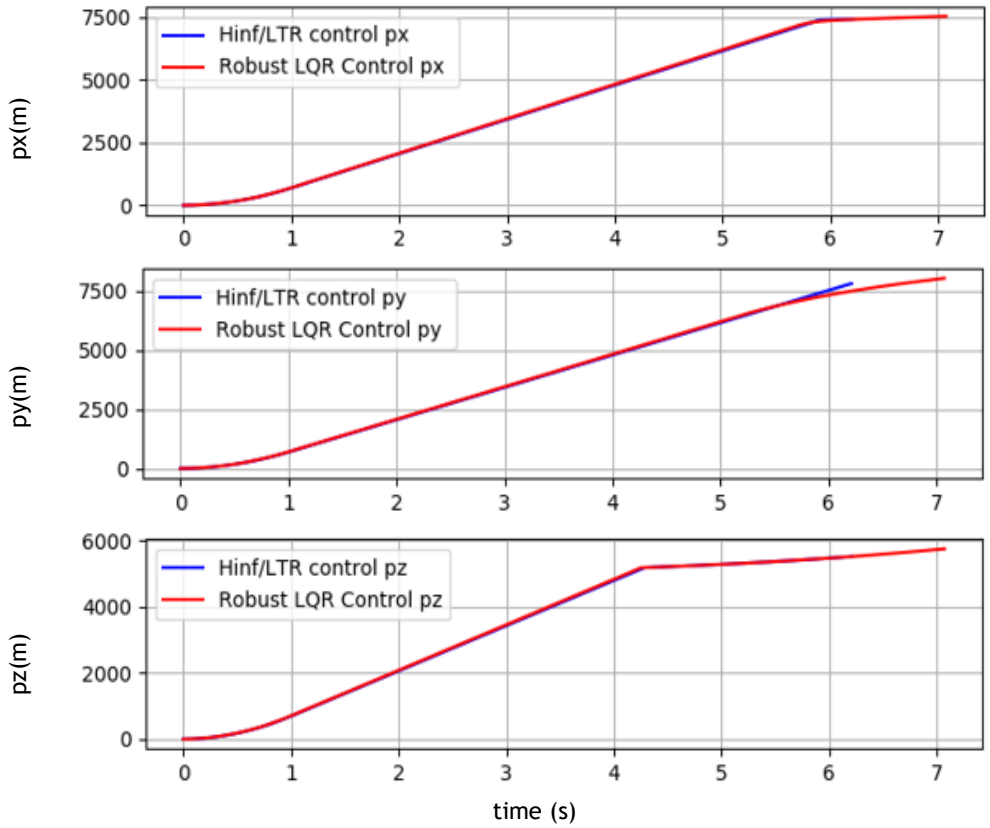

Figure 4.8. Missile and target positions until the intersection occurs using Hinfinit/LTR and Robust LQR methods for X1

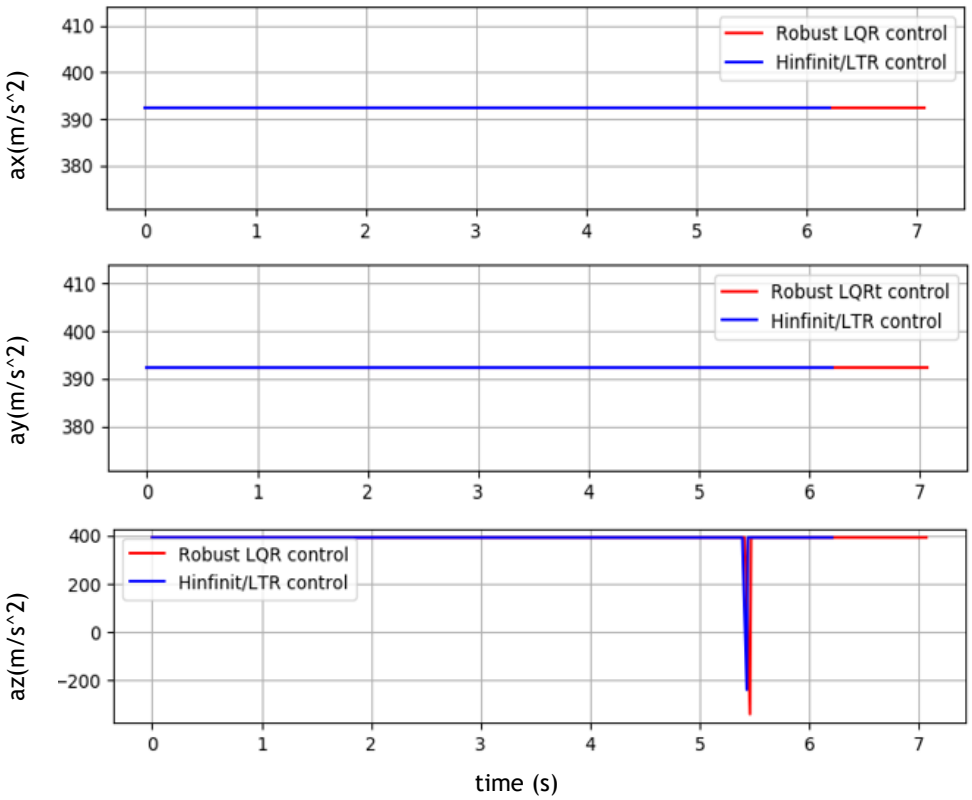

Figure 4.9. Missile accelerations until the intersection occurs using Hinfinit/LTR and Robust LQR methods for X1

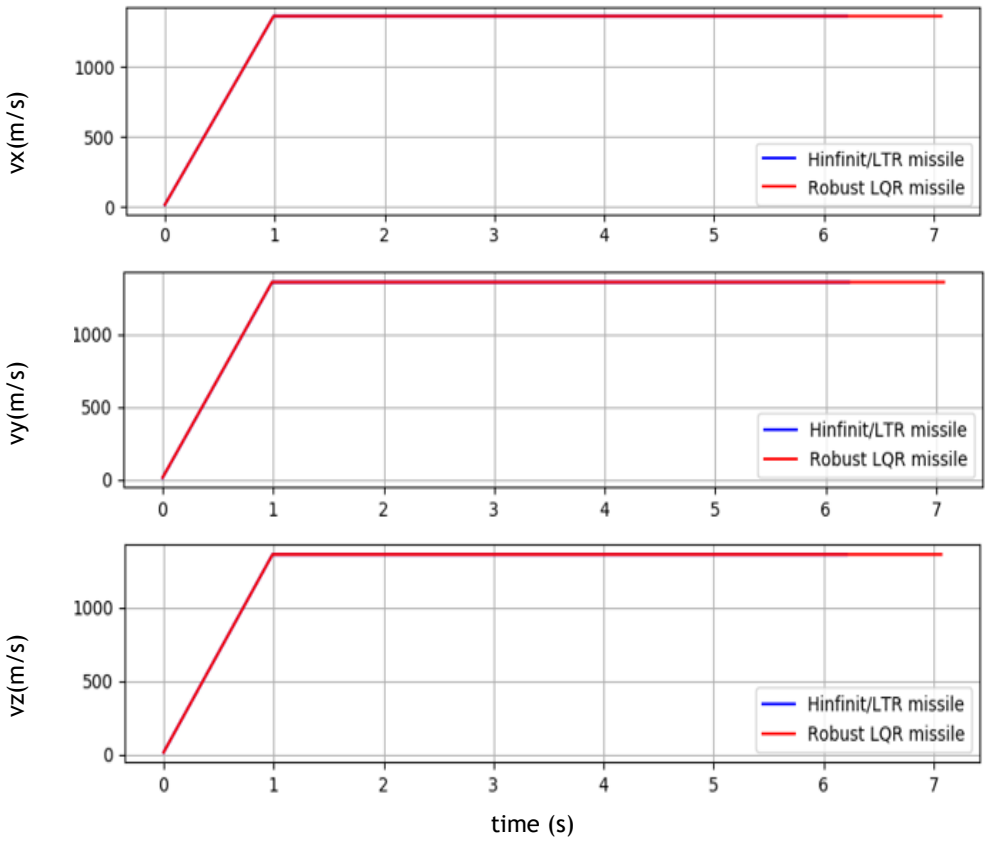

Figure 4.10. Missile velocities until the intersection occurs using Hinfinit/LTR and Robust LQR methods for X1

Missile velocity and acceleration for both methods are very similar because of the maximum g force supported and the structural limitation, as already explained before. Therefore, the persecutor behaviour relatively to the velocity will always be to reach the maximum speed as fast as possible and maintain it, so the intersection occurs in the minimum possible time. Regarding the acceleration, since the launch the missile reaches the maximum allowed g force, so that it can as quickly as possible reach the intended collision course with the target and maintain it until a successful interception is made. That is why figure 4.9 presents a very similar data for both controllers, as well as figure 4.10.

However, missile and target velocities don't tend to intercept as time goes by, as it is possible to verify from figures 4.3 and 4.6, because missile's controller is only for the acceleration and not for velocity and in matrix Q (given in (4.4 a)), the data for velocity is equal to zero, unlike what happens with the position. Therefore, only the missile and target positions are intended to coincide. Another important consideration is that the initial velocity of the missile is given by the state-vector X1, where its values are zero meters per second.

The missile and target route during the intersection can be analysed in figure 4.7, where it's quite visible that the intersection occurs first for the H_∞/LTR controller and from figure 4.8, the missile course with the application of both methods is presented in 2D, being the biggest difference on py.

Regarding figures 4.2, 4.5 and 4.9, an analysis for the missile acceleration is made, being the conclusions as follows: for x plane and the y plane, the data is the same, except for the z plane, where a variation of the acceleration appears first for the H_∞/LTR.

From the above data regarding the position, velocity and acceleration, it is possible to observe that both controllers have a very similar performance for a non manoeuvrable target, except for the final stage of the intersection. However, in a real combat situation, every millisecond counts and the H_∞/LTR controller showed to be more efficient and effective.

4.1.2. Implementation of the first analysis (X2)

This second analysis aims to prove that the missile also intersects the target from a different position, as well as demonstrates that H_∞/LTR controller continues to have a better performance than the Robust LQR controller.

4.1.2.1. Robust LQR Control

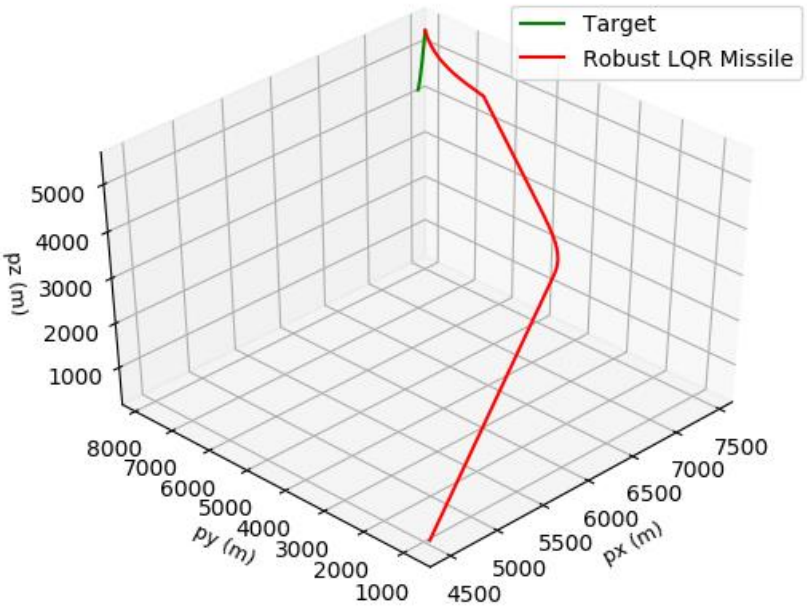

Figure 4.11. Intersection of target and missile using Robust LQR control in three dimensions for X2

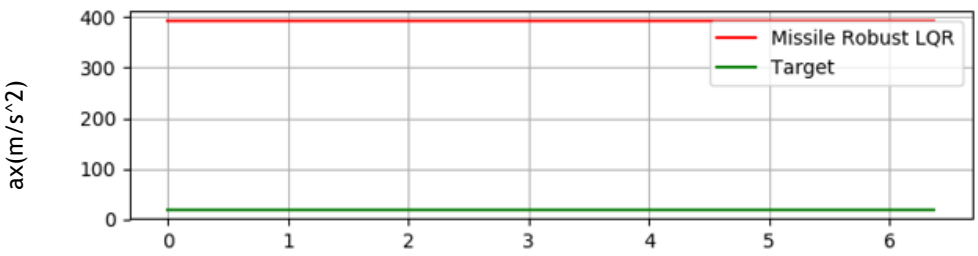

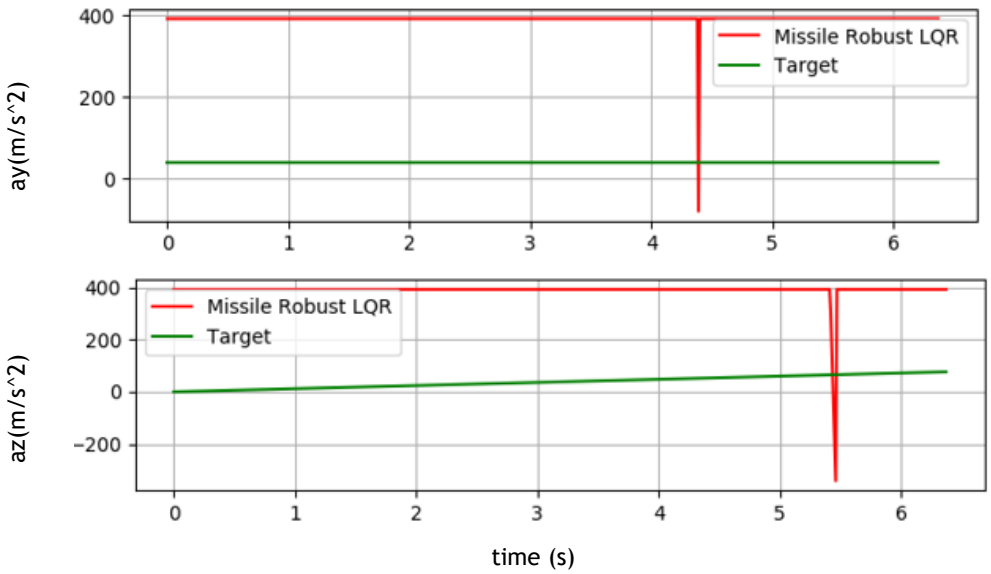

Figure 4.12. Missile and target acceleration until the intersection occurs using Robust LQR method for X2

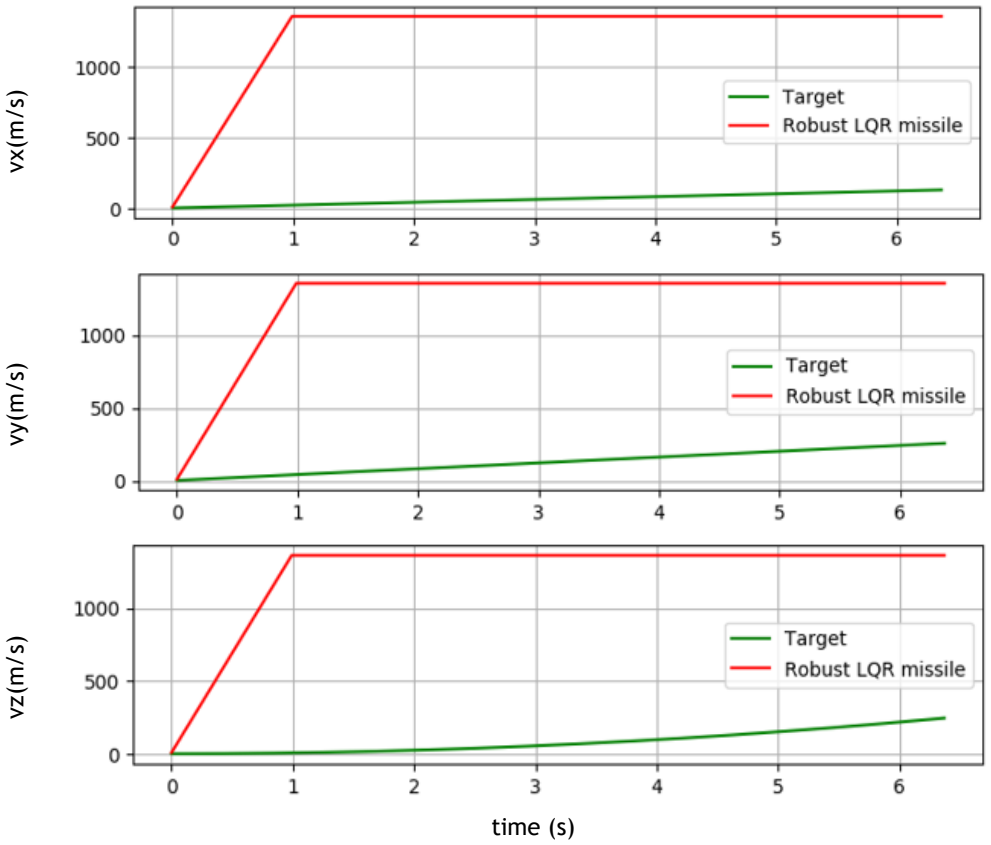

Figure 4.13. Missile and target velocities until the intersection occurs using Robust LQR method for X2

4.1.2.2. Hinfinit/LTR Control

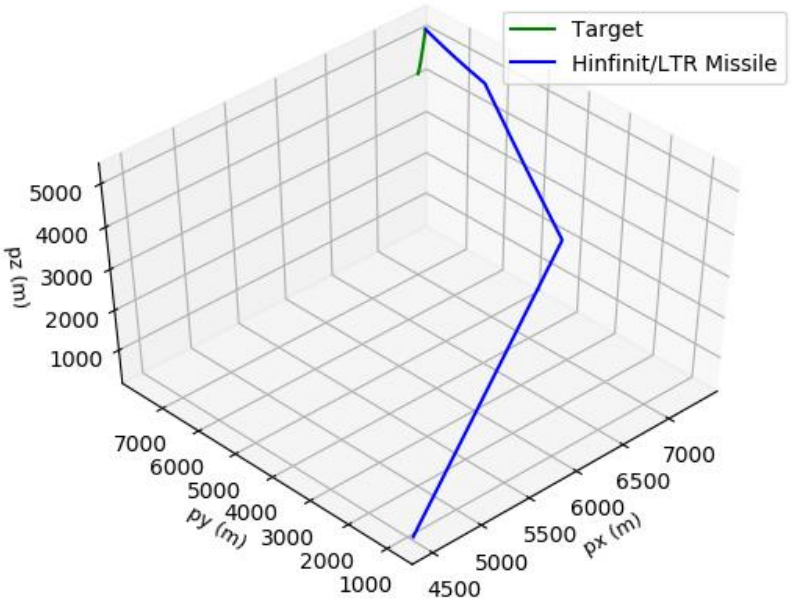

Figure 4.14. Intersection of target and missile using Hinfinit/LTR control in three dimensions for X2

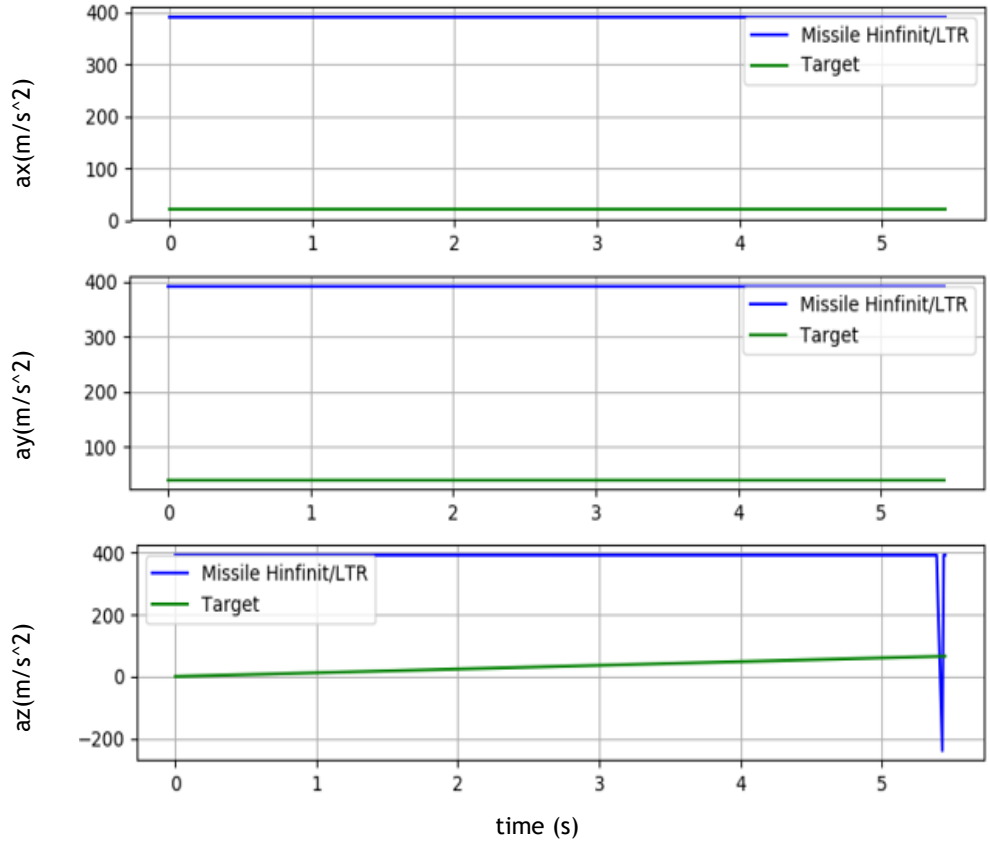

Figure 4.15. Missile and target acceleration until the intersection occurs using Hinfinit/LTR method for X2

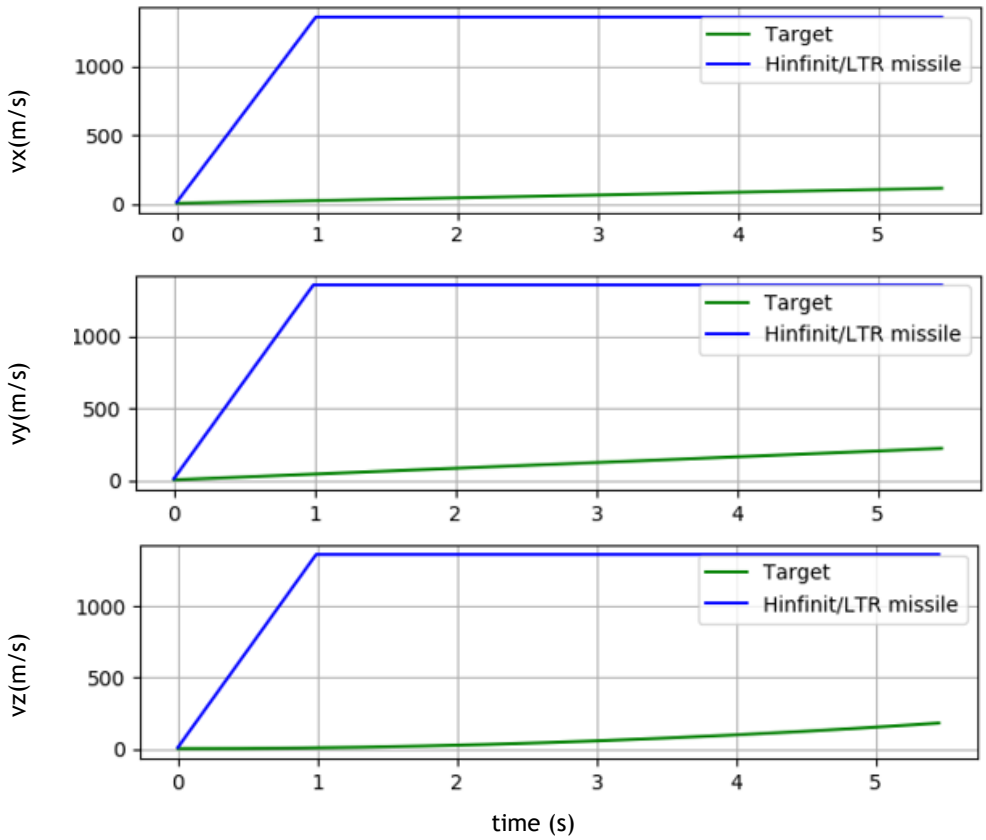

Figure 4.16. Missile and target velocity until the intersection occurs using Hinfinit/LTR method for X2

4.1.2.3. Comparison between Robust LQR and Hinfinit/LTR methods

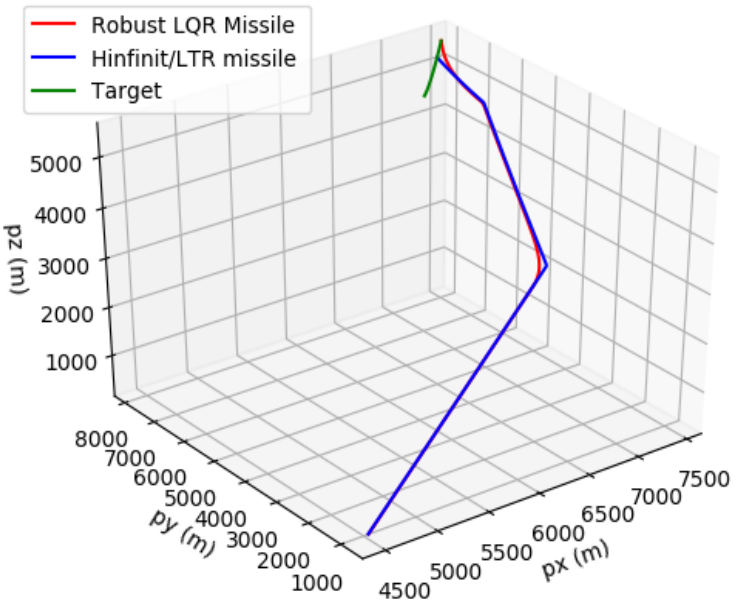

Figure 4.17. Intersection of target and missile using Hinfinit/LTR and Robust LQR control in three dimensions for X2

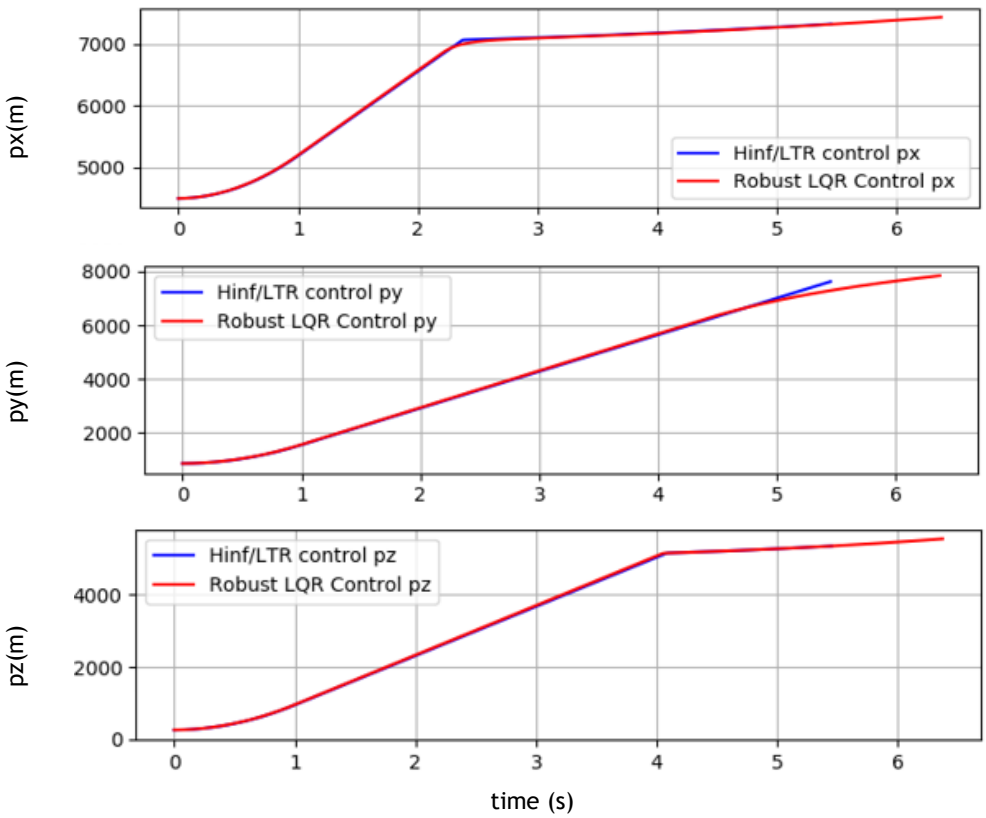

Figure 4.18. Missile position until the intersection occurs using Hinfinit/LTR and Robust LQR methods for X2

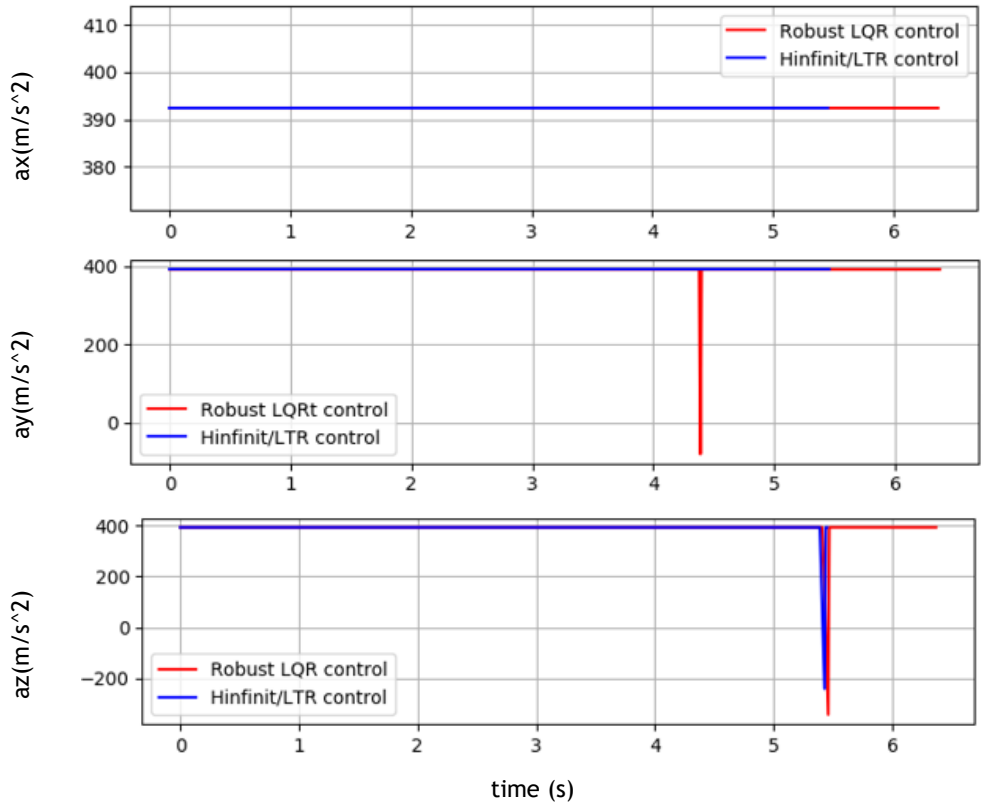

Figure 4.19 Missile acceleration until the intersection occurs using Hinfinit/LTR and Robust LQR methods for X2

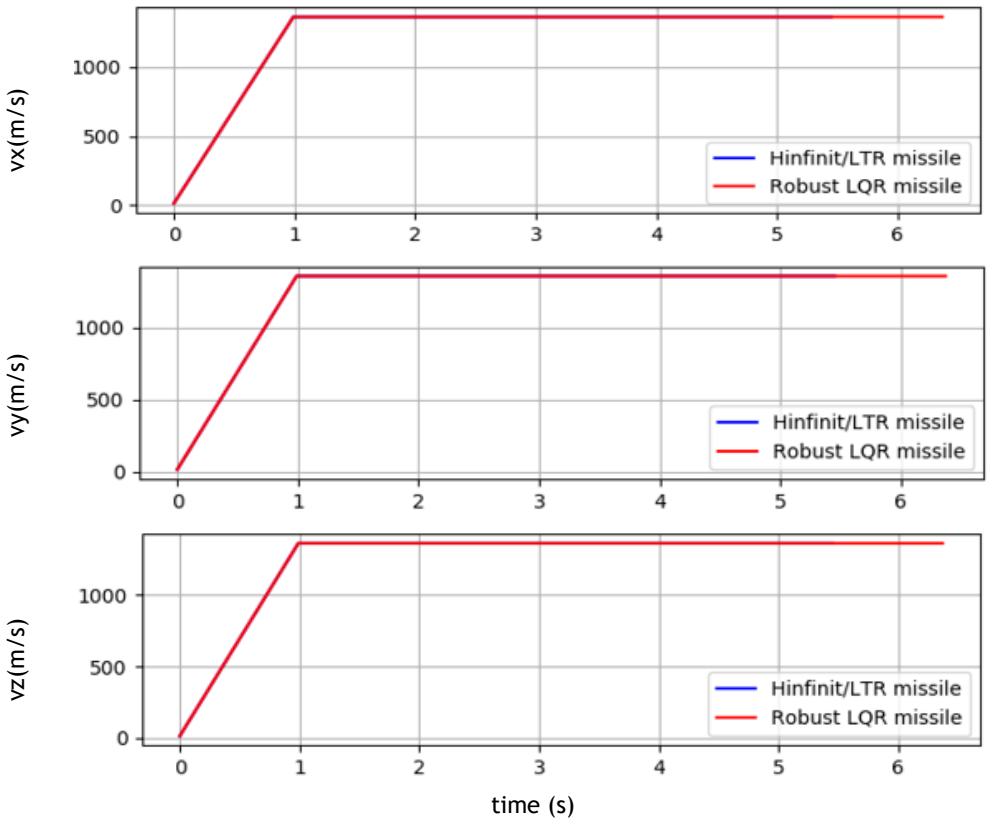

Figure 4.20. Missile velocity until the intersection occurs using Hinfinit/LTR and Robust LQR methods for X2

From this second analysis concerning the implementation of a different state vector, the differences between both methods are more visible. H_∞/LTR controller takes a more aggressive approach regarding the Robust LQR and for this reason, the first method reaches the target faster, as it is possible to verify from figures 4.11, 4.14 and 4.17. Also, from figure 4.18, the position in 2D of both controllers is presented.

The Velocity behaves exactly as in the first study case, being given by figures 4.13, 4.16 and 4.20, where due to the structural limitations and a top speed of Mach 4, the missile begins with a speed of zero meters per second and soon after, it reaches the top speed and maintains it, so the intersection occurs as fast as possible.

Regarding missile acceleration, it behaves differently from the first study case, where the maximum g force is reached from the beginning and maintained until the end of the simulation, with the exception of when it is necessary to correct the persecutor course, as shown in figures 4.12, 4.15 and 4.19, where the data are presented.

4.2. Implementation of the problem, using a manoeuvring target

For the implementation of a manoeuvring target, matrixes Q and R were also obtained recurring to modified Bryson, where the same considerations were made. Therefore, the matrices obtained were:

$$Q = \begin{bmatrix} 9500000 & 0 & 0 & 0 & 0 & 0 \\ 0 & 9000000 & 0 & 0 & 0 & 0 \\ 0 & 0 & 7000000 & 0 & 0 & 0 \\ 0 & 0 & 0 & 0 & 0 & 0 \\ 0 & 0 & 0 & 0 & 0 & 0 \\ 0 & 0 & 0 & 0 & 0 & 0 \end{bmatrix} \quad (4.5\ a)$$

$$R = \begin{bmatrix} 0.0012 & 0 & 0 \\ 0 & 0.068 & 0 \\ 0 & 0 & 0.001 \end{bmatrix} \quad (4.5\ b)$$

In this sub-chapter, the target from sub-chapter 4.1 is still used but this time, when the missile is detected, the target tries to escape, using two different trajectories (these trajectories were also generated randomly by the program). Besides the implementation of evasive manoeuvres, the detection time also is subjected to an analysis, to determine if it is directly related to the success or failure of the mission. Therefore, the target initiates the engagement maneuverers at two different times (4 and 5 seconds) and then, the two different trajectories are applied. Note that during the data analysis of sub-chapter 4.2, the target starts the trajectory in a defined state vector (X = [7000, 7000, 5000, 0, 0, 0]). In order to be easier to explain the four different cases, a similar methodology regarding the previous sub-chapter is applied, where X3.1 represents the first engagement manoeuver starting at 4 seconds, X3.2 represents the second engagement manoeuver starting at 5 seconds, X4.1 is for the target starting the first engagement manoeuver at 4 seconds and finally, X4.2 is for the target starting the manoeuver at 5 seconds.

4.2.1. Implementation of the first evasive manoeuvre trajectory X3

4.2.1.1. Engagement Manoeuvres for X3.1

4.2.1.1.1. Robust LQR Control

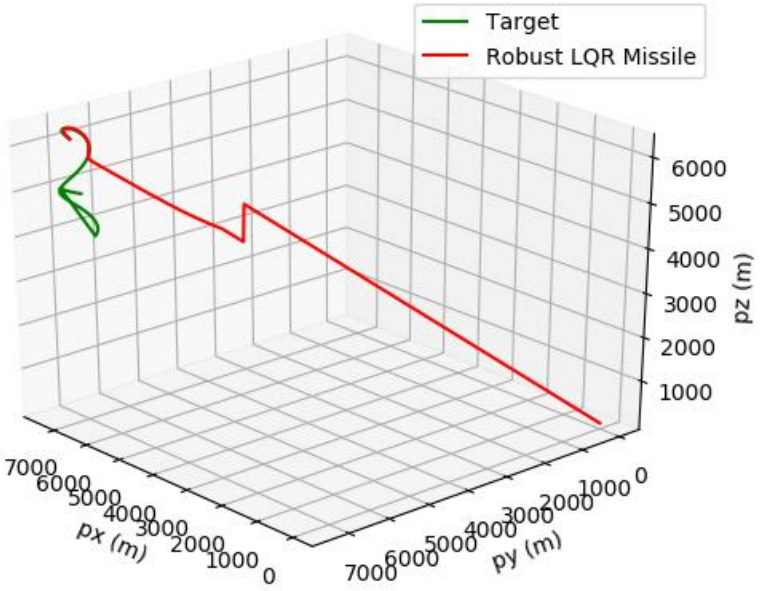

Figure 4.21. Intersection of target and missile using Robust LQR control in three dimensions for X3.1

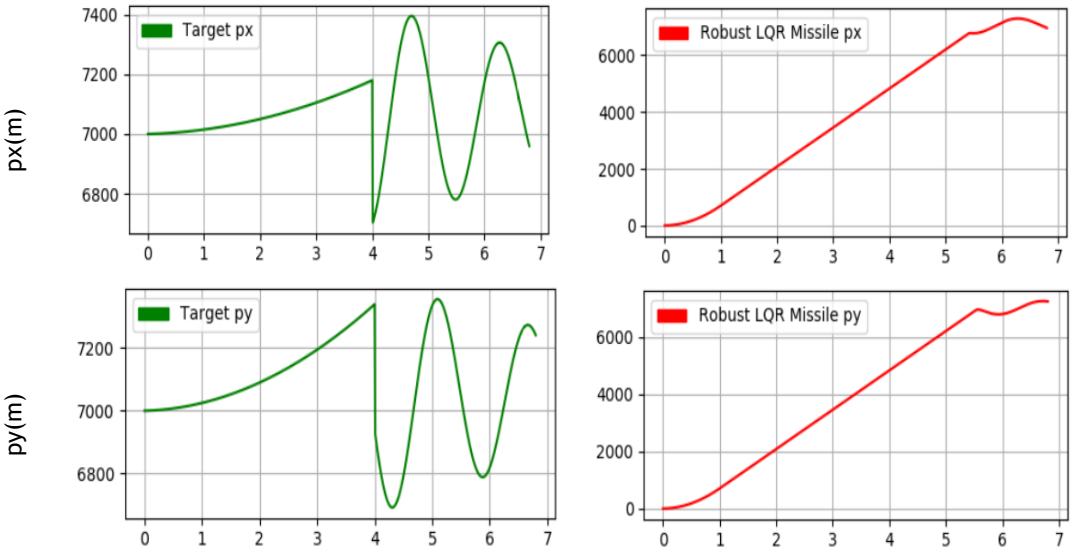

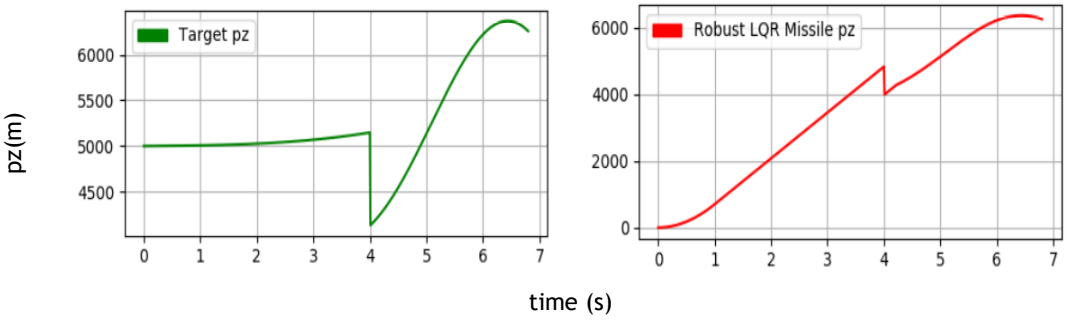

Figure 4.22. Target and missile course using Robust LQR control in two dimensions for X3.1

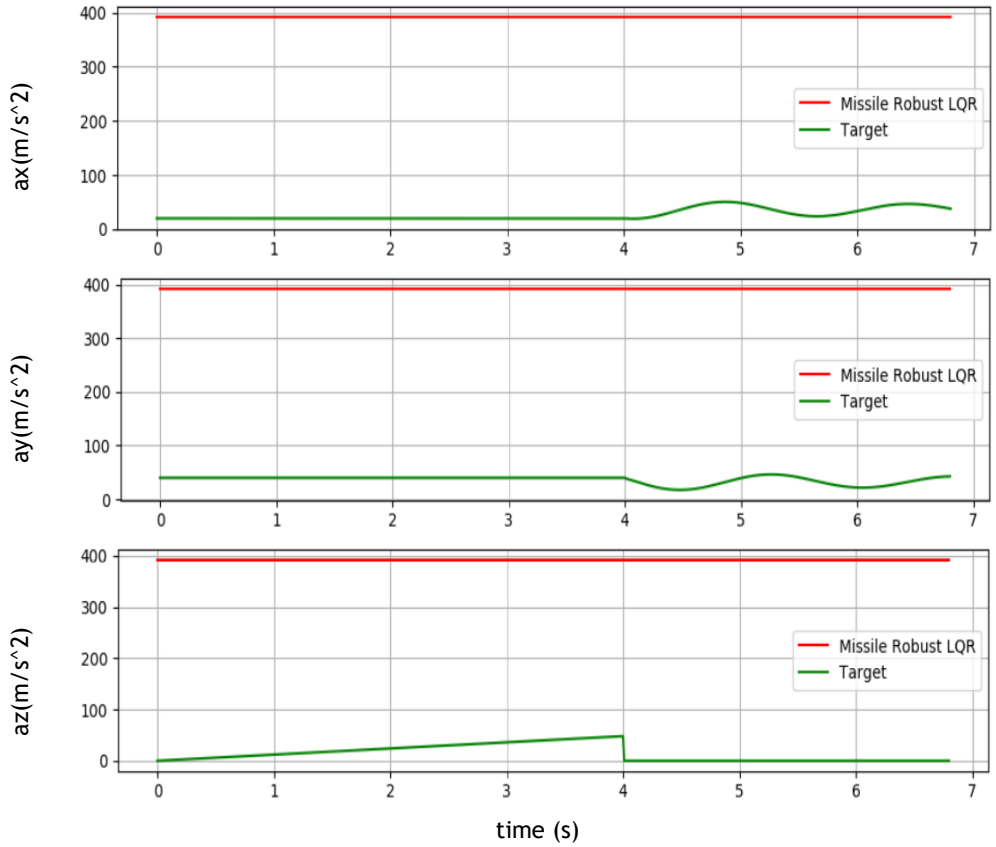

Figure 4.23. Missile and target acceleration until the intersection occurs using Robust LQR method for X3.1

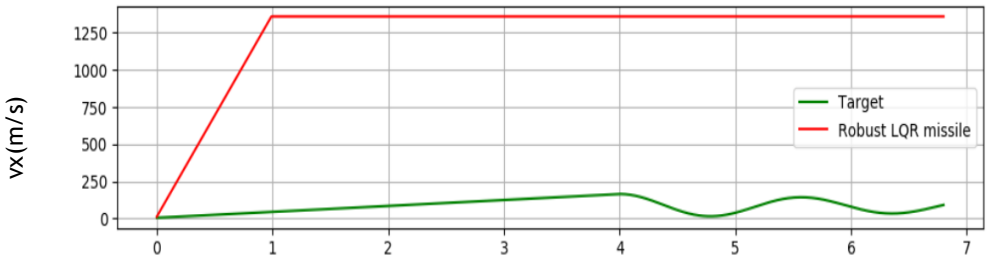

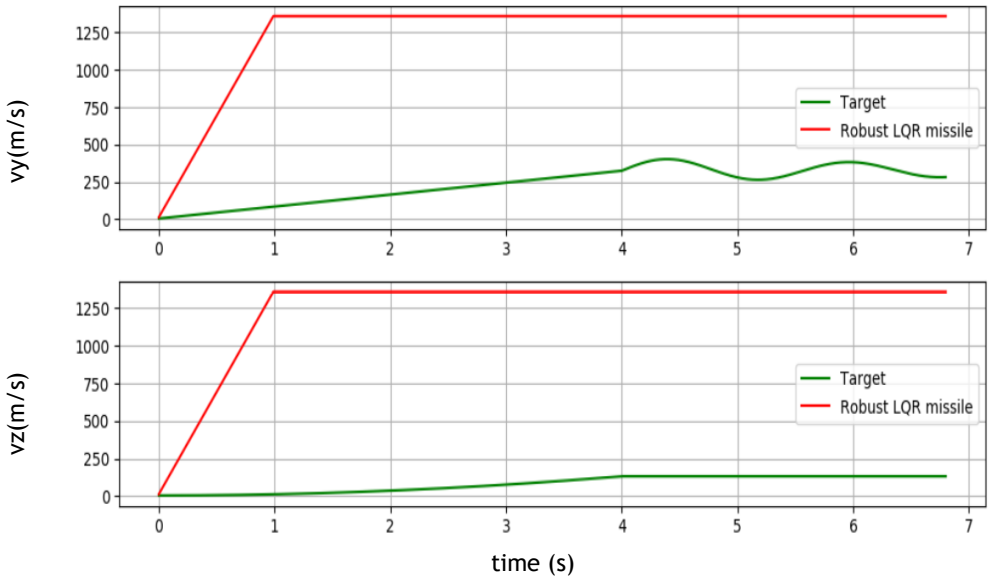

Figure 4.24. Missile and target velocity until the intersection occurs using Robust LQR method for X3.1

4.2.1.1.2. Hinfinit/LTR Control

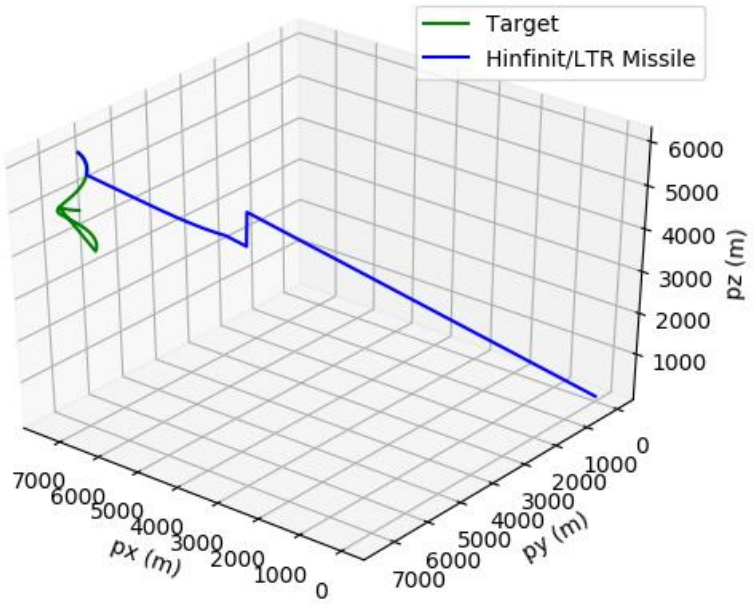

Figure 4.25. Intersection of target and missile using Hinfinit/LTR control in three dimensions for X3.1

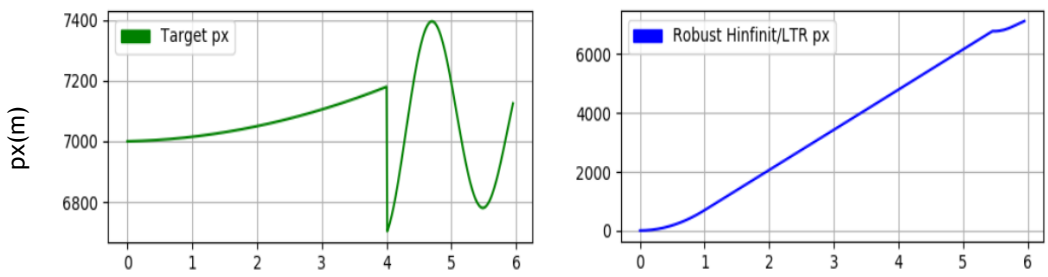

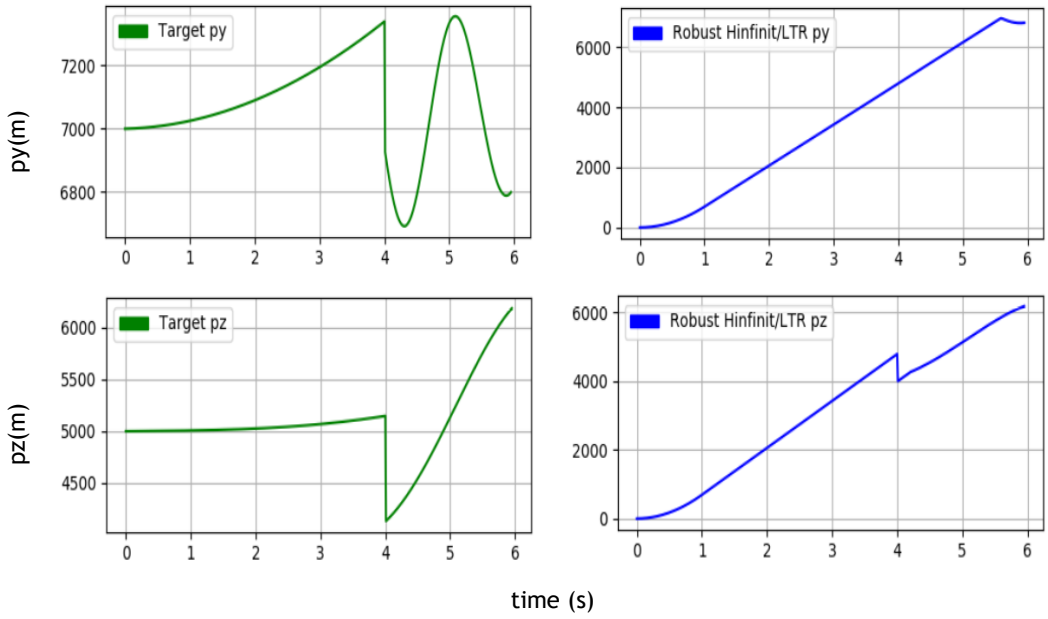

Figure 4.26. Target and missile course using Hinfinit/LTR control in two dimensions for X3.1

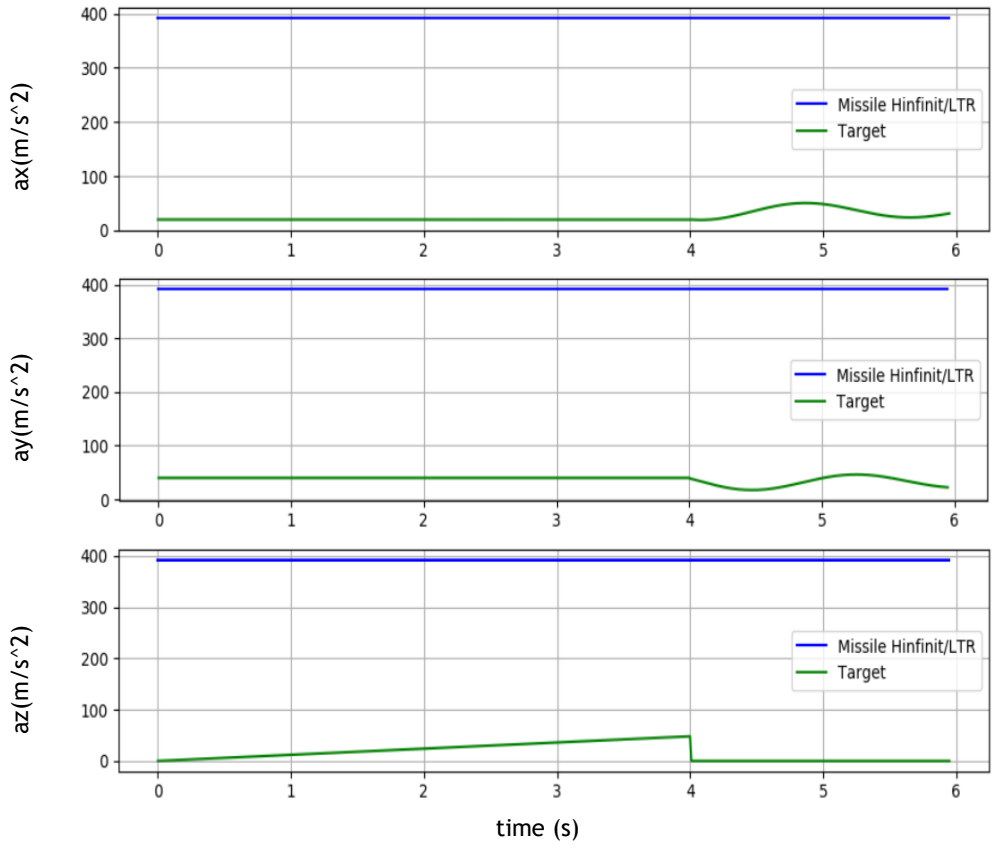

Figure 4.27. Missile and target acceleration until the intersection occurs using Hinfinit/LTR method for X3.1

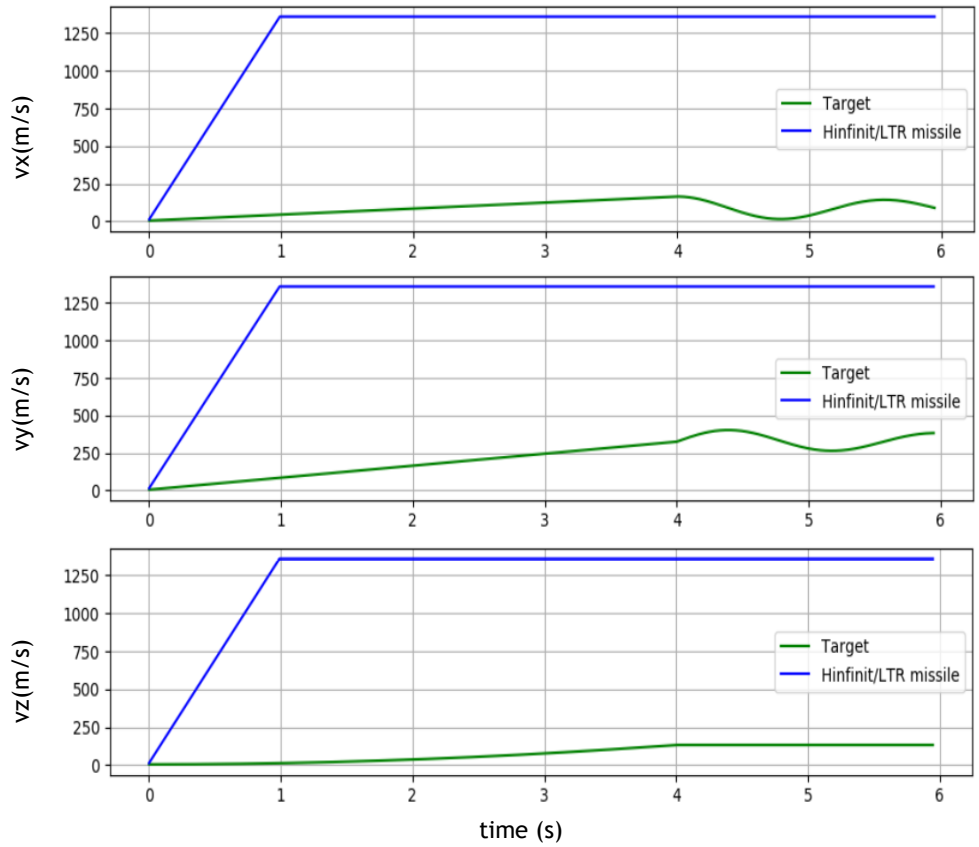

Figure 4.28. Missile and target velocity until the intersection occurs using Hinfinit/LTR method for X3.1

In this study case, where the target detects the pursuer and initiates the evasive manoeuvres at 4 seconds, it is already possible to determine that the H_∞/LTR controller is faster than the Robust LQR controller, from the analysis shown in figures 4.21 and 4.25. More precisely, Hinfinit/LTR controller is able to intersect the target at 5.95 seconds, while Robust LQR intersects at 6.78 seconds.

Missile course is maintained until the evasive manoeuvres are initiated. From this point, it will be necessary to adjust the course to the new target trajectory. From figures 4.22 and 4.26, target and missile course can be analysed in 2D, where it is visible the moment when the trajectory of both vehicles changes.

Now, as explained on sub-chapter 4.1, missile's behaviour regarding velocity and acceleration is expected and the target maintains a constant speed in vz and a constant speed variation in vx and vy, which directly influences the acceleration, as shown in figures 4.23, 4.24, 4.27 and 4.28.

4.2.1.2. Engagement Manoeuvres for X3.2

4.2.1.2.1. Robust LQR Control

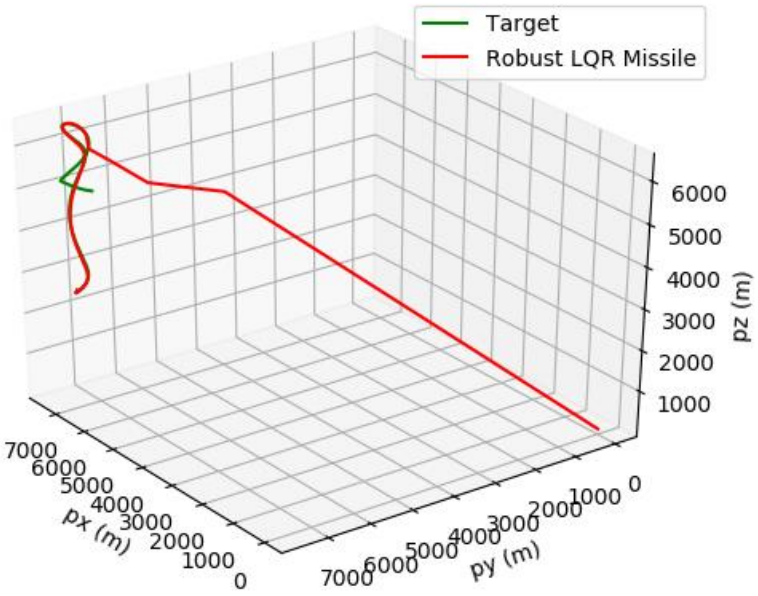

Figure 4.29. Intersection of target and missile using Robust LQR control in three dimensions for X3.2

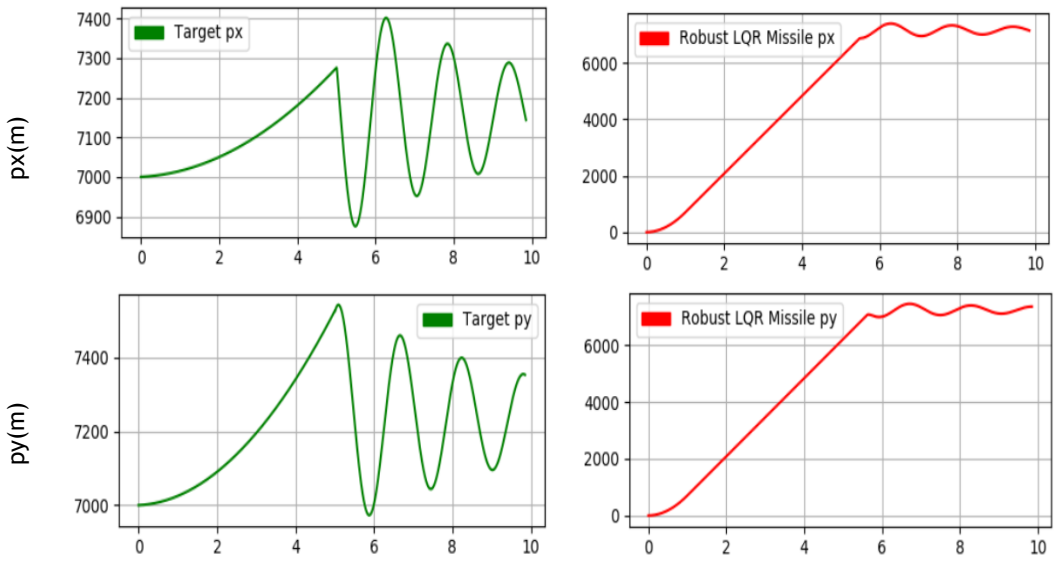

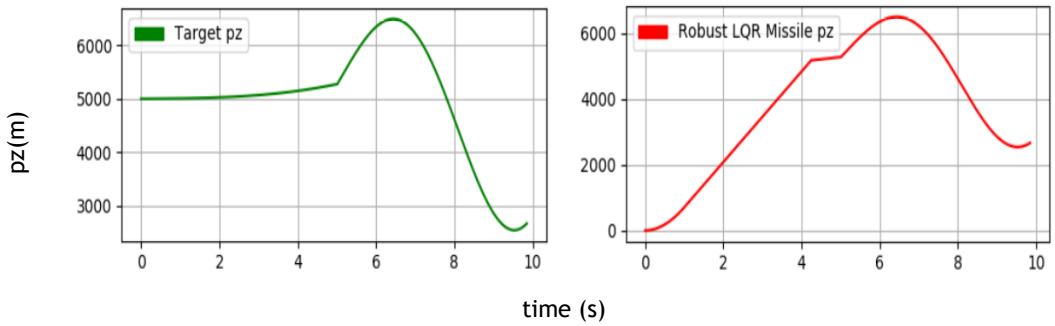

Figure 4.30. Target and missile course using LQR Robust control in two dimensions for X3.2

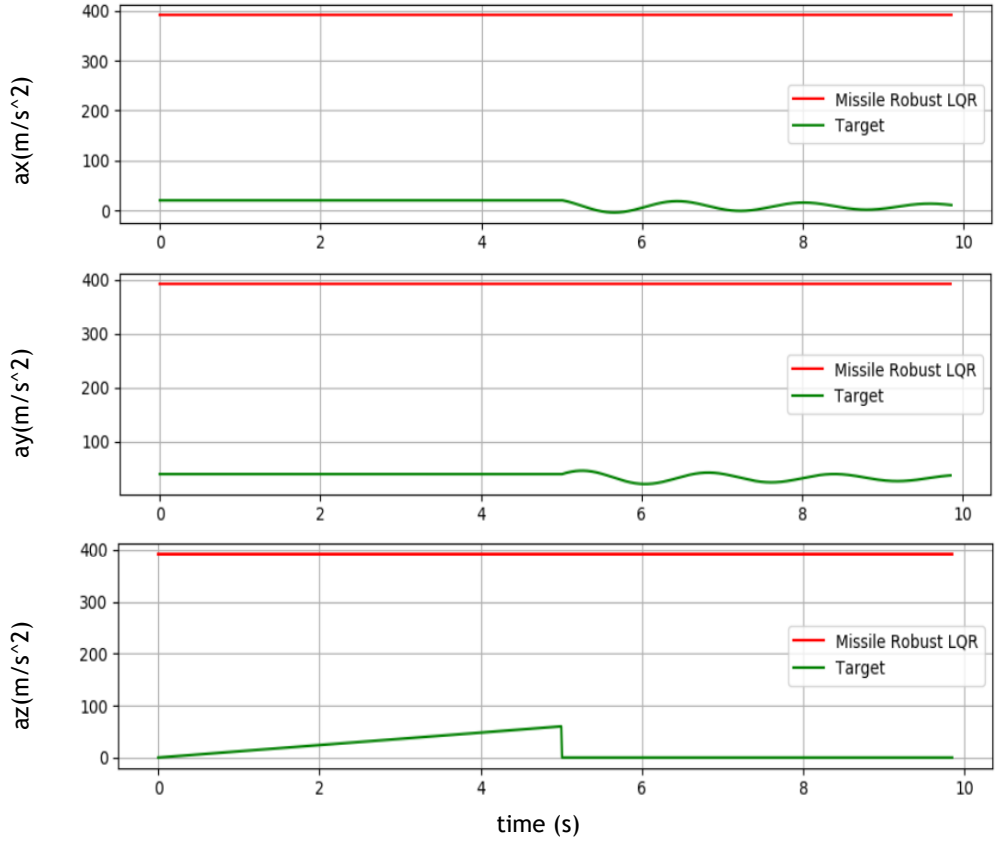

Figure 4.31. Missile and target acceleration until the intersection occurs using Robust LQR method for X3.2

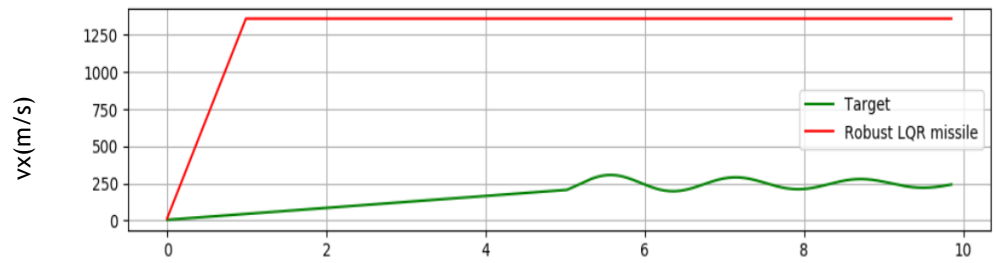

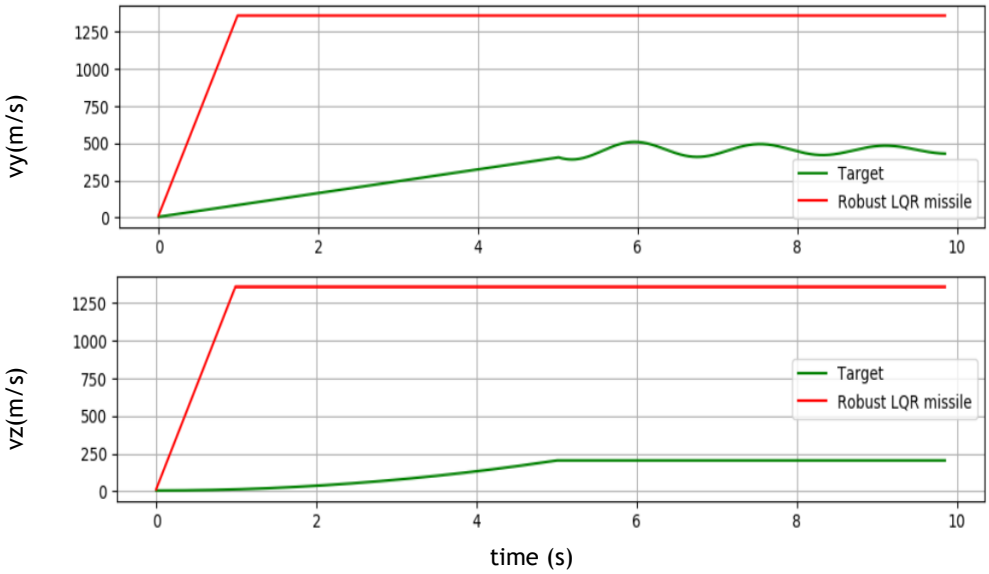

Figure 4.32. Missile and target velocity until the intersection occurs using Robust LQR method for X3.

4.2.1.2.2. Hinfinit/LTR Control

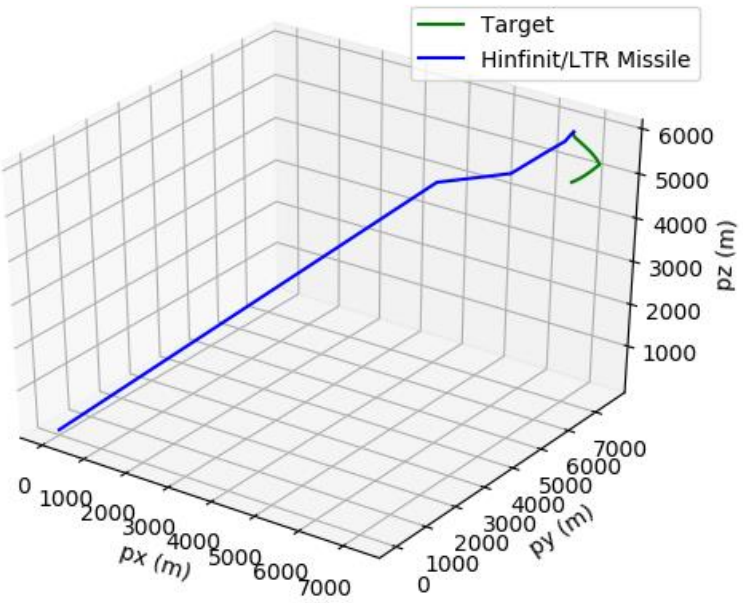

Figure 4.33. Intersection of target and missile using Hinfinit/LTR control in three dimensions for X3.2

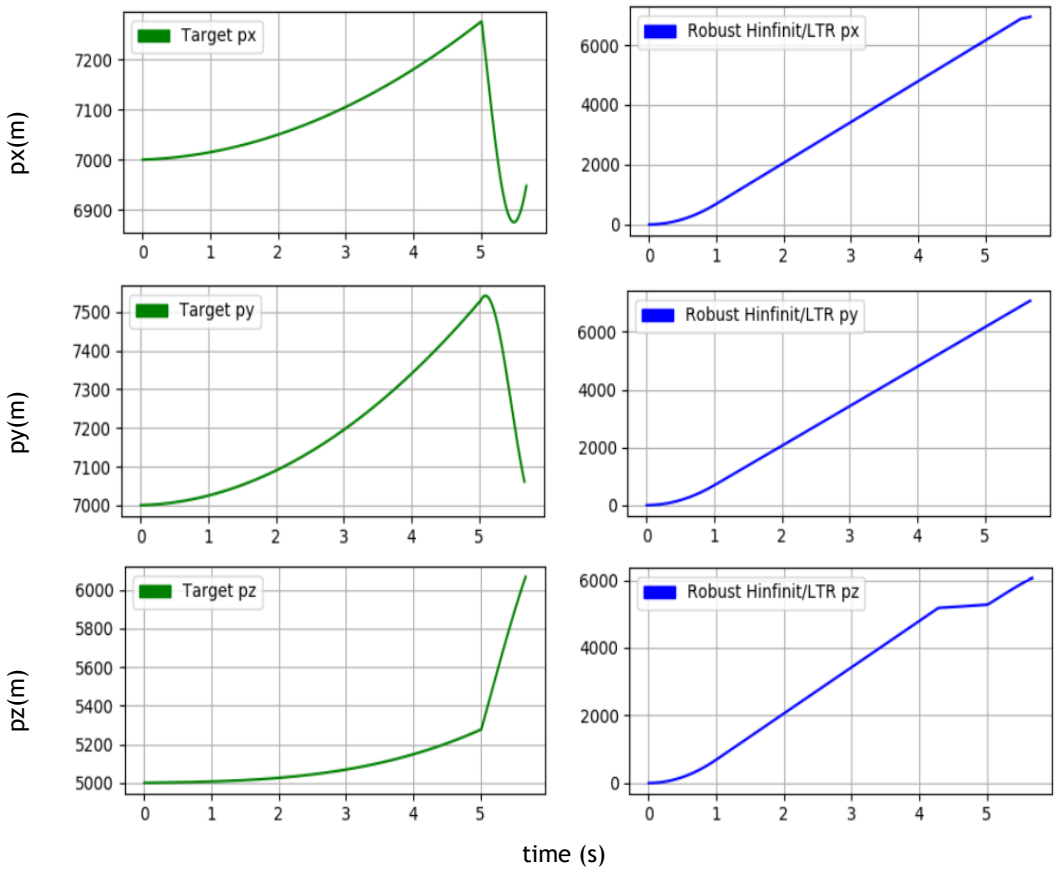

Figure 4.34. Target and missile course using Hinfinit/LTR control in two dimensions for X3.2

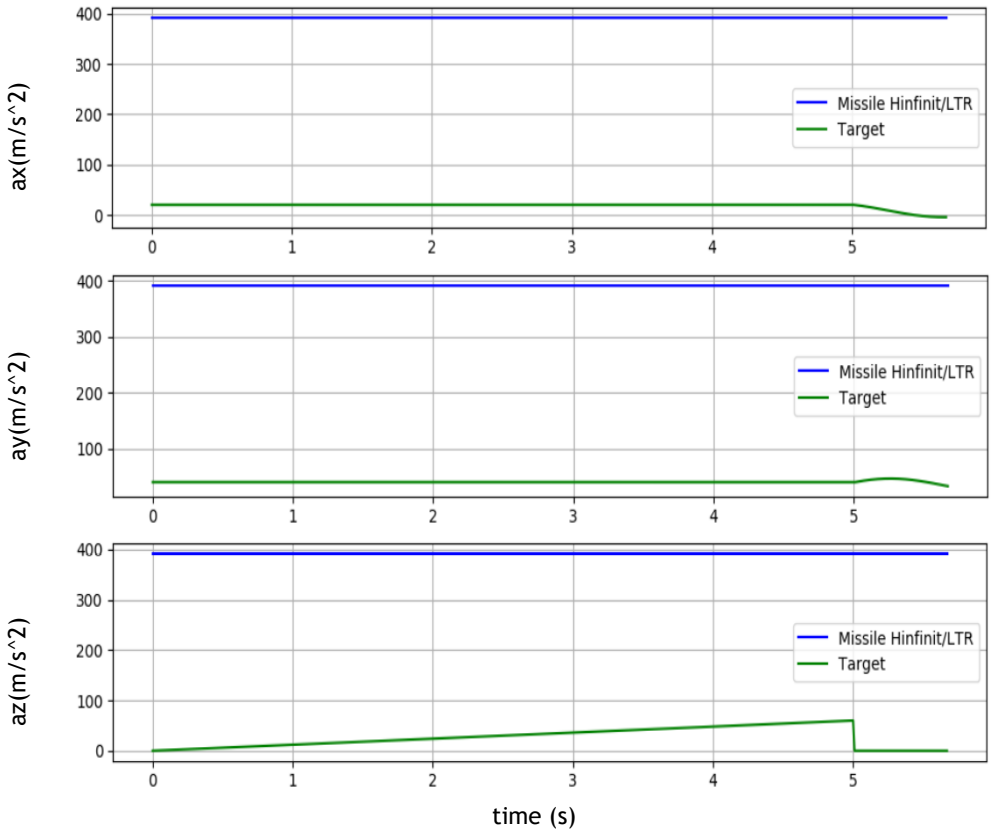

Figure 4.35. Missile and target acceleration until the intersection occurs using Hinfinit/LTR method for X3.2

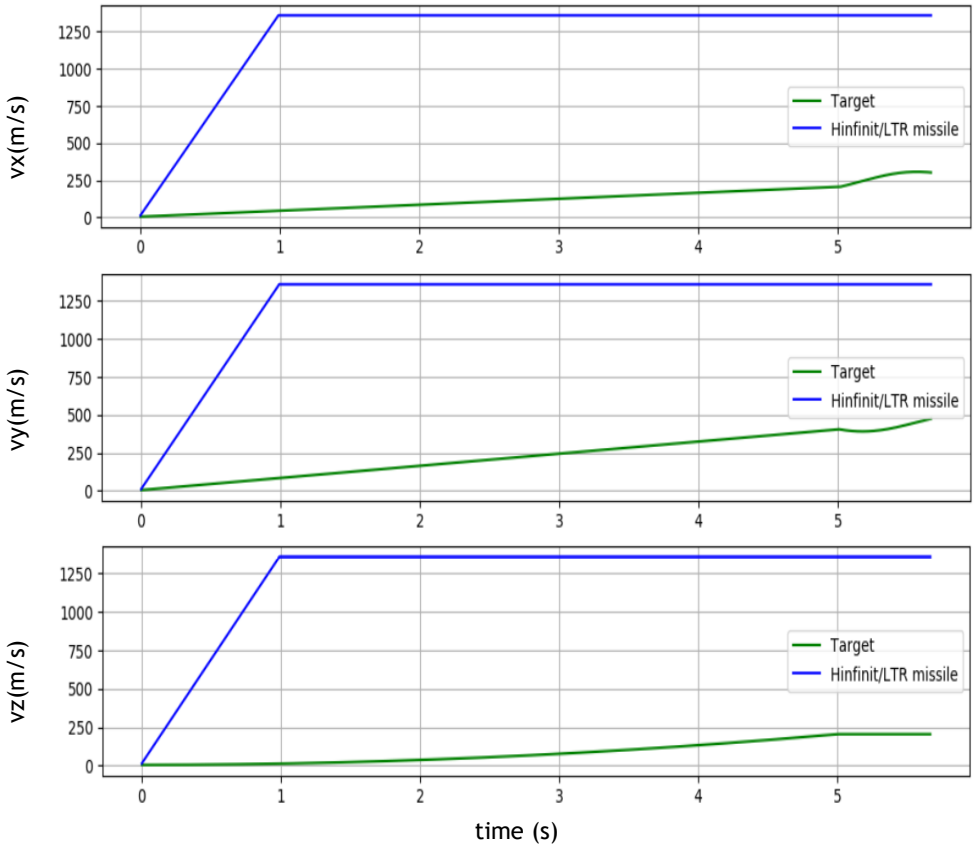

Figure 4.36. Missile and target velocity until the intersection occurs using Hinfinit/LTR method for X3.2

Still for the first evasive manoeuvre, but now with the detecting time starting at 5 seconds, H_∞/LTR method continues to be faster than the Robust LQR method, where the intersection for the first method occurred at 5.67 seconds while for the second method occurred at 9.85 seconds (the difference between both methods is more visible in this case with a difference of 4.18).

As explained before, missile course is maintained until the evasive manoeuvres are initiated. Therefore, for the Robust LQR controller, the missile does not have time to adjust the route for the new target trajectory, needing more time to calculate and follow the course. However, for the H_∞/LTR controller, the fact that the target initiates a new trajectory almost at the impact time does not affect the missile behaviour and the proper corrections are made to ensure the mission success.

4.2.2. Implementation of the first evasive manoeuvre trajectory X4

4.2.2.1. Engagement Manoeuvres for X4.1

4.2.2.1.1. Robust LQR Control

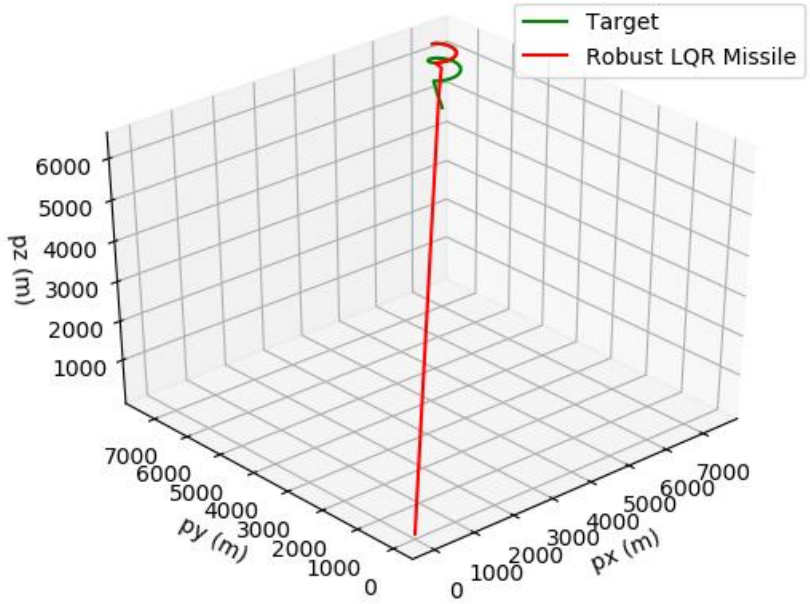

Figure 4.37. Intersection of target and missile using Robust LQR control in three dimensions for X4.1

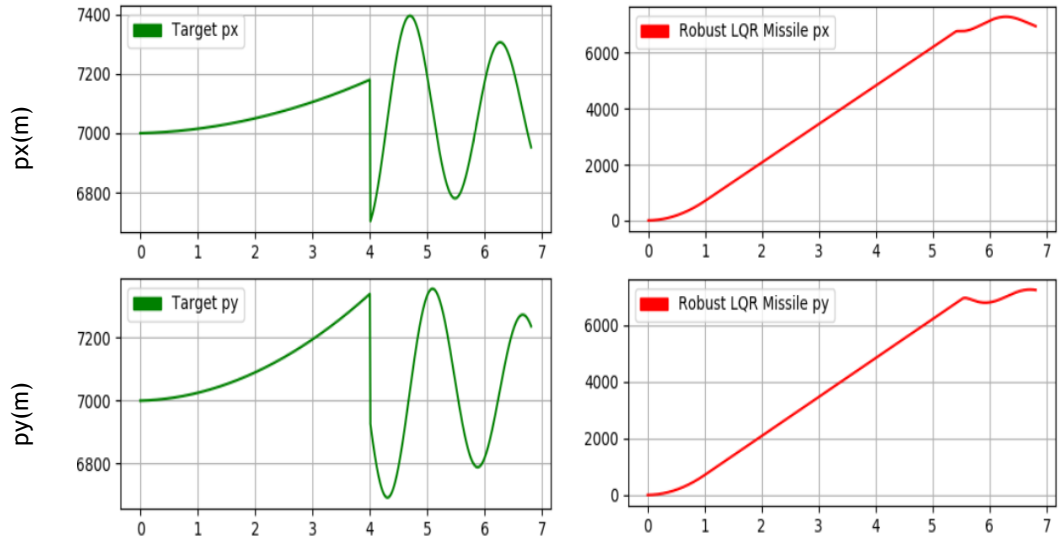

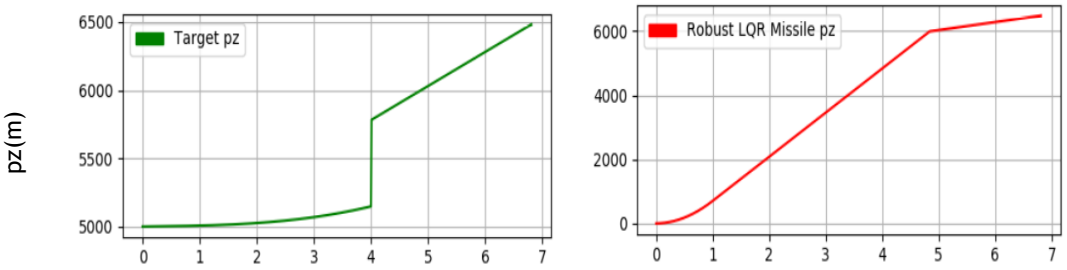

Figure 4.38. Target and missile course using LQR Robust control in two dimensions for X4.1

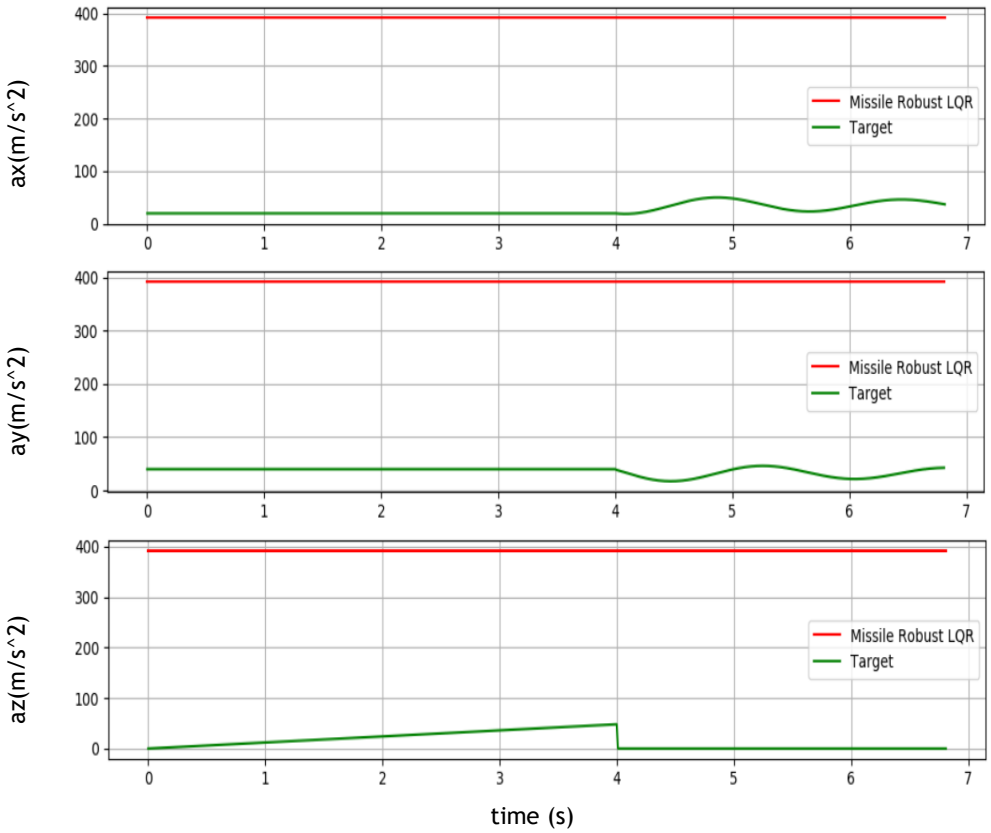

Figure 4.39. Missile and target acceleration until the intersection occurs using Robust LQR method for X4.1

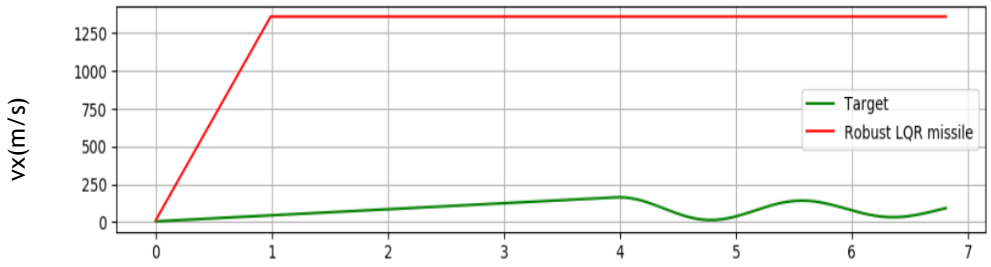

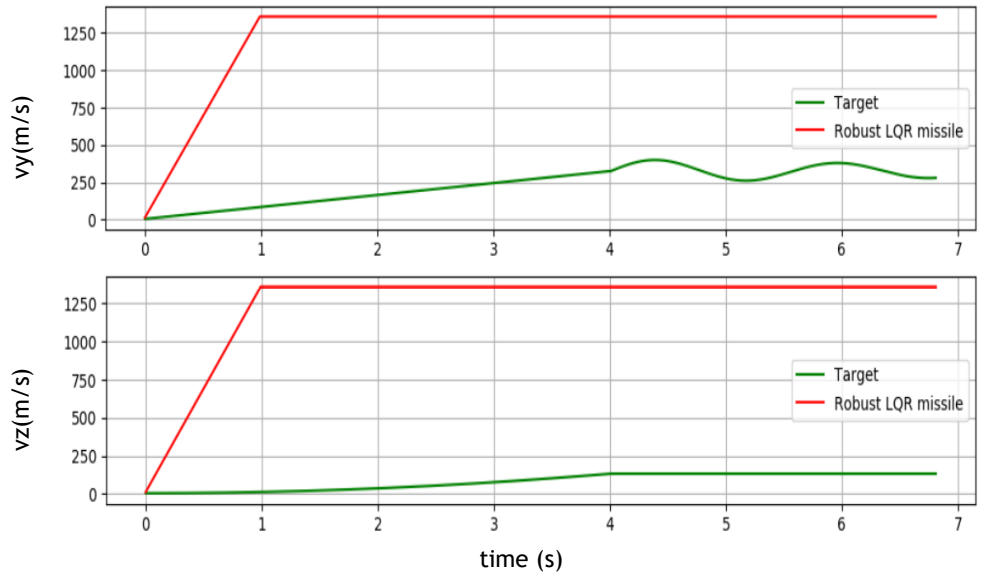

Figure 4.40. Missile and target velocity until the intersection occurs using Robust LQR method for X4.1

4.2.2.1.2. Hinfinit/LTR Control

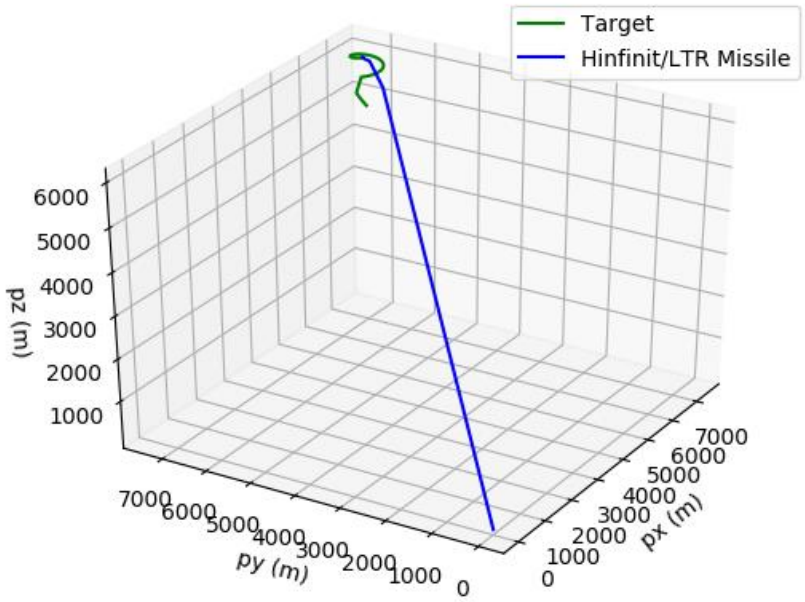

Figure 4.41. Intersection of target and missile using Hinfinit/LTR control in three dimensions for X4.1

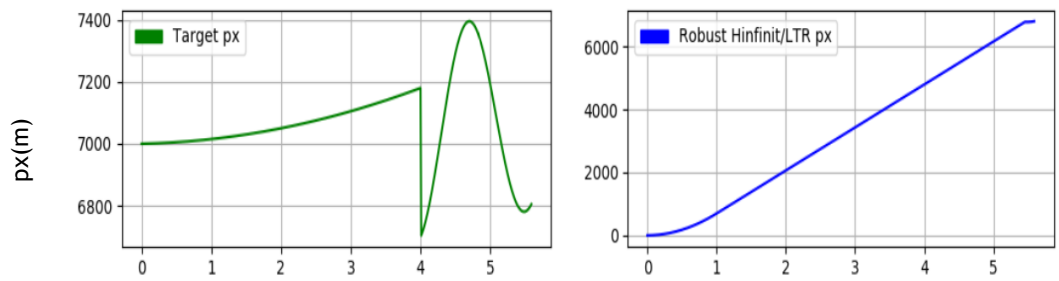

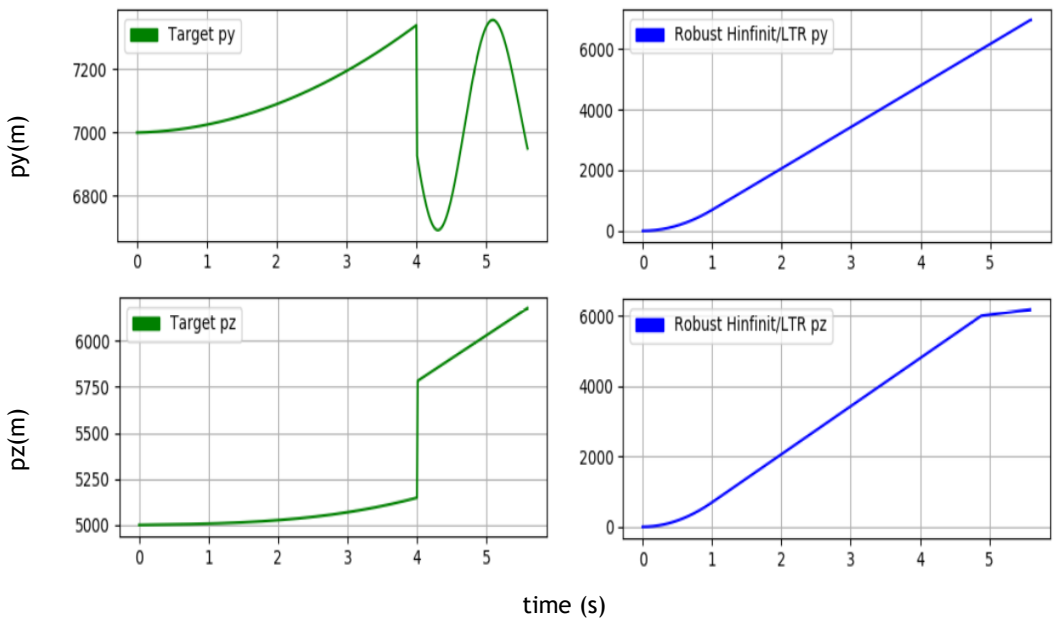

Figure 4.42. Target and missile course using Hinfinit/LTR control in two dimensions for X4.1

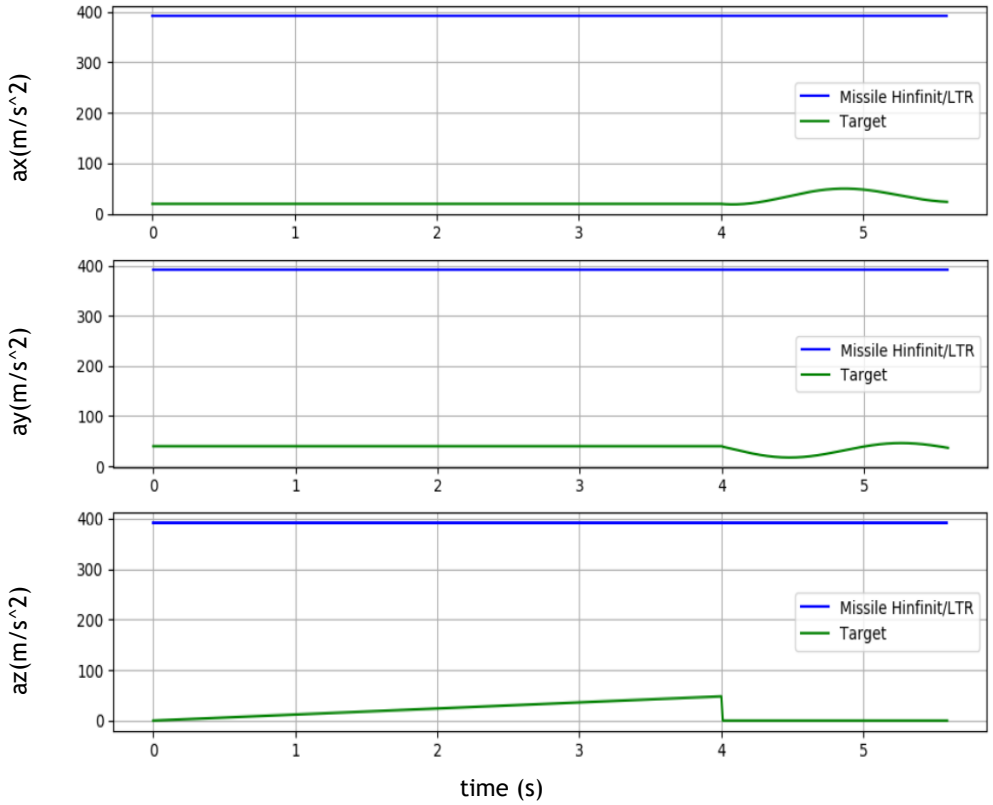

Figure 4.43. Missile and target acceleration until the intersection occurs using Hinfinit/LTR method for X4.1

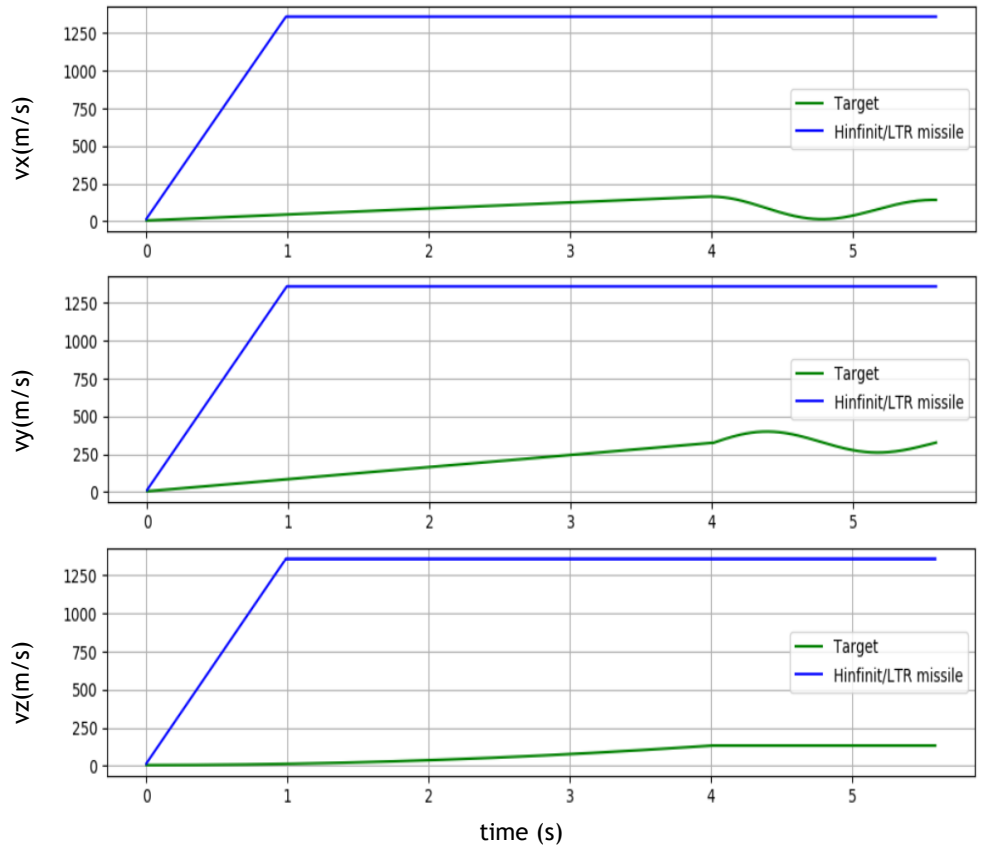

Figure 4.44. Missile and target velocity until the intersection occurs using Hinfinit/LTR method for X4.1

For this simulation, where the target detects the pursuer and initiates the respective evasive manoeuvres at 4 seconds, the H_∞/LTR controller as a better performance, as expected. It is possible to analyse the trajectory of both methods in figures 4.37 and 4.41 in 3D, where the required time for a successful intersection on the H_∞/LTR controller is 5.59 seconds, while on the Robust LQR controller is 6.81 seconds.

As in the previous case, missile course is maintained until the evasive manoeuvres are initiated. After that, it needs to adjust the new route. From figures 4.38, 4.40, 4.42 and 4.44, the velocity, as well the new target and missile course can be analysed in 2D, where an abrupt climb and a variation of speed while performing a spiral is made by the target. Target and missile velocity influence directly the acceleration, as shown in figures 4.39 and 4.43.

4.2.2.2. Engagement Manoeuvres for X4.2

4.2.2.2.1. Robust LQR Control

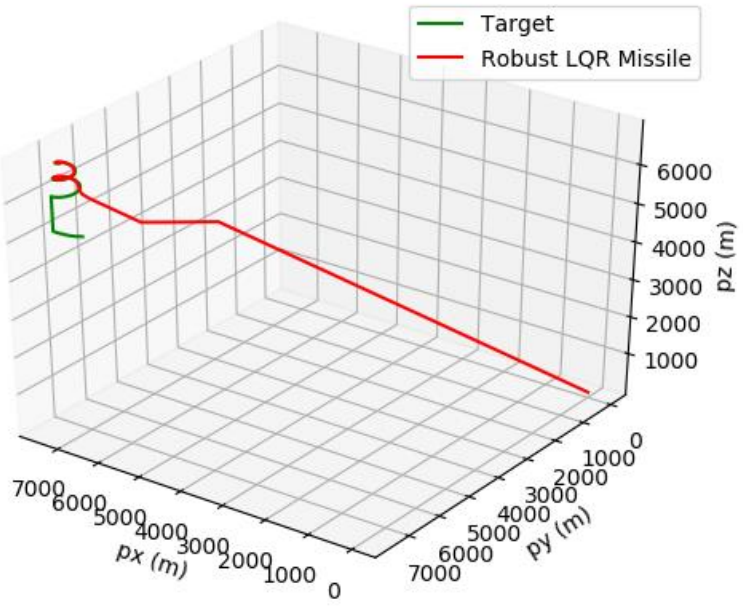

Figure 4.45. Intersection of target and missile using Robust LQR control in three dimensions for X4.2

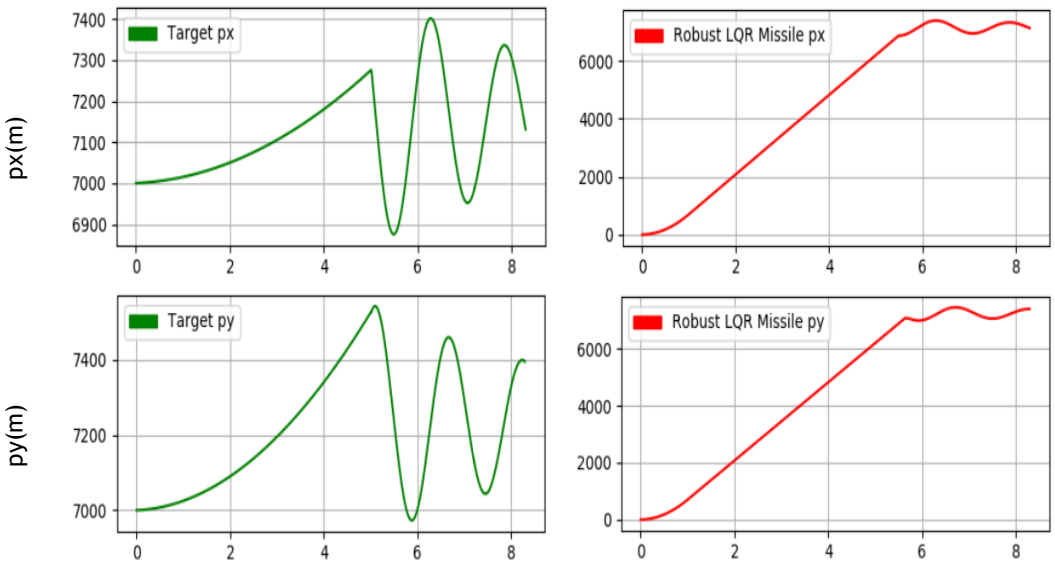

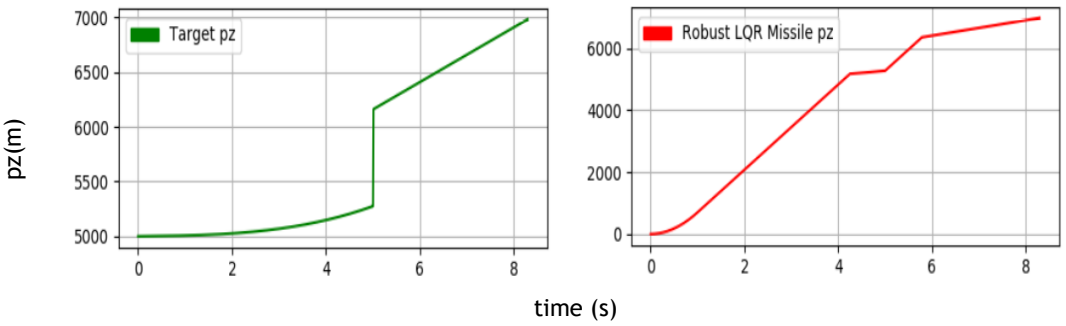

Figure 4.46. Target and missile course using Robust LQR control in two dimensions for X4.2

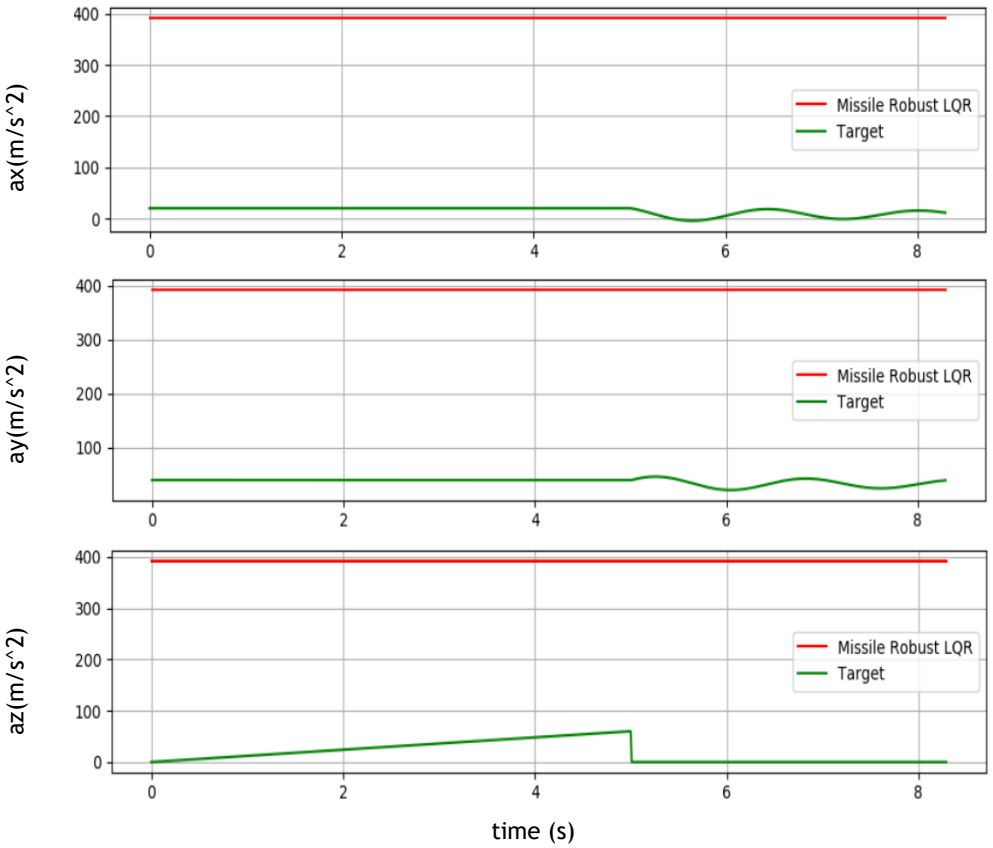

Figure 4.47. Missile and target acceleration until the intersection occurs using Robust LQR method for X4.2

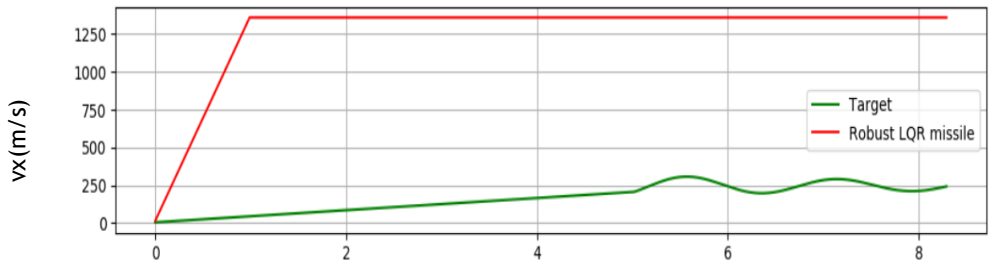

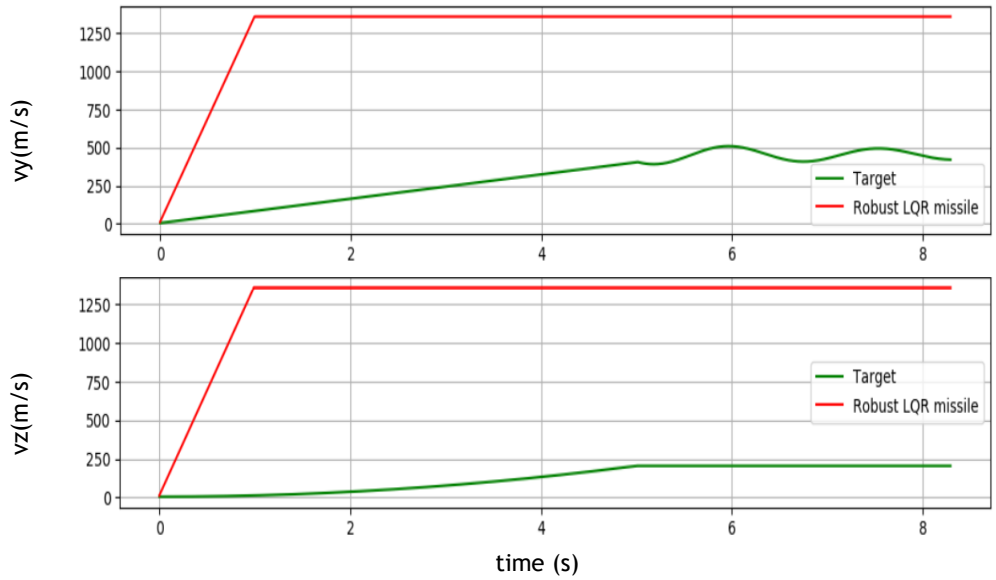

Figure 4.48. Missile and target velocity until the intersection occurs using Robust LQR method for X4.2

4.2.2.2.2. Hinfinit/LTR Control

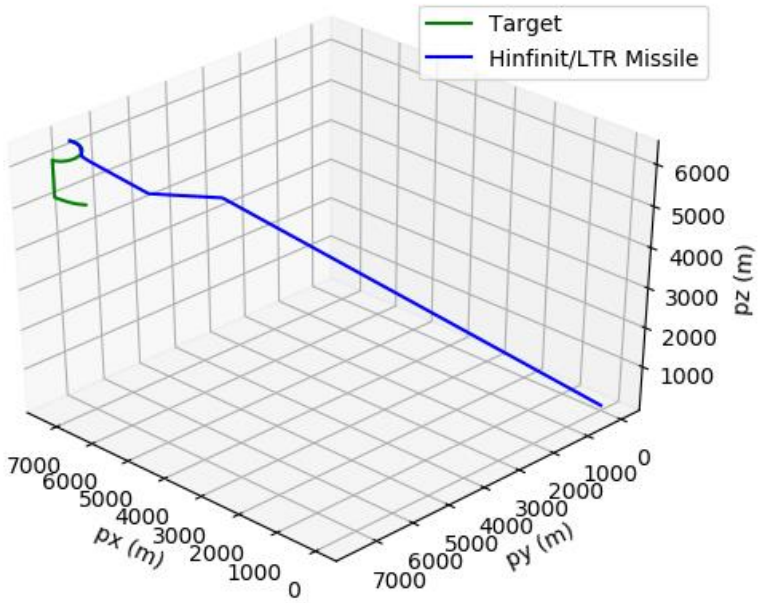

Figure 4.49. Intersection of target and missile using Hinfinit/LTR control in three dimensions for X4.2

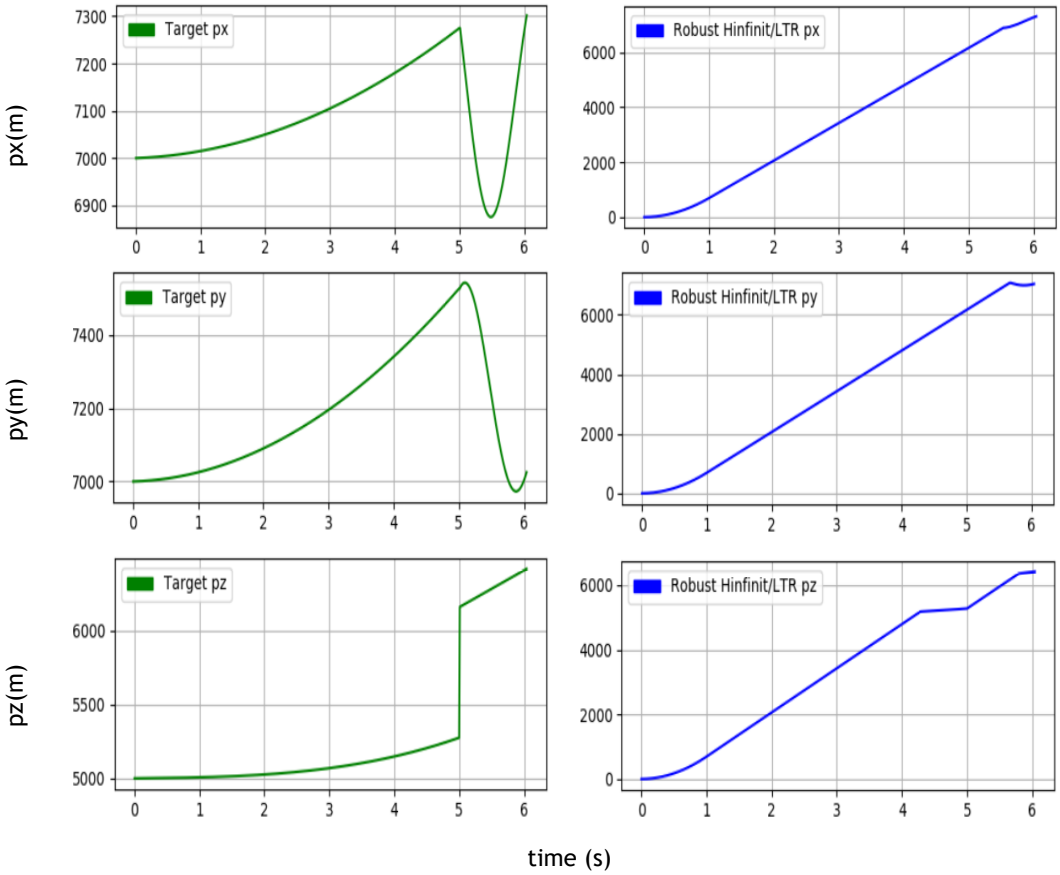

Figure 4.50. Target and missile course using Hinfinit/LTR control in two dimensions for X4.2

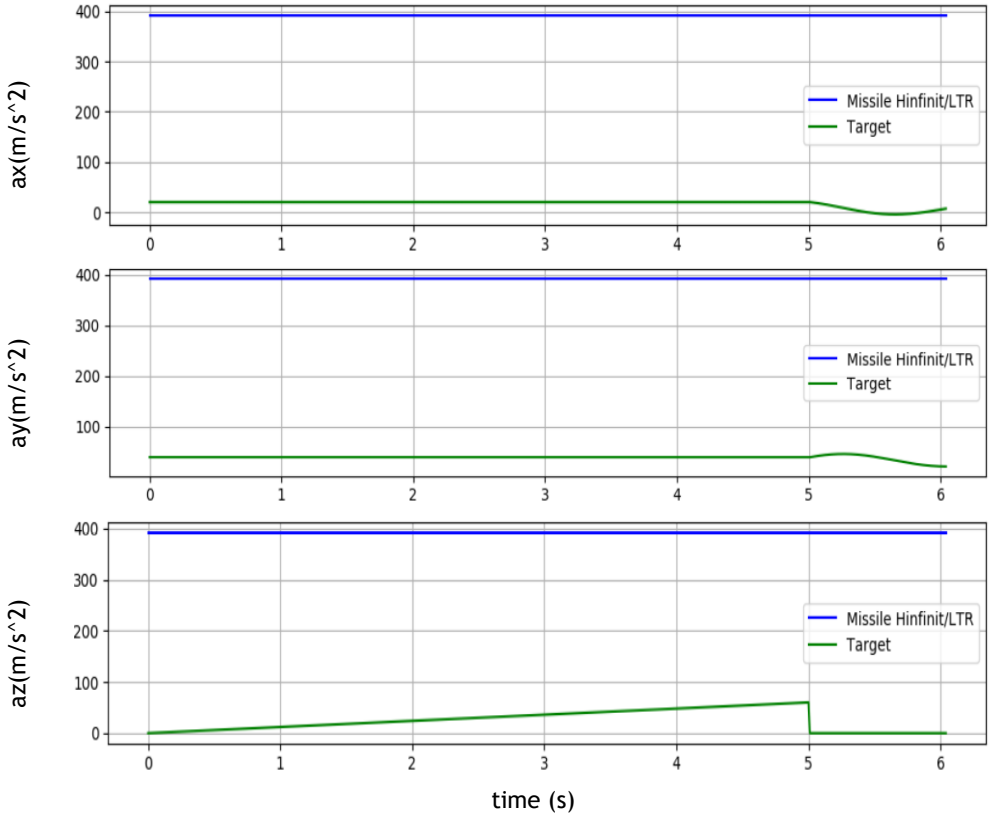

Figure 4.51. Missile and target acceleration until the intersection occurs using Hinfinit/LTR method for X4.2

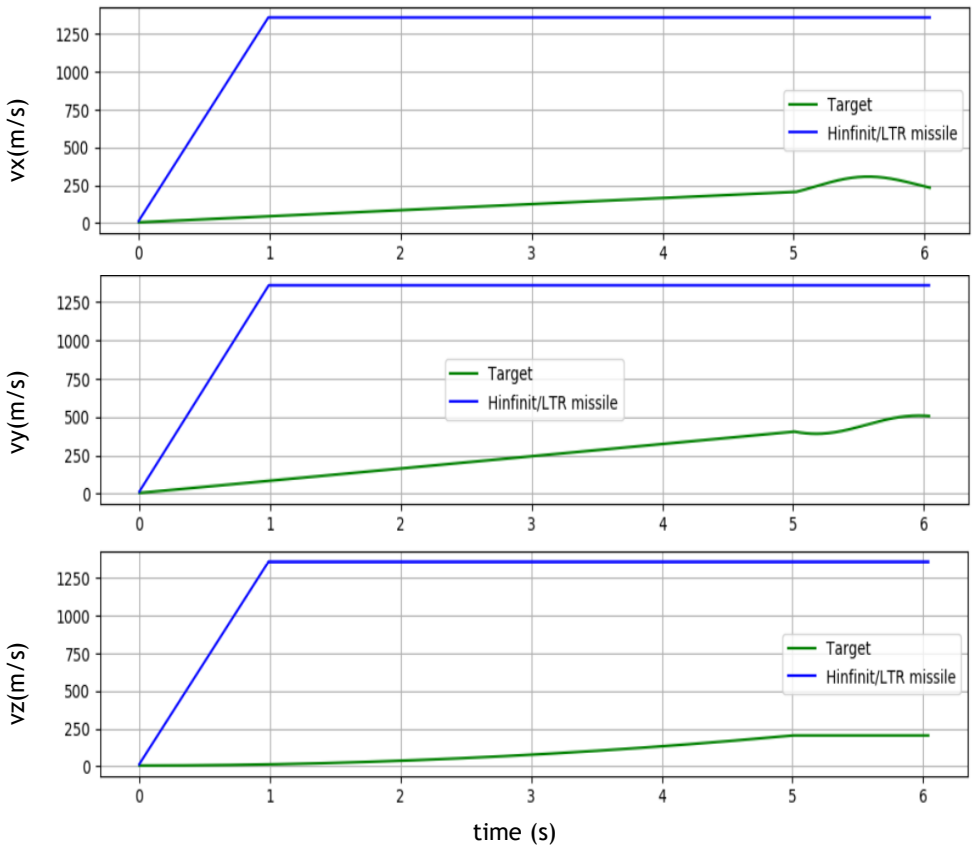

Figure 4.52. Missile and target velocity until the intersection occurs using Hinfinit/LTR method for X4.2

For this specific case with the evasive manoeuvres starting at 5 seconds, the H_∞/LTR controller is 2.25 seconds faster than the Robust LQR controller (missile intersection using Hinfinit occurs at 6.04 seconds while Robust LQR intersection occurs at 8.29 seconds).

As in the study case X3.2, Robust LQR controller needs more time to calculate and follow the new target trajectories. However, for the H_∞/LTR controller, the fact that the target initiates a new trajectory almost at the time of impact does not affect the missile behaviour, being the proper corrections made and the difference between the case X4.1 and X4.2 less than 1 second.

Chapter 5

Contributions and Future works

5.1. Contributions

The law of orientation is the feedback of the algorithm in which the geometrical rule is implemented, being this a line passing through the object being guided (LOS). In the first generation of CLOS guided missiles, the tracing was manual, an operator had to keep the target image in its FOV, which could range from a simple pair of binoculars to a radar or a television screen. Already in the second generation of CLOS-guided missiles, only the target tracking is manual, all other functions, including those of tracking the missile, are made automatically. In the auto-tracking case, a seeker is mounted on a platform that has sufficient mechanical mobility to allow the fulfilment of the mission (in most cases two degrees of freedom are sufficient, being these the azimuth, which is the angular distance measured on the horizon, and the elevation). Finally, in a two-point system, the seeker is implemented on the missile, in a platform named gimbal.

As technology evolves, the interaction between man and machine is becoming smaller, making the systems more and more precise. However, no system is infallible.

Being the main objective of this research the implementation of a H_∞/LTR controller in a SAM and AAM, it is possible to conclude that it allows a slightly faster intersection than the robust LQR controller for a non-manoeuvring target, but can have a much better performance regarding a manoeuvring target. For the first study case, although the differences between both methods are in the thousandths of a second (more precisely 0.86 seconds for X1 and 0.92 seconds for X2), in a tactical missile this difference may lead to the success or failure of the mission. Regarding the manoeuvring target with two different routes, the differences between both methods are more significant. H_∞/LTR controller has a much more systematic trajectory, with very similar results and times for the impact, where the fact of changing the evasive manoeuvres initiating time does not present a problem to this method. Nevertheless, the same cannot be concluded from Robust LQR controller. This method has a worst performance for all the cases presented and when the evasive manoeuvres initiating time is changed, this controller needs more time to calculate and follow the new target trajectories, having significant differences on the impact time.

However, it is necessary to take into consideration that changing the missile and target g-force and Mach number will have a direct impact on the results, which also depends on the matrices Q and R. Moreover, the change in the parameter values will also have a direct impact on the operation of the H_∞/LTR controller.

5.2. Future Works

In the context of this dissertation, many topics can be developed given its complexity. The development of a Homing Guided missile (being explored the active, semi-active and passive controllers), the implementation of a command guidance and a beam-rider guidance, as well as the application of the velocity pursuit would complement this work.

Regarding the pursuit modelling associated to guidance (proportional navigation or collision Homing), the implementation of its variants (PPN, GTPN and IPN) would be significant because it is by far the most important approach regarding all the classical guidance laws.

Also, the implementation of a H_∞ controller would be a good addiction to the work already developed in this dissertation.

Bibliography

[1] N.A. Shneydor, *Missile guidance and pursuit: kinematics, dynamics and control* (Coll House, Westergate, Chichester, West Sussex ,1998)
[Online]. Available: https://doi.org/10.1533/9781782420590.129 (Consultation date: 08/02/2018).

[2] Ross Jr., Frank, *Guided missiles: rockets & torpedoes* (Lothrop, Lee & Shepard, 1951).

[3] Gatland, Keneeth W., *Development of the guided missile* (Iliffe, 1952).

[4] Spearman, M. Leroy, Historical development of worldwide guided missiles, *NASA Technical Memorandum 85658* (1983).

[5] Zarchan, P., *Ballistic missile defense guidance and control issues* (Gordon and Breach Science Publishers SA, 1998, pp. 99-124).
[Online]. Available: https://doi.org/10.1080/08929889908426470 (Consultation date: 12/02/2018).

[6] N. Jack, *Missile Aerodynamics* (United Sates of America, McGraw-Hill Company, Inc, 1960).

[7] R. L. Robert, *Fighter Combat: Tactics and Maneuvering* (United States of America, United States Naval Institute, 1987). [Online]. Available:
http://books.google.nl/books/about/Fighter_Combat.html?id=hBxBdKr0beYC&redir_esc=y
(Consultation date: 12/02/2018).

[8] Yu M., Oh H., Chen W., Multiple Model Ballistic Missile Tracking with State-Dependent Transitions and Gaussian Particle Filtering, *Institute of Electrical and Electronics Engineers (IEEE) 54(3), (2017), 1066-1081.*

[9] Ghose D., *Guidance of Missiles,* NPTEL COURSE of Guidance, Control and Decision Systems Laboratory, Department of Aerospace Engineering (Bangalore, India, 2012). [Online]. Available:
http://nptel.ac.in/courses/101108054/1 (Consultation date: 20/02/2018).

[10] Neil. F. Palumbo, Guest Editor's Introduction : Homing Missile Guidance and Control, *Johns Hopkins APL Technical Digest, 29(1), (2010), 2-8.* [Online]. Available:
http://www.jhuapl.edu/techdigest/td/td2901/palumbo_guesteditor.pdf (Consultation date: 12/02/2018).

[11] Puertas A. A., Echevarría J. A., *ARMAMENTO NAVAL I*, División de Publicaciones de la Escuela Superior de Guerra Naval (Peru, 2013) [Online]. Available:

http://virtual.esup.edu.pe/bitstream/ESUP/29/1/Armamento%20Naval%20I.pdf (Consultation date: 02/03/2018).

[12] SAN FRANCISCO MARITIME NATIONAL PARK ASSOCIATION, (2013), 126-200. [Online]. Available: https://maritime.org/doc/missile/part2.htm (Consultation date: 02/03/2018).

[13] Naval Education, *Gunner's Mate Missile M 3 & 2* (Periscope Film LLC, 2013). [Online].Available: https://www.okieboat.com/GMM/GMM%203%20and%202%20CHAPTER%203%20Principles%20of%20Missile%20Flight%20and%20Jet%20Propulsion.pdf (Consultation date: 03/03/2018).

[14] Aránguez P. S., ESCUELA TÉCNICA SUPERIOR DE INGENIEROS AERONÁUTICOS (Madrid). Misiles, Temas 18 a 33. Cuarto Curso (Plan 95), 2º Cuatrimestre (1998).

[15] 4º Ingenieros Aeronáuticos (Valencia). Aeronaves, Astronáutica e Ingeniería Espacial. Misiles I.

[16] Siouris G. M., Missile Guidance and Control Systems, *The American Society of Mechanical Engineers (ASME) (2005) 57(6).* [Online] Available: https://doi.org/10.1115/1.1849174 (Consultation date: 10/03/2018).

[17] SAN FRANCISCO MARITIME NATIONAL PARK ASSOCIATION, (2013), *INTRODUCTION TO ROCKET AND GUIDED MISSILE FIRE CONTROL*, PART J, 1-23. [Online]. Available: https://maritime.org/doc/firecontrol/partj.htm (Consultation date: 10/03/2018).

[18] Costa M., *Orientação de mísseis interceptores com base no método dos Reguladores Quadráticos Lineares (LQR) com estimação de trajetórias*, MSc. Dissertation, Dept. Aero. Sci., University of Beira Interior (UBI), Covilhã, 2017.

[19] Berglund E., *Guidance and Control Technology*, Defense Technical Information Center Compilation Part Notice ADP010953, *Proceedings of the RTO SCI Lecture Series on "Technologies for Future Precision Strike Missile Systems" (2001).*

[20] Raj K. D. S., Performance Evaluation of Proportional Navigation Guidance for Low-Maneuvering Targets, *International Journal of Scientific & Engineering Research* 5(9), *(2014),* 93–99.

[21] Palumbo N. F., Blauwkamp R. A., Lloyd J. M., Basic principles of homing guidance, *Johns Hopkins APL Technical Digest (Applied Physics Laboratory) 29(1), (2010), 25–41.*

[22] Zarchan P., *Tactical and Strategic Missile Guidance* (Fifth Edition), American Institute of Aeronautics and Astronautics (AIAA) (2007).

[23] István P., László S. V., Gyula Ó, Derivation of the Fundamental Missile Guidance Equations, *Atlantic Association for Research in the Mathematical Science (AARMS) 14(4), (2015), 341-348.*

[24] Siouris, G. M., An Engineering Approach to Optimal Control and Estimation Theory, *IEEE Aerospace and Electronic Systems Magazine (1997)* (Vol. 12).

[25] Williams II R., Lawrence D., *Linear State-Space Control Systems*, Wiley (2007).

[26] Tan H., Shu S, Lin F., An optimal control approach to robust tracking of linear systems, International Journal of Control 82(3), (2009), 525-540 [Online]. Available: http://www.ece.eng.wayne.edu/~flin/Journal/Robust%20Tracking%20IJC.pdf (Consultation date: 15/03/2018).

[27] Liu X., Wu Y., Xiao S., A Control Method to Make LQR Robust: A Planes Cluster Approaching Mode, *International Journal of Control, Automation and Systems (IJCAS) 12(2), (2014), 302-308*. [Online]. Available: https://link.springer.com/content/pdf/10.1007/s12555-012-0435-0.pdf (Consultation date: 15/03/2018).

[28] Tripathy N. S., Kar I. N., Paul K., Stabilization of Uncertain Discrete-Time Linear System with Limited Communication, *Institute of Electrical and Electronics Engineers (IEEE) 62(9), (2016), 4727-4733*. [Online]. Available: https://doi.org/10.1109/TAC.2016.2626967 (Consultation date: 18/03/2018).

[29] PETERSEN I. R., HOLLOT C. V., A Riccati Equation Approach to the Stabilization of Uncertain Linear Systems, *International Federation of Automatic Control (IFAC) 22(4), (1986), 397-411.*

[30] Lin L. G., *Nonlinear Control Systems: A "State-Dependent (Differential) Riccati Equation" Approach" Approach*. (Faculteit Ingenieurswetenschappen KU Leuven, 2014). [Online]. Available: https://lirias.kuleuven.be/bitstream/123456789/460411/1/thesis.pdf (Consultation date: 20/03/2018).

[31] Margarido P., *Flight dynamics and simulation of a generic aircraft for aeroservoelastic design,* Instituto Superior Técnico de Lisboa (2016).

[32] Jia Luo, C. E. Lan. Determination of weighting matrices of a linear quadratic regulator, *Journal of Guidance, Control, and Dynamics (JGCD), 18(6), (1995), 1462-1463.*

[33] S. Antunes, *Controlo Óptimo Robusto de Osciladores Caóticos*, MSc. dissertation, Dept. Aero. Sci., University of Beira Interior (UBI), Covilhã, 2009.

[34] Z. Artstein, Stabilization with Relaxed Controls*, Nonlinear Analysis, Theory, Methods & Applications* 7(11), *(1983),* 1163-1173.

[35] O. Föllinger, *Regulation Technology*, (Hüthig Heidelberg, 1990).

[36] Jackson P. B., Overview of missile flight control systems, *Johns Hopkins APL Technical Digest 29(1), (2010), 9-24.*

[37] Watts G. L., McCarter J. W., Missile Aerodynamics for Ascent and Re-entry, *Marshall Space Flight Center under Contract of National Aeronautics and Space Administration (NASA), (2012).*

[38] Diseño de un Sistema Avanzado de Guiado y Control para Misiles con Doble Mando Aerodinámico, UNIVERSIDAD POLITÉCNICA DE MADRID, (2016).

[39] Savkin A. V., Pathirana P. N., Faruqi F. A., Problem of Precision Missile Guidance: LQR and H_∞ Control Frameworks, *Institute of Electrical and Electronics Engineers (IEEE) 39(3), (2003), 901-910.*

[40] Shinar J., Rotsztein Y., Bezner E., (1978). Analysis of Three-Dimensional Optimal Evasion with Linearized Kinematics, *American Institute of Aeronautics and Astronautics (AIAA) 2(5), (1979), 353-360.*

[41] Toivonen H. T., *Robust Control Methods,* Abo Akademi University, Finland (1998). [Online]. Available: http://users.abo.fi/htoivone/courses/robust/rob4.pdf (Consultation date: 30/03/2018).

[42] Ferreira L. H. C., Cunha F. H. R., Paula C. F., *Um Procedimento Simplificado De Síntese De Controladores H_∞/ LTR Para O PROBLEMA DE SENSIBILIDADE MISTA*, Proceedings of the 18th National Brazilian of automatic conference (2010) [Online]. Available: https://www.researchgate.net/profile/Luis_Ferreira3/publication/228902226_UM_PROCEDIMENTO_SIMPLIFICADO_DE_SINTESE_DE_CONTROLADORES_HLTR_PARA_O_PROBLEMA_DE_SENSIBILIDADE_MISTA/links/553d587d0cf245bdd76ab8e8/UM-PROCEDIMENTO-SIMPLIFICADO-DE-SINTESE-DE-CONTROLADORES-H-LTR-PARA-O-PROBLEMA-DE-SENSIBILIDADE-MISTA.pdf (Consultation date: 02/04/2018).

[43] Doyle J. C., Glover K., Khargonekar P. P., Francis B. A., State-space solutions to standard H2 and Hinf control problems, *Institute of Electrical and Electronics Engineers (IEEE) 34(8), (1989), 831-847.* [Online]. Available:

https://authors.library.caltech.edu/3087/1/DOYieeetac89.pdf (Consultation date: 05/04/2018).

[44] Yamaguchi R., Higuchi T., State-space approach with the maximum likelihood principle to identify the system generating time-course gene expression data of yeast, *International Journal of Data Mining and Bioinformatics, 1(1), (2006), 77-87.*

[45] Chen C., On the Robustness of Linear Quadratic Regulator via Perturbation Analysis of the Riccati Equation, Ph.D. dissertation, Dublin City University (DCU), (2014). Available: http://doras.dcu.ie/20260/1/PhD_Thesis_Ci_Chen_DCU_Blue_2_Hard_Copies.pdf (Consultation date: 07/04/2018).

[46] Dray T., Manogue C., The Geometry of the Dot and Cross Products, *Journal of Online Mathematics and Its Applications*, (2006) Article ID 1156.

[47] Fresconi F., Celmins I., Silton S., *Theory, Guidance, and Flight Control for High Maneuverability Projectiles*, U.S. Army Research Laboratory (2014). Available: http://www.arl.army.mil/arlreports/2014/ARL-TR-6767.pdf (Consultation date: 09/04/2018).

[48] Gkritzapis D., Kaimakamis G., Siassiakos K., Chalikias M., A Review of Flight Dynamic Simulation Model of Missiles, *Proceedings of the 2nd European Computing Conference (ECC) (2008), 257-261.*

Appendix A

A.1. Numerical Resolution of Ordinary Equations (Butcher Algorithm)

Butcher Algorithm allows to obtain the state x from the differential equation $\dot{x}$.This algorithm comes from the Runge Kutta method of order six (consisting in six equations that make Butcher Algorithm very precise) to be able to establish the next state (x_{n+1}).
The model of a controlled system is described as:

$$\dot{x} = f(x, u) \qquad \text{(A.1)}$$

where $x \in R^n$ is the state vector and $u \in R^r$ is the control vector. Now, the six functions of the Runge Kutta method are given by:

$$\begin{aligned}
k_1 &= h * f(x_k, u_k) \\
k_2 &= h * f\left(x_k + \frac{k_1}{4}, u_k\right) \\
k_3 &= h * f\left(x_k + \frac{k_1}{8} + \frac{k_2}{8}, u_k\right) \\
k_4 &= h * f\left(x_k - \frac{k_2}{2} + k_3, u_k\right) \\
k_5 &= h * f\left(x_k + \frac{3k_1}{16} + \frac{9k_4}{16}, u_k\right) \\
k_6 &= h * f\left(x_k - \frac{3k_1}{7} + \frac{2k_2}{7} + \frac{12k_3}{7} - \frac{12k_4}{7} + \frac{8k_5}{7}, u_k\right)
\end{aligned} \qquad \text{(A.2)}$$

where h is the simulation step, $x_k \equiv x(t_k)$, $u_k \equiv u(t_k)$, $k \in [0,6]$ and $t_k = t_{k-1} + h$.
Finally, the system solution over time taking into account the control u and the initial conditions (t_0 and x_0) is given by:

$$x_{n+1} = x_n + \frac{1}{90}(7k_1 + 32k_3 + 12k_4 + 32k_5 + 7k_6) \qquad \text{(A.3)}$$

Appendix B

A. Costa, K. Bousson

Abstract – *Missiles development are constantly evolving. This is mainly due to the significantly increase in the performance of the missiles means of transportation, allowing bigger and heavier armament, which results directly in much more precise control systems, with a capacity for different types of warheads, as well as an ability to store larger amounts of fuel. Regarding the subject addressed in this document, it should be taking into consideration that a tactical missile has to be quite versatile, as it can either aim to shoot down an aircraft with high manoeuvrability or a cruise missile with a predefined trajectory. A control system for a missile is responsible for its attitude, while the missile guidance system is responsible for controlling its trajectories and, therefore, being able to put it back on the collision course if necessary. The focus of this paper is on the tactical missile trajectory control, which has to be capable of performing the basic function of detecting the signals received by the command, which in its turn will be applied to the control system. An H_∞/LTR controller and the Artstein method applied on a Robust LQR controller were applied to the missile, where it's concluded that the first one shows a better performance for manoeuvrable or non-manoeuvrable targets. However, Robust LQR method reveals a strong potential when implemented to solve systems in which perturbations predominate, thus making the behaviour of the two methods in question very similar*

Keywords: *H_∞ , H_∞ / LTR , Robust LQR, Tactical Missile, Artstein Method*

Nomenclature

A	State Matrix
a	Acceleration
AAM	Air-to-Air Missile
B	Control Matrix
C	Output Matrix
CLOS	Command to Line-of-Sight
FOV	Field of View
G(s)	Process Plant
H	Hamiltonian Matrix
J	Performance Index
K	Controller
K_C	Feedback Matrix
K_F	State Observer Matrix
LFT	Linear Fraction Transformation
LQR	Linear Quadratic Regulator
LTR	Loop Transfer Recovery
LOS	Line-of-Sight
m	Meters
N'	Constant of Proportionality
P	Riccati Solution
p	Positions
Q	Weighting Matrix for the State Variables
R	Real Symmetric Positive Defined Matrix
SAM	Surface-to-Air Missile
SISO	Single Input and Single Output
SI	International System of Units
T	Transposed Matrix
t_0	Initial Time
t_f	Terminal Time
u(.)	Given Element of Ω
u	Plant control input vector
v	Velocity
w	External inputs
x	State vector
y	Measured Variables
z	Error signal
3D	Three-Dimensional Space

I. Introduction

In 1870, the first theory application of a guidance law was made, when Werner von Siemens submitted a proposal to the Prussian ministry of war for a project of guided torpedoes to destroy the enemy vessels and in 1916, it had become the first operational guided-weapon system in history. [1]

To understand the definition of a guided-weapon, first it's necessary to distinguish guidance from navigation. So, guidance is "the process for guiding the path of an object towards a given point, which in general may be moving, which means that the target moves in a way that is not quite predictable and there will be an evader and a pursuer. On the other hand, in navigation there will be one given point (the target) that is fixed, so the pursuer doesn't need to predict the trajectory to occur the intersection. [2]

Since the first operational guided-weapon (the guidance of the proposed torpedo would have been of LOS), this technology has evolved into an exponential way and today guidance is being treated in technological disciplines from the point of view of kinematics, dynamics and control, trying to predict zones of interception, launch envelopes, stability of guidance process, trajectories, accuracy effects, structural limits, costs, energy expenditure and many other topics. [3]-[4]

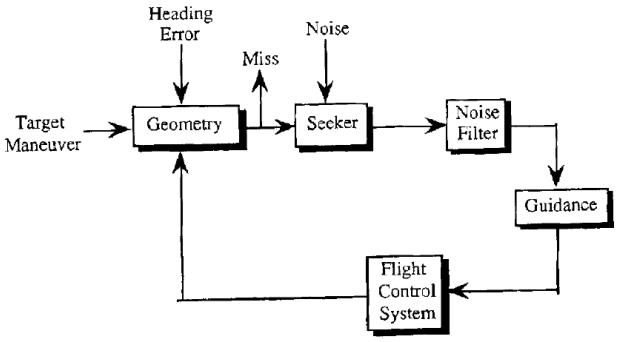

Fig. 1. Missile Guidance system in the form of a control loop [5]

From Fig. 1, it's possible to see how control engineers in today's society implement a guidance system on a missile. Starting with the Geometry section, the missile acceleration is subtracted from target acceleration to obtain a relative acceleration. After that, two integrations will occur to provide the distance and the miss distance will be obtained through the relative separation between the missile and the target (in conventional missiles systems, it is used a warhead to destroy the target, because the missile designer can't eliminate the miss distance).

The missile seeker will attempt to track the target (with the use of a certain filter to smooth the noisy seeker signal) and then a guidance command is generated from the noise filter output. Finally, the flight control system must enable the missile to manoeuvre until the achieved acceleration matches the acceleration commands from the guidance law. [5]

All guidance laws are subjects to errors associated with the law itself, and for this reason, it's impossible to have a 100% flawless law. For example, in the case of the velocity pursuit method, a high demand of lateral acceleration is required, being in most cases infinite at the final phase of the interception. Moreover, it's also very sensitive to target velocity or even the wind, resulting in a finite miss distance. Another example is the proportional navigation, where most of the time the constant of proportionality N' is not a constant, because of the manoeuvrability of the target, which causes errors in the guidance law.

Besides those, one of the most used method, the LQR is also subject to errors (uncertainties), that can't be predicted and will cause instability to the controller.

Taking into account the motivating factors previously discussed, the research carried out in this article has as main objective the implementation of a H_∞/LTR controller, in a SAM and AAM. For the approval of this method, the performance trajectories are compared to a Robust LQR controller using the Artstein Method.

II. LQR Method

Regulator design for a linear time-invariant state equation with the goal of minimizing a quadratic performance index naturally is referred to as a linear quadratic regulator problem. [6]

Consider the continuous-time linear deterministic system that is characterized by the following first equation that concerns the state equation and the second equation that concerns the output equation: [7]-[8]

$$\begin{cases} \dot{x}(t) = A(t)x(t) + B(t)u(t) + \text{ uncertainties} \\ y(t) = C(t)x(t) + \text{ others\_uncertainties} \end{cases} \quad (1)$$

Regarding the performance index (it may also be designated as cost function or objective function) to be minimized, it can be represented by equation:

$$J(x, t_0, t_f, u(.)) = \frac{1}{2}\int_{t_0}^{\infty} \left[x^T(t)Qx(t) + u^T(t)Ru(t) \right] dt \quad (2)$$

For the study of the LQR optimization, it is known that the Riccati equation is directly related to it. If the pair (A, B) is controllable (the solution is always greater than zero) and the pair (Q, A) is detectable, the use of the Riccati equation is valid and possible and its algebraic form is: [9]-[10]

$$0 = PA + A^T P + Q - PBR^{-1}B^T P \quad (3)$$

Note that the pair (A, B) is given by "design" and can't be modified at this stage and the pair (Q, R) is the controller design parameter. Large Q penalizes transients of x and large R penalizes usage of control action u.

Therefore, the assigned weight of the matrices Q and R must be chosen very carefully and for that, two examples are given for the implementation of the respective matrices, being those the Bryson method and the Hamiltonian matrix. Regarding the first example, it suggests that each term of the diagonal matrices is the inverse square of the maximum value expected for the variable on the simulation time. These equations are:

$$Q = diag(Q_i) \quad \text{with} \quad Q_i = \frac{1}{x_{i\max}^2} \quad (4)$$

$$R = diag(R_i) \quad \text{with} \quad R_i = \frac{1}{u_{i\max}^2} \tag{5}$$

where $x_{i\max}^2$ and $u_{i\max}^2$ are the values indicating the extreme of the perturbations wanted for u_i or x_i for the closed loop. [11]

Meanwhile, the second given example suggests that it's possible to determine Q in its ideal form using the following matrix: [12]

$$H = \begin{bmatrix} A & -BR^{-1}B^T \\ -Q & -A^T \end{bmatrix} \tag{6}$$

After obtaining P through the Riccati equation, it's possible to parameterize the control vector with the time varying feedback gain matrix as a linear function of the state vector, being given by: [13]

$$u = -R^{-1}B^T Px \tag{7}$$

III. H_∞ / LTR method

To understand the H_∞-optimal control problem, consider a linear dynamic system with finite dimension and invariant on time, designated as LFT, which can be shown as a basic block diagram (control system diagram) as it follows: [14]

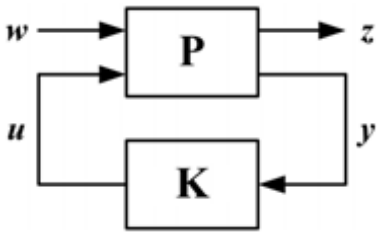

Fig. 2. Block Diagram of the feedback control system [14]

The generalized plant P (also called coefficient matrix for the LFT) contains what is usually called the plant in a control problem, plus all weighting functions, and it is expressed as:

$$P = \begin{cases} \dot{x} = Ax + Bu + Lw_x \\ z_x = Hx \\ z_u = \rho lu \\ y = Cx + \mu lw_y \end{cases} \tag{8}$$

The signal w (w_x and w_y) contains all external inputs (disturbance inputs), including Gaussian disturbances, sensor noises and commands; the output z (z_x and z_u) is an error signal (controlled output); y is the measured variables (measured output); and u is the control input. Note that the resulting closed-loop transfer function from w to z is denoted by T_{zw} and it's obtained from a fractional linear transformation.

The matrices A, B and C form an embodiment in state variables of the usually called transfer matrix (or transfer function to the system SISO) of G(s): [14]-[15]

$$G := \begin{bmatrix} A & B \\ C & 0 \end{bmatrix} = C\Phi(s)B \tag{9}$$

where Φ(s) is represented as:

$$\Phi(s) = (sI - A)^{-1} \tag{10}$$

Therefore, if both pairs (A B and A L) are stable and the both (A C and A H) are detectable, the plant P may be submitted to an optimization recurring to H_∞ and the problem will be based in finding a controller K, which with the information provided by y, generates a control signal u capable of commanding the generalized plant P and neutralizes the influence of w and z, using the minimization of the matrix T_{zw}. [16]

The controller K admissible and represented in terms of state variable can be given as:

$$K := \begin{bmatrix} A_\infty + BK_C + ZK_F & ZK_F \\ K_C & 0 \end{bmatrix} \tag{11}$$

where A_∞ and Z are represented as:

$$A_\infty = A + \gamma^{-2}LL^T X \tag{12}$$

$$Z = (I - \gamma^{-2}YX)^{-1} \tag{13}$$

Finally, the solution for the generalized algebraic Riccati equation is given by the symmetric matrices X and Y: [16]

$$A^T X + XA + \gamma^{-2}XLL^T X - \rho^{-2}XBB^T X + H^T H = 0 \tag{14}$$

$$K_C = \rho^{-2}B^T X \tag{15}$$

$$YA^T + AY + \gamma^{-2}YHH^T - \mu^{-2}YCC^T + L^T L = 0 \tag{16}$$

$$KF = \mu^{-2}YC^T \tag{17}$$

Now, it will be presented the problem regarding the H_∞ / LTR controller for the mixed sensibility and through the exit. Beginning with the H_∞ / LTR for the mixed sensibility, a set of the feedback matrix K_C represented by (15) is projected to ensure that the transfer matrix with

open mesh $(G(s)K(s))$ becomes the transfer matrix with the objective mesh $(C\Phi(s)K_F)$, which is reached using the sate observer. Regarding the H_∞ / LTR through the exit, it can be divided into two steps. First, it is necessary to project one state observer matrix K_F (by choosing the L, μ and γ), to obtain the objective mesh and then, design the feedback matrix K_C by reducing the value of ρ iteratively in order to approximate the open mesh to the objective mesh established in the beginning. If the value of ρ tends to zero, then the matrix X given by (14) will also tend to zero.

Note that if the pairs (A B and A L) are stabilized and the pair (A, C) is detectable, K_C will be chosen depending on the values obtained in (16). In the generalized plant P that is given by (8), if matrix H is equal to matrix C and ρ tends to zero, the controller K will tend to: [18]

$$\lim_{\rho\to 0^+} K(s) = \left[C\Phi(s)B\right]^{-1} C\Phi(s)K_F \tag{18}$$

IV. Artstein Method

To be able to use a robust controller, first a system needs to meet a number of requirements, being those: the system must be able to resist to the disturbances while performing the function for the purpose it was created; the controller must accomplish the objective, even when subject to disturbances;

The application of the Artstein method ensures that regardless of the input signal, the output signal will be controlled and stabilized as developed. Therefore, the Robust controller using this method will adopt the following structure: [19]-[20]

$$u = -R^{-1}B^T(P(x - x_{ref}(t)) + r) \tag{19}$$

where r and z are represented as:

$$r = -(A^T - PBR^{-1}BT)^{-1}Pz \tag{20}$$

$$z = -Ax_{ref}(t) \tag{21}$$

Note that the solution of the matrix *P* is still obtained using the Riccati equation given by (3).

V. Simulation Results

For the simulations obtained, the pursuer is a tactical missile with the ability for 40 g force and a top speed of Mach 4 and the target course, as well as the top speed and g force, were generated randomly using Python 3.6, having this the ability for a maximum 3 g force and a top speed of Mach 1.5.

For the H_∞ / LTR controller, the system that describes the missile movement is represented in (8), where the state vector concerns the position and velocity as in (22), the control vector concerns the acceleration as in (23), the measured output and the controlled output are represented by the position as in (24) and (25), respectively and the disturbance input concerns the position and velocity disturbances as in (26). For the Robust LQR controller, the system that describes the missile movement is represented in (1), where as in the first method, the state vector is represented in (22), the control vector is represented in (23) and the measured output is represented in (24). All this vectors are in 3D and in SI, being represented as:

$$x = \begin{bmatrix} p_x & p_y & p_z & v_x & v_y & v_z \end{bmatrix}^T \tag{22}$$

$$u = \begin{bmatrix} a_x & a_y & a_z \end{bmatrix}^T \tag{23}$$

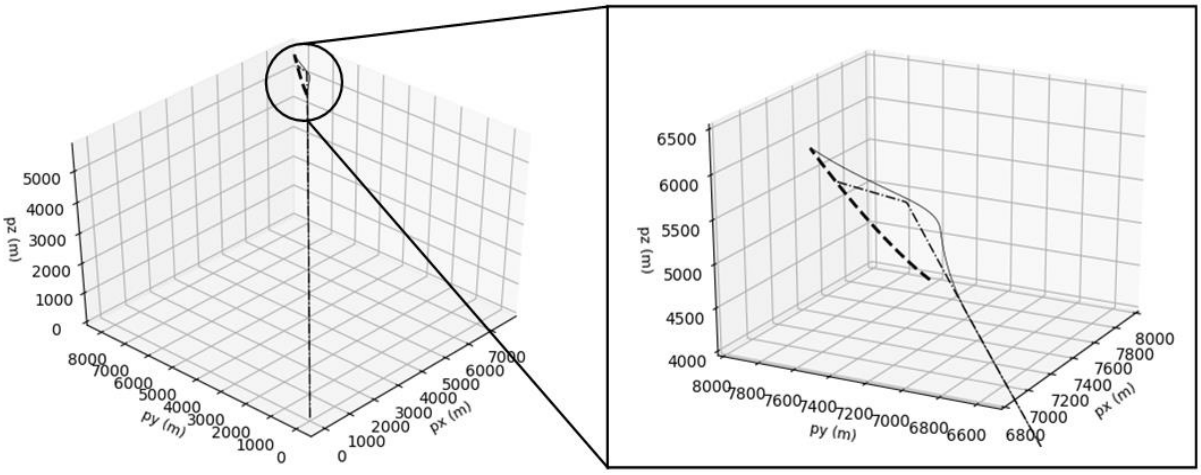

Fig 3. Missile and Target (densely dashed) persecution until the intersection occurs for the state vector X1, using Robust LQR (solid line) and Hinfinit/LTR (densely dashdotted) controllers in 3D

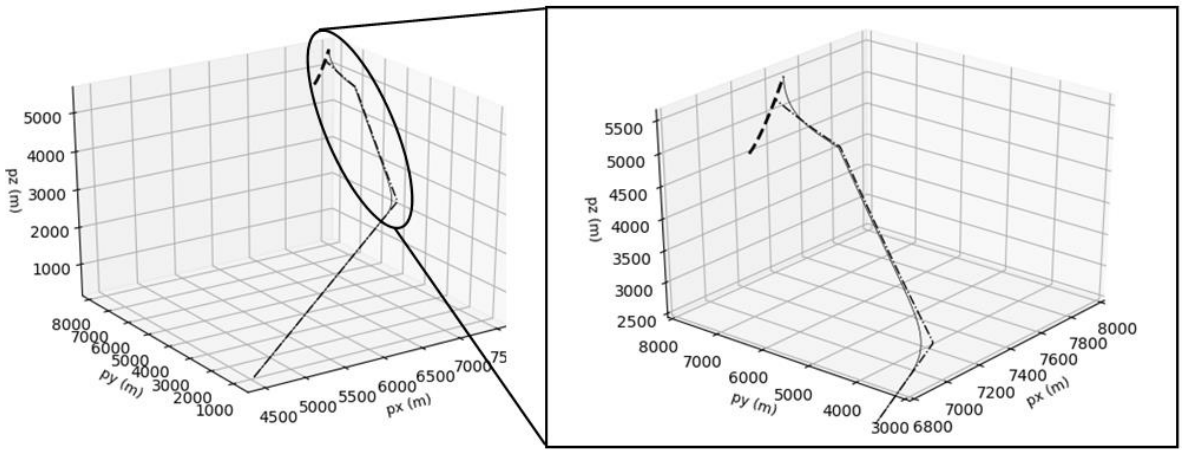

Fig 4. Missile and Target (densely dashed) persecution until the intersection occurs for the state vector X2, using Robust LQR (solid line) and Hinfinit/LTR (densely dashdotted) controllers in 3D

$$y = \begin{bmatrix} p_x & p_y & p_z \end{bmatrix} \tag{24}$$

$$z = \begin{bmatrix} p_x & p_y & p_z \end{bmatrix}^T \tag{25}$$

$$w = \begin{bmatrix} \dot{p}_x & \dot{p}_y & \dot{p}_z & \dot{v}_x & \dot{v}_y & \dot{v}_z \end{bmatrix} \tag{26}$$

Both methods have matrices A and B in common, being those represented in (27) and (28), respectively. Matrices L, H, C, ρI and μI, are represented in (29), (30), (31), (32) and (33), respectively and only concerns the H_∞ / LTR method.

$$A = \begin{bmatrix} 0 & 0 & 0 & 1 & 0 & 0 \\ 0 & 0 & 0 & 0 & 1 & 0 \\ 0 & 0 & 0 & 0 & 0 & 1 \\ 0 & 0 & 0 & 0 & 0 & 0 \\ 0 & 0 & 0 & 0 & 0 & 0 \\ 0 & 0 & 0 & 0 & 0 & 0 \end{bmatrix} \tag{27}$$

$$B = \begin{bmatrix} 0 & 0 & 0 \\ 0 & 0 & 0 \\ 0 & 0 & 0 \\ 1 & 0 & 0 \\ 0 & 1 & 0 \\ 0 & 0 & 1 \end{bmatrix} \tag{28}$$

$$L = \begin{bmatrix} 1 & 0 & 0 & 0 & 0 & 0 \\ 0 & 1 & 0 & 0 & 0 & 0 \\ 0 & 0 & 1 & 0 & 0 & 0 \\ 0 & 0 & 0 & 0 & 0 & 0 \\ 0 & 0 & 0 & 0 & 0 & 0 \\ 0 & 0 & 0 & 0 & 0 & 0 \end{bmatrix} \tag{29}$$

$$H = \begin{bmatrix} 1 & 0 & 0 & 0 & 0 & 0 \\ 0 & 1 & 0 & 0 & 0 & 0 \\ 0 & 0 & 1 & 0 & 0 & 0 \end{bmatrix} \tag{30}$$

$$C = \begin{bmatrix} 1 & 0 & 0 & 0 & 0 & 0 \\ 0 & 1 & 0 & 0 & 0 & 0 \\ 0 & 0 & 1 & 0 & 0 & 0 \end{bmatrix} \tag{31}$$

$$\rho I = \begin{bmatrix} \rho & 0 & 0 \\ 0 & \rho & 0 \\ 0 & 0 & \rho \end{bmatrix} \tag{32}$$

$$\mu I = \begin{bmatrix} \mu & 0 & 0 \\ 0 & \mu & 0 \\ 0 & 0 & \mu \end{bmatrix} \tag{33}$$

V.1. Implementation of the Problem, using a non-maneuvering target

For the implementation of a non-maneuvering target, matrixes Q and R were obtained recurring to modified Bryson:

$$Q = \begin{bmatrix} 2000000 & 0 & 0 & 0 & 0 & 0 \\ 0 & 2000000 & 0 & 0 & 0 & 0 \\ 0 & 0 & 2000000 & 0 & 0 & 0 \\ 0 & 0 & 0 & 0 & 0 & 0 \\ 0 & 0 & 0 & 0 & 0 & 0 \\ 0 & 0 & 0 & 0 & 0 & 0 \end{bmatrix} \tag{34}$$

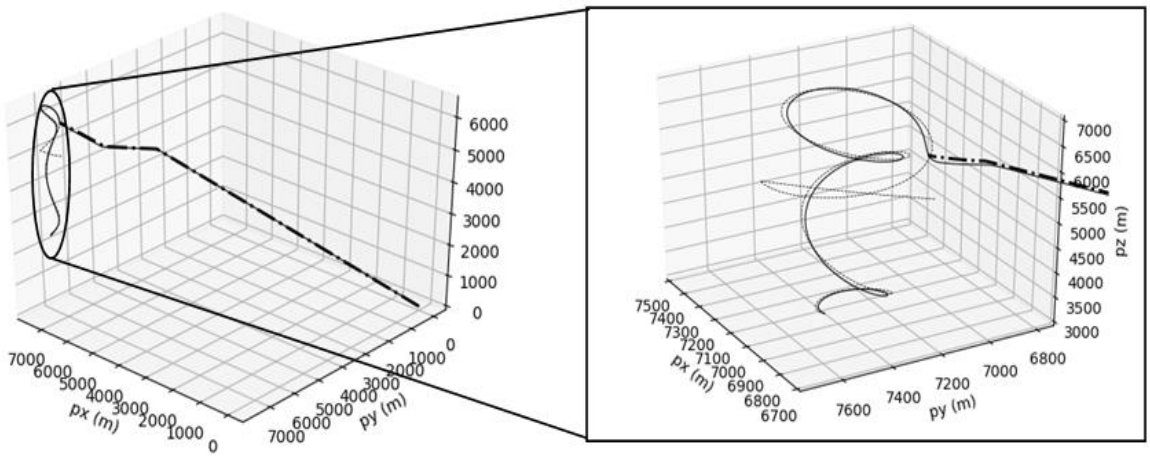

Fig 5. Missile and Target (dotted) persecution using evasive maneuvers starting at 5 seconds of the simulation, until the intersection occurs, using Robust LQR (solid line) and Hinfinit/LTR (densely dashdotted) controllers in 3D

$$R = \begin{bmatrix} 0.001 & 0 & 0 \\ 0 & 0.001 & 0 \\ 0 & 0 & 0.001 \end{bmatrix} \quad (35)$$

As it's possible to observe from matrix Q given in (34), the data for velocity is equal to zero, where only the missile and target positions are intended to coincide. In other words, Missile propulsion is independent of the target. Two different analysis were performed, by altering the initial persecutor position, with the initial velocity equal to zero. Therefore, two different state vectors were applied for the systems in question, being those respectively: X1 = [0, 0, 0, 0, 0, 0] and X2 = [4500, 850, 250, 0, 0, 0]. Regarding the target, for both simulations, it started from the same position and also with initial velocity equal to zero The state vector regarding the target is equal to X = [7000, 7000, 5000, 0, 0, 0].

From Fig.3, where the sate vector X1 was applied, it's possible to observe that both controllers have a very similar performance for a non manoeuvrable target, with the exception of the final intersection stage, where the H_∞ / LTR controller shows a better performance than the Robust LQR. More precisely, the missile using H_∞ / LTR controller needs 6.21 seconds for the impact to occur, while the missile using Robust LQR controller needs 7.07 seconds.

When state vector X2 was applied, H_∞ / LTR controller continued to have a better performance regarding the other controller, as it's possible to observe from Fig. 4. In this simulation, the intersection for H_∞ / LTR controller occurred at 5.45 seconds, while for Robust LQR controller occurred at 6.37 seconds

V.2. Implementation of the Problem, using a maneuvering target

As in the previous case V.1, for the implementation of a maneuvering target matrices Q and R were also obtained recurring to modified Bryson, being represented as (36) and (37), respectively.

Two different escape trajectories were generated randomly by the program, where the missile detection time by the target was also subjected to an analysis. Therefore, the first escape route starts at 5 seconds of simulation and it will be referred as X3 and the second escape route will start at 4 seconds of simulation and it will be referred as X4.

Now, note that the initial state vector for the missile is X = [0, 0, 0, 0, 0, 0] and the initial state vector for the target is the same as in V.1.

$$Q = \begin{bmatrix} 9500000 & 0 & 0 & 0 & 0 & 0 \\ 0 & 9000000 & 0 & 0 & 0 & 0 \\ 0 & 0 & 7000000 & 0 & 0 & 0 \\ 0 & 0 & 0 & 0 & 0 & 0 \\ 0 & 0 & 0 & 0 & 0 & 0 \\ 0 & 0 & 0 & 0 & 0 & 0 \end{bmatrix} \quad (36)$$

$$R = \begin{bmatrix} 0.0012 & 0 & 0 \\ 0 & 0.068 & 0 \\ 0 & 0 & 0.001 \end{bmatrix} \quad (37)$$

From Fig.5, where the case X3 is applied, it's possible to conclude that the missile using the H_∞ / LTR controller against a maneuvering target continues to have a better performance than the missile using Robust LQR controller. More preciselly, the intersection for the first method referred occurs at 5.67 seconds, while for the second method occurs at 9.85 seconds, which corresponds to a more significant difference regarding the analysis made to a non-maneuvering target.

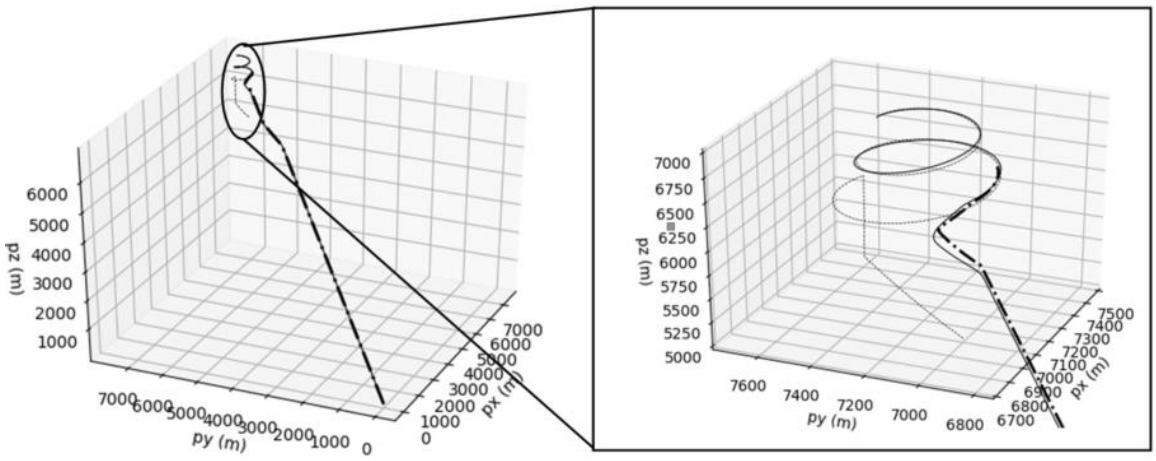

Fig 6. Missile and Target (dotted) persecution using evasive maneuvers starting at 4 seconds of the simulation, until the intersection occurs, using Robust LQR (solid line) and Hinfinit/LTR (densely dashdotted) controllers in 3D

Missile course is maintained until the evasive maneuvers are initiated. Therefore, for the Robust LQR controller, the missile doesn't have time to adjust the course before the new blank trajectory starts and needs more time to calculate and follow the route. However, for the H_∞ / LTR controller, the fact that the target initiates a new trajectory during the simulation, doesn't affect the missile behaviour, and the proper corrections were made.

Fig.6 represents the second study case referred as X4, where the evasive maneuvers were applied at 4 seconds of the simulation, so that the blank had a better chance of excaping from the persecutor. The intersection for the H_∞ / LTR controller occurred at 5.59 seconds, while for the Robust LQR controller occurred at 6.81 seconds, thus occuring what would already be expected. In this simulation, an abrupt climb and a variation of speed while performing a spiral is made by the target, where the Robust LQR method requires more time to calculate the new path and to apply an inpact trajectory.

VI. Conclusion

The law of orientation is the feedback of the algorithm in which the geometrical rule is implemented, being this a line passing through the object being guided (LOS). In the first generation of CLOS guided missiles, the tracing was manual, an operator had to keep the target image in its FOV, which could range from a simple pair of binoculars to a radar or a television screen. Already in the second generation of CLOS-guided missiles, only the target tracking is manual, all other functions, including those of tracking the missile, are made automatically. In the auto-tracking case, a seeker is mounted on a platform that has sufficient mechanical mobility to allow the fulfilment of the mission (in most cases two degrees of freedom are sufficient, being these the azimuth, which is the angular distance measured on the horizon, and the elevation). Finally, in a two-point system, the seeker is implemented on the missile, in a platform named gimbal.

As technology evolves, the interaction between man and machine is becoming smaller, making the systems more and more precise. However, it is necessary to understand that no system is infallible.

From this article, it is possible to conclude that the H_∞ / LTR controller has a better performance regarding the Robust LQR controller. For the first case of study, corresponding to V.1, although the differences between both methods are in the thousandths of a second, more precisely 0.86 seconds for X1 and 0.92 seconds for X2, in a tactical missile, this difference may lead to the success or failure of the mission. Now, regarding V.2, where a manoeuvring target with two different routes is tested, differences between the two methods are more significant. H_∞ / LTR controller has a more systematic trajectory, with very similar results and times for the impact, where the fact that changing the evasive manoeuvres initiating time, as well as the target path, do not present a problem to this specific method. Nevertheless, the same cannot be concluded from Robust LQR controller. This method has a worst performance for all the cases presented, specifically for the simulations in V.2, where this controller needs more time to calculate and follow the new blank trajectories, when the initial evasive manoeuvres time and the escape path is changed, having significant differences on the impact time.

However, it is necessary to take into consideration that changing the target and missile maximum g force as well as the Mach number, will have a direct impact on the missile behaviour. The results presented also depend on the values applied to matrices Q and R. Moreover, the change of the values ρ and μ will also have a direct impact on the performance of the H_∞ / LTR controller.

References

[1] N.A. Shneydor, *Missile guidance and pursuit: kinematics, dynamics and control* (Coll House, Westergate, Chichester, West Sussex ,1998).

[2] Ross Jr., Frank, *Guided missiles: rockets & torpedoes* (Lothrop, Lee & Shepard, 1951).
[3] Gatland, Keneeth W., *Development of the guided missile* (Iliffe, 1952).
[4] Spearman, M. Leroy, Historical development of worldwide guided missiles, *NASA Technical Memorandum 85658* (1983).
[5] Zarchan, P., *Ballistic missile defense guidance and control issues* (Gordon and Breach Science Publishers SA, 1998, pp. 99-124).
[6] Siouris, G.M., *An engineering approach to optimal control and estimation theory* (Wiley-Interscience 1996).
[7] W. L. Robert, L. A. Douglas, *Linear state-space control systems* (John Wiley & Sons, 2007).
[8] Liu X., Wu Y., Xiao S., A control method to make LQR robust: a planes cluster approaching mode, *International Journal of Control, Automation, and Systems (2014) 12(2), 302-308.*
[9] Tripathy N. S., Kar I. N., Paul K., Stabilization of Uncertain Discrete-time Linear System with Limited Communication, *Institute of Electrical and Electronics Engineers (IEEE) (2017) 62(9), 4727-4733.*
[10] Peterson I. R., Holoot C. V., A riccati equation approach to the stabilization of uncertain linear systems, *International Federation of Automatic Control (IFAC) (1986) 22(4), 397- 411.*
[11] Lin L. G., *Nonlinear control systems: a "state-dependent (differential) riccati equation" approach*, Ph.D. dissertation, Dept. Elect. Eng. , National Chiao Tung Univ., Shanghai, 2014.
[12] Jia Luo, C. E. Lan, Determination of weighting matrices of a linear quadratic regulator, *Journal of Guidance, Control, and Dynamics(JGCD) (1995) 18(6), 1462-1463*
[13] A. Sandra, *Controlo óptimo robusto de osciladores caóticos, MSc dissertation, Dept. Aero. Eng., University of Beira Interior, Covilhã, 2009.*
[14] Toivonen H., *Lecture notes on robust control by state-space methods*, Dept. Chem. Eng., Abo Akademi Univ., Finland, 1998.
[15] Caio F. de Paula, Felipe H. R. Cunha, Luís H. C. Ferreira, Um procedimento simplificado de síntese de controladores Hinfinit/LTR para o problema de sensibilidade mista, *Proceedings of the 18th National Brazilian of automatic conference.*
[16] C. D. John, K. Glover, K. P. Pramod, F. A. Bruce, State.space solutions to standard H2 and Hintinit control problems, *Institute of Electrical and Electronics Engineers (IEEE) (1989) 34(8), 831-847.*
[17] Y. Rui, H. Tomoyuki, State-space approach with the maximum likelihood principle to identify the system generating time-course gene expression data of yeast, Proceedings of the *International Journal Data Mining and Bioinformatics (IJDMB) (2006) 1(1), 77-87.*
[18] J. Shinar, Y. Rotsztein, E. Bezner, Analysis of three-dimensional optimal evasion with linearized kinematics, *Conference of guidance and control for the American Institute of Aeronautics and Astronautics (AIAA) (1978)*
[19] Artstein Z., Stabilization with relaxed controls, *International Mathematical Journal Nonlinear Analysis (1983) 7(11), 1163-1173.*
[20] Jackson P. B., Overview of missile flight control systems, *Johns Hopkins University Applied Physics Laboratory (APL) (2010) 29(1), 9-24.*

Authors' information

Department of Aerospace Science
University of Beira Interior, 6201-001 Covilhã, Portugal